VOLUME 35 | SUPPLEMENT 2 | MARCH 2022

MODERN PATHOLOGY

ABSTRACTS (1018–1075)

LIVER PATHOLOGY

2022

USCAP 111TH ANNUAL MEETING

REAL INTELLIGENCE

MARCH 19–24, 2022 LOS ANGELES, CALIFORNIA

Published by
SPRINGER NATURE
www.ModernPathology.org

USCAP
Creating a Better Pathologist
AN OFFICIAL JOURNAL OF THE UNITED STATES AND CANADIAN ACADEMY OF PATHOLOGY

EDUCATION COMMITTEE

Rhonda K. Yantiss
Chair

Kristin C. Jensen
Chair, CME Subcommittee

Laura C. Collins
Chair, Interactive Microscopy Subcommittee

Yuri Fedoriw
Short Course Coordinator

Ilan Weinreb
Chair, Subcommittee for Unique Live Course Offerings

Carla L. Ellis
Chair, DEI Subcommittee

Adebowale J. Adeniran
Kimberly H. Allison
Sarah M. Dry
William C. Faquin
Karen J. Fritchie
Jennifer B. Gordetsky
Levon Katsakhyan, Pathologist-in-Training
Melinda J. Lerwill
M. Beatriz S. Lopes
Julia R. Naso, Pathologist-in-Training
Liron Pantanowitz
Carlos Parra-Herran
Rajiv M. Patel
Charles "Matt" Quick
David F. Schaeffer
Lynette M. Sholl
Olga K. Weinberg
Maria Westerhoff

ABSTRACT REVIEW BOARD

Benjamin Adam
Oyedele Adeyi
Mariam Priya Alexander
Daniela Allende
Catalina Amador
Vijayalakshmi Ananthanarayanan
Tatjana Antic
Manju Aron
Roberto Barrios
Gregory R. Bean
Govind Bhagat
Luis Zabala Blanco
Michael Bonert
Alain C. Borczuk
Tamar C. Brandler
Eric Jason Burks
Kelly J. Butnor
Sarah M. Calkins
Weibiao Cao
Wenqing (Wendy) Cao
Barbara Ann Centeno
Joanna SY Chan
Kung-Chao Chang
Hao Chen
Wei Chen
Yunn-Yi Chen
Sarah Chiang
Soo-Jin Cho
Shefali Chopra
Nicole A. Cipriani
Cecilia Clement
Claudiu Cotta
Jennifer A. Cotter
Sonika M. Dahiya
Elizabeth G. Demicco
Katie Dennis
Jasreman Dhillon
Anand S. Dighe
Bojana Djordjevic
Michelle R. Downes
Charles G. Eberhart
Andrew G. Evans
Fang Fan
Julie C. Fanburg-Smith
Gelareh Farshid
Michael Feely
Susan A. Fineberg
Dennis J. Firchau
Gregory A. Fishbein
Agnes B. Fogo
Andrew L. Folpe
Danielle Fortuna
Billie Fyfe-Kirschner
Zeina Ghorab
Giovanna A. Giannico
Anthony J. Gill
Tamar A. Giorgadze
Alessio Giubellino
Carolyn Glass
Carmen R. Gomez-Fernandez
Shunyou Gong
Purva Gopal
Abha Goyal
Christopher C. Griffith
Ian S. Hagemann
Gillian Leigh Hale
Suntrea TG Hammer
Malini Harigopal
Kammi J. Henriksen
Jonas J. Heymann
Carlo Vincent Hojilla
Aaron R. Huber
Jabed Iqbal
Shilpa Jain
Vickie Y. Jo
Ivy John
Dan Jones
Ridas Juskevicius
Meghan E. Kapp
Nora Katabi
Francesca Khani
Joseph D. Khoury
Benjamin Kipp
Veronica E. Klepeis
Christian A. Kunder
Stefano La Rosa
Stephen M. Lagana
Keith K. Lai
Goo Lee
Michael Lee
Vasiliki Leventaki
Madelyn Lew
Faqian Li
Ying Li
Chieh-Yu Lin
Mikhail Lisovsky
Lesley C. Lomo
Fang-I Lu
aDeqin Ma
Varsha Manucha
Rachel Angelica Mariani
Brock Aaron Martin
David S. McClintock
Anne M. Mills
Richard N. Mitchell
Hiroshi Miyamoto
Kristen E. Muller
Priya Nagarajan
Navneet Narula
Michiya Nishino
Maura O'Neil
Scott Roland Owens
Burcin Pehlivanoglu
Deniz Peker Barclift
Avani Anil Pendse
Andre Pinto
Susan Prendeville
Carlos N. Prieto Granada
Peter Pytel
Stephen S. Raab
Emilian V. Racila
Stanley J. Radio
Santiago Ramon Y Cajal
Kaaren K Reichard
Jordan P. Reynolds
Lisa M. Rooper
Andrew Eric Rosenberg
Ozlen Saglam
Ankur R. Sangoi
Kurt B. Schaberg
Qiuying (Judy) Shi
Wonwoo Shon
Pratibha S. Shukla
Gabriel Sica
Alexa Siddon
Anthony Sisk
Kalliopi P. Siziopikou
Stephanie Lynn Skala
Maxwell L. Smith
Isaac H. Solomon
Wei Song
Simona Stolnicu
Adrian Suarez
Paul E. Swanson
Benjamin Jack Swanson
Sara Szabo
Gary H. Tozbikian
Gulisa Turashvili
Andrew T. Turk
Efsevia Vakiani
Paul VanderLaan
Hanlin L. Wang
Stephen C. Ward
Kevin M. Waters
Jaclyn C. Watkins
Shi Wei
Hannah Y. Wen
Kwun Wah Wen
Kristy Wolniak
Deyin Xing
Ya Xu
Shaofeng N. Yan
Zhaohai Yang
Yunshin Albert Yeh
Huina Zhang
Xuchen Zhang
Bihong Zhao
Lei Zhao

To cite abstracts in this publication, please use the following format: **Author A, Author B, Author C, et al. Abstract title (abs#). In "File Title."** ***Modern Pathology*** **2022; 35 (suppl 2): page#**

1018 Impact of Age and Gender on the Severity of Non-Alcoholic Steatohepatitis (NASH)

Eesha Acharya[1], Robert Lam[2], Joseph Lim[2], Dhanpat Jain[2]
[1]University of Michigan, Ann Arbor, MI, [2]Yale School of Medicine, New Haven, CT

Disclosures: Eesha Acharya: None; Robert Lam: None; Joseph Lim: *Grant or Research Support*, Intercept, Allergan, Genfit, Pfizer, Viking; Dhanpat Jain: None

Background: Men and post-menopausal women are at increased risk of developing non-alcoholic steatohepatitis (NASH) compared to pre-menopausal women. However, the impact of age and gender on NASH progression remains controversial. We sought to investigate whether age and gender were associated with severity of nonalcoholic steatohepatitis (NASH).

Design: From a cohort of adult patients with biopsy-proven NASH from 2012-2019, we conducted a cross-sectional study with patients stratified by age and gender (men 18-50 years, women 18-50 years, men >50 years, women >50 years). Twenty-five patients were randomly selected into each group. Patients with a prior liver transplant or alternative etiologies were excluded, including autoimmune and viral hepatitis, alcoholic liver disease, and genetic and other metabolic disorders. Baseline anthropometric data at the time of the index liver biopsy date were obtained. Each patient's liver biopsy was evaluated for a variety of histologic factors, including steatosis, fibrosis (NASH-CRN criteria) and nonalcoholic fatty liver disease activity score (NAS). ANOVA tests were performed to calculate differences between age and gender groups for various clinical and histologic parameters.

Results: A summary of descriptive results for the various age and gender groups is show in Table 1. Baseline mean age was similar among corresponding age groups, and BMI was similar across all groups. Among histologic features, there was a significant difference among age and gender groups for NAS (p=0.02) and fibrosis (p<0.001). The degree of steatosis (mean 2.3, SD 0.8) and NAS (mean 4.5, SD 0.9) were highest in 18-50 year-old women compared to >50 year-old women and men of all ages. Fibrosis scores were higher in men compared to women for all age groups, and was highest in >50 year-old men (mean 2.8, SD 1.2).

	Men, 18-50 years Mean (SD)	Female, 18-50 years Mean (SD)	Male, >50 years Mean (SD)	Female, >50 years Mean (SD)	Total (n=100) Mean (SD)	p-value
Age	37.0 (9.5)	39.0 (7.2)	62.0 (8.4)	60.0 (6.1)	49.5 (14.0)	<0.001
BMI (kg/m^2)	33.0 (5.0)	32.1 (7.8)	34.7 (5.9)	32.3 (7.6)	33.0 (6.6)	0.5
NAS	3.7 (1.4)	4.5 (0.9)	3.5 (1.3)	4.1 (1.2)	4.0 (1.2)	0.02
Steatosis	2.2 (0.7)	2.3 (0.8)	1.8 (0.8)	2.1 (0.8)	2.1 (0.8)	0.09
Fibrosis	1.5 (1.2)	1.6 (1.0)	2.8 (1.2)	2.1 (1.3)	2.0 (1.3)	<0.001

Conclusions: An association between age and gender with severity of NASH was observed. Women have higher steatosis and NAS compared to men. However, liver fibrosis tends to be more severe in men, and tends to increase with age irrespective of gender. Estrogen-related sex hormones may play a protective role against fibrosis in young pre-menopausal women. This phenomenon may have therapeutic implications and needs further evaluation.

1019 Unique Somatic Mutational Landscape in Cirrhotic-Like (Cirrhotomimetic) Hepatocellular Carcinoma

Sameer Al Diffalha[1], Chirag Patel[1], Prachi Bajpai[1], Amr Elkholy[1], Michael Behring[1], Brandon Wilk[1], Manavalan Gajapathy[1], Felipe Massicano[1], Tarun Karthik Kumar Mamidi[1], Donna Brown[1], Gurpreet Kaur[1], Abby Shelton[2], Erin Smithberger[1], George Netto[1], C Ryan Miller[1], Elizabeth Worthey[1], Upender Manne[1]
[1]The University of Alabama at Birmingham, Birmingham, AL, [2]UAB Hospital, Birmingham, AL

Disclosures: Sameer Al Diffalha: None; Chirag Patel: None; Prachi Bajpai: None; Amr Elkholy: None; Michael Behring: None; Brandon Wilk: None; Manavalan Gajapathy: None; Felipe Massicano: None; Tarun Karthik Kumar Mamidi: None; Donna Brown: None; Gurpreet Kaur: None; Abby Shelton: None; Erin Smithberger: None; George Netto: None; C Ryan Miller: None; Elizabeth Worthey: None; Upender Manne: None

Background: Hepatocellular carcinoma (HCC) is the second highest cause of cancer-related death globally. The majority of HCCs occur in background cirrhosis. Although diagnosis of most of HCCs can be made by imaging, some HCC variants cannot be detected. This misleads the radiologists to infer them as cirrhosis and misses tumor nodules. They are discovered at time of histologic examination of explanted livers. Thus, they are termed cirrhotic-like HCC (CL-HCC).

Design: Based on histology, we classified samples from 15 patients into 3 groups of 5: HCC without background cirrhosis (HCC W/O-C), HCC with background cirrhosis (HCC W-C), and CL-HCC (Figure 1). DNA was extracted from formalin-fixed, paraffin-embedded tumors and were processed for whole-exome sequencing. Following base calling, sequences were aligned to current genome reference (GRCh38) with BWA-MEM and processed via GATK for base quality score recalibration, indel realignment and duplicate removal. QC was run to ensure samples were of sufficient coverage and quality. GATK HaplotypeCaller and Mutect2 were used to call variants. Tertiary analysis and interpretation of variants was performed using the Codicem software, using a pairwise approach to identify tumor specific and background variation. Variant interpretation and classification was done according to ACMG-AMP criteria. Classification across the entire cohort and known or predicted functional impact were used to generate an Oncoprint using the cBioPortal Oncoprinter (Figure 2).

Results: In HCC W/O-C, we identified 9 unique somatic mutations, including alterations at 3 sites each in *CTNNB1* and *KMT2C* and at 1 site each in *CYP21A2, JAK1,* and *NBAS*. In HCC W-C , six mutations were found, including alterations at 2 sites in *AXIN1*, and at 1 site each in *KMT2C, MSH6, RBM10,* and *SEC63.* CL-HCCs exhibited 4 unique mutations in *APC, BRCA1, PCDH15,* and *TP53*, and 1 in *CYP21A2*, which was also identified in HCC W/O-C. A missense mutation in *BRCA1* and a stop mutation in *PCDH15* . The stop mutation in *APC*, a regulator of the WNT signaling pathway, is associated with HCC, and colon cancer. The variant in *TP53* is predicted to cause altered splicing, leading to an abnormal or absent protein (Table 1).

Table 1: Pathogenic somatic mutations in all 3 groups of HCC.

Gene symbol	Variant	Classification	GROUPS			Mutation type
			Non cirrhotic-HCC	Cirrhotic-HCC	Cirrohotic-Like-HCC	(All somatic)
KMT2C	c.1013-2A>G:	likely pathogenic	(2/5)	(3/5)	-	Splice site
KMT2C	c.906T>A:p.C302*	likely pathogenic	(1/5)	-	-	STOP
KMT2C	c.2639G>A:p.W880*	likely pathogenic	(1/5)	-	-	STOP
MSH6	c.3992G>A:p.R1331Q	likely pathogenic	-	(1/5)	-	Missense
AXIN1	c.1597C>T:p.R533*	likely pathogenic	-	(1/5)	-	STOP
AXIN1	c.1020-3C>A:	likely pathogenic	-	(1/5)	-	Splice site
RBM10	c.292delC:p.R98Efs*36	likely pathogenic	-	(1/5)	-	Frame shift
SEC63	c.1605delA:p.K535Nfs*28	likely pathogenic	-	(1/5)	-	Frame shift
CTNNB1	c.94G>T:p.D32Y	pathogenic	(1/5)	-	-	Missense
CTNNB1	c.98C>G:p.S33C	pathogenic	(1/5)	-	-	Missense
CTNNB1	c.100G>A:p.G34R	likely pathogenic	(1/5)	-	-	Missense
CYP21A2	c.955C>T:p.Q319*	likely pathogenic	(2/5)	-	(2/5)	STOP
JAK1	c.2729T>C:p.L910P	pathogenic	(1/5)	-	-	Missense
NBAS	c.3285G>A:p.W1095*	likely pathogenic	(1/5)	-	-	STOP
APC	c.694C>T:p.R232*	pathogenic	-	-	(1/5)	STOP
BRCA1	c.4730C>T:p.S1577F	likely pathogenic	-	-	(1/5)	Missense
PCDH15	c.4693C>T:p.R1565*	pathogenic	-	-	(1/5)	STOP
TP53	c.672+2T>A:	likely pathogenic	-	-	(1/5)	Splice site

Figure 1 - 1019

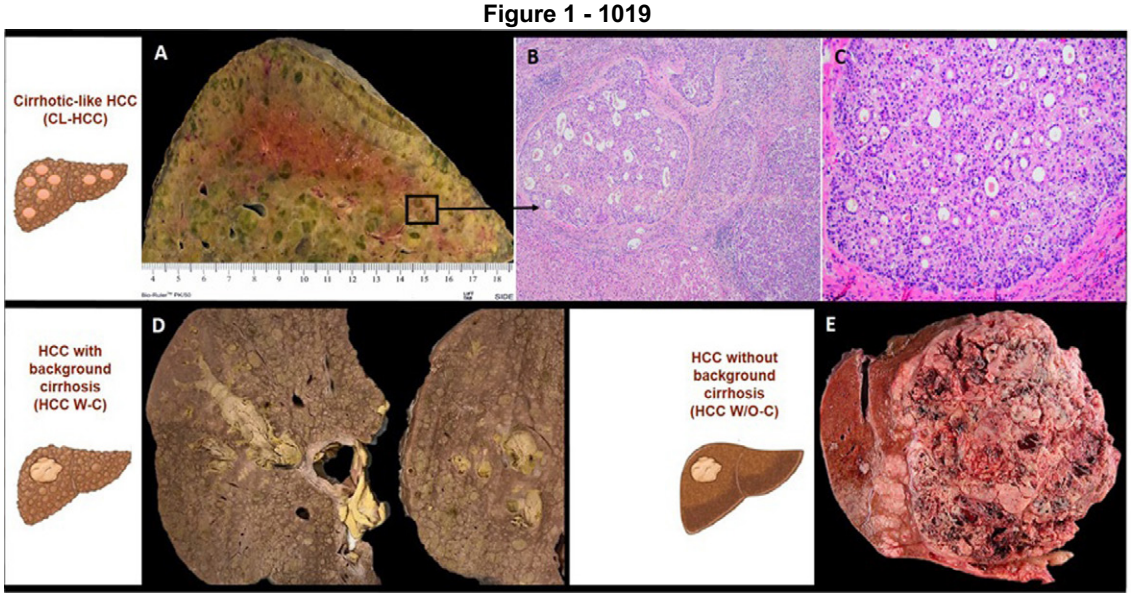

Figure 2 - 1019

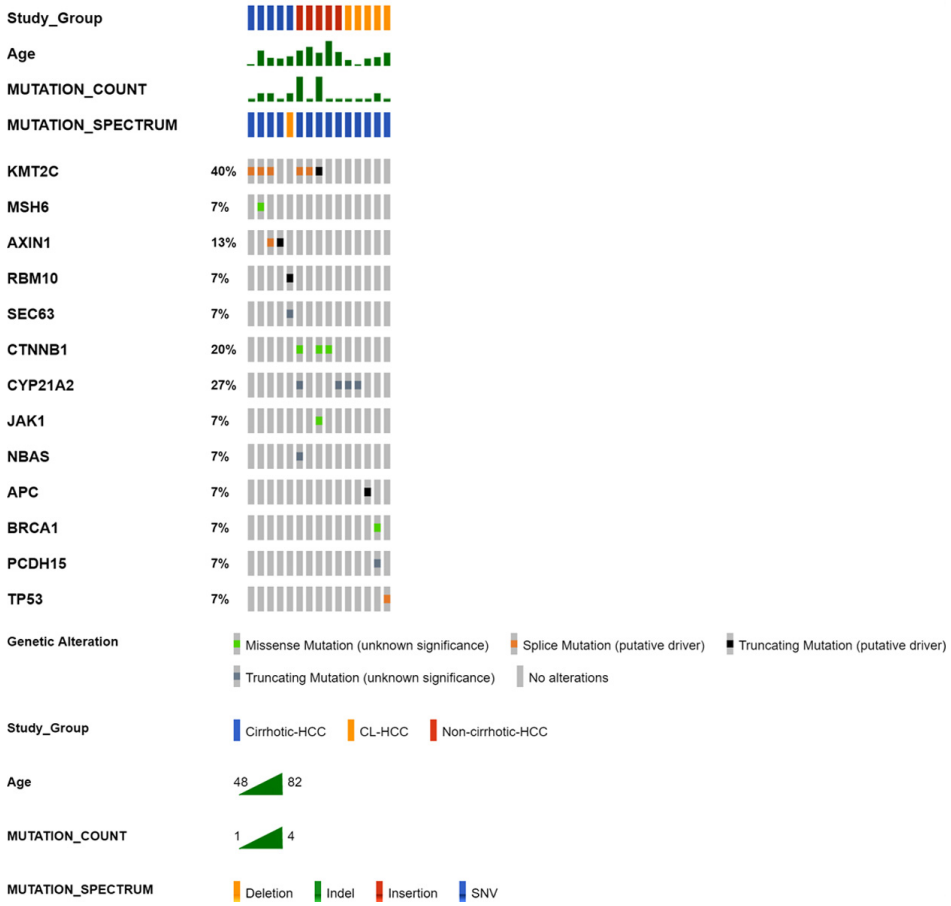

Conclusions: Our study is first to identify stop mutations in *APC, CYP21A2*, and *PCDH15*; missense mutations in *BRAC1*; and a splice variant in TP53 in CL-HCCs. Mutational profiling of suspicious cirrhotic scars could help in accurate diagnosis of CL-HCCs.

1020 Influence of the I148M Variant of Patatin-like Phospholipase Containing 3 Gene (PNPLA3) on the Histological Severity of Non-alcoholic Fatty Liver Disease in Mexican Population

Leticia Bornstein-Quevedo[1], CENTRO SC[2], Claudia Bautista-Wong[2], Zaira Mojica-Gonzalez[2], Eunice Molina[2], Gabriel Herrera-Maya[2]
[1]INMUNOQ, Mexico City, Mexico, [2]Mexico City, Mexico

Disclosures: Leticia Bornstein-Quevedo: *Consultant*, Bayer; CENTRO SC: *Primary Investigator*, Galmed pharmaceuticals, Novo Nordisk, Viking; Claudia Bautista-Wong: None; Zaira Mojica-Gonzalez: None; Eunice Molina: None; Gabriel Herrera-Maya: None

Background: PNPLA3 codifies a protein that is normally expressed in the liver and is involved in lipid metabolism. It has been recently identified as a major determinant for fat content. Several studies confirmed that the I148M variant plays an important role in the development of fatty liver disease, from simple steatosis to progressive fibrosis, and it influences fibrogenesis. The aim of this study was to determine the association between the single nucleotide polymorphism (SNP) variant I148M in PNPLA3 and the histological severity of Non-alcoholic Fatty Liver Disease (NAFLD) in the Mexican population.

Design: Two hundred and twenty-three liver biopsies were included; diagnosis was made using the NASH CRN system. Clinical and biochemical profiles were determined. The genotyping was made using 5' exonuclease TaqMan assay for rs738409 SNP in Rotor-Gene 5Plex thermocycler. The associations of this allele with clinical, anthropometric, and biochemical profiles were investigated. Univariate analysis was made using Student's T for continuous variables and Square chi for nominal variables. Kruskal Wallis test was used for categorical variables at SPSS V20.

Results: The SNP was found in 90% of the cases with the following distribution: female 91.8%% (135 cases) and male 88% (66 cases) (p 0.35). The presence of the SNP was not different among any of the variables but only in those with a higher HOMA index (p 0.001), insulin level (p.000) and histological activity (p 0.04). The fibrosis score was as follows: F0 23% (51 cases), F1: 22% (50 cases), F2: 22.5% (56 cases), F3: 17.1% (38 cases), F4 12.1% (27 cases). In the F4 subgroup the presence of homozygous SNP was higher than the others subgroups (55%) barely reaching significance (p 0.05). Hypertension was significantly higher in the F4 subgroup (59.3%, p 0.016). The levels of glucose showed a trend to be higher in the F4 compared to other fibrosis subgroups (p 0.075) as the cholesterol level (p 0.072). Insulin, HOMA index and HbA1c levels were also significantly higher in the F4 subgroup (p 0.000).

Conclusions: There is a high prevalence of SNP rs 738409 in the NAFLD Mexican population and correlates with clinical history of Hypertension, histological activity and insulin levels. In the subgroup F4, the insulin levels and HOMA index are significantly higher (p 0.000).

1021 Miz-1 Reduced Expression Coupled with Variable c-Myc and ZEB-1 Expression in High Grade Hepatocellular Carcinoma

Joeffrey Chahine[1], Sumeyye Culfaci[1], Dong Hyang Kwon[1], Pamela Tuma[2], Bhaskar Kallakury[3]
[1]MedStar Georgetown University Hospital, Washington, DC, [2]Catholic University of America, Washington, DC, [3]Georgetown University Hospital, Washington, DC

Disclosures: Joeffrey Chahine: None; Sumeyye Culfaci: None; Dong Hyang Kwon: None; Pamela Tuma: None; Bhaskar Kallakury: None

Background: Myc-Interacting Zinc Finger (Miz-1) is a transcription factor that can be an activator or a repressor depending on its interaction with the Myc oncoprotein, which can impact cellular proliferation. Zinc Finger E-Box Binding Homeobox-1 (ZEB-1) is an EMT-inducing transcriptional factor and a major stimulator of this process. Increased expression of ZEB-1 is associated with aggressive behavior in many tumor types.

Design: Since all three transcription factors are known to play crucial roles in tumor progression and metastatic potential, 147 hepatocellular carcinoma (HCC) resection cases including juxtaposing benign hepatic parenchyma are identified and the following panel of immunohistochemistry is performed to investigate the association: Miz-1 (ZBTB17), ZEB-1 (OT13G6), c-Myc (Y69), and Ki-67 (Mib-1). Clinicopathologic variables, including status of viral hepatitis, degree of fibrosis, tumor size, grade, lymphovascular invasion, and tumor-node-metastasis (TNM) stage, were obtained and correlated with the IHC results.

Results: Compared to the adjacent benign liver section, reduction of Miz-1 expression was observed in 145/147 (98.6%) *(P<0.0001)* cases, while positive expression of c-Myc, Ki-67 (> 5%), and ZEB-1 was observed in 26/147 (17.7%) *(p<0.0001)*, 47/147 (31.9%) *(p=0.00004)*, and 14/147 (9.5%) *(p<0.0001)* cases respectively. Of note, complete loss of Miz-1 expression was noted in 21/48 (43.75%) high grade tumors (III/IV) associated with positive c-Myc, Ki-67 (>5%), and ZEB-1 expression in 10/21 (47.6%) *(P=0.0000756)* cases. All 10 cases with positive ZEB-1 had confirmed positive lymph node involvement.

n=147	HCC Grade 1 (n=14)	HCC Grade 2 (n=85)	HCC Grade 3 (n=33)	HCC Grade 4 (n=15)
Miz-1 Reduced Cytoplasmic Expression	14/14 (100%, p=0.00006)	84/85 (98.82%, p <0.000001)	32/33 (96.96%, p <0.000001)	15/15 (100%, p=0.00003)
C-Myc Expression	1/14 (7.14%, p=0.00085)	7/85 (8.23%, p <0.000001)	10/33 (30.3%, p=0.010775)	8/15 (53.33%, p=0.19638)
Ki-67 Expression	4/14 (28.57%, p=0.0610)	10/85 (11.76%, p <0.000001)	19/33 (57.57%, p=0.093219)	14/15 (93.33%, p=0.000457)
Zeb-1 Expression	0/14 (0%, p=0.00006)	1/85 (1.17%, p <0.000001)	6/33 (18.18%, p=0.0001289)	7/15 (46.66%, p=0.19638)

Conclusions: These results support the role of Miz-1 as one of the intermediary checkpoints required for the induction of cell cycle arrest and apoptosis. Positive c-Myc/ZEB-1 coupled with Miz-1 reduced expression confirms the transcriptional repressor role of the Myc/Miz-1 complex and the activation of the ZEB-1 gene as a predictor of increased metastatic expansion, therapy resistance, and poor survival in high grade HCC cases. These studies are extended to cholangiocarcinoma including a cohort with mixed

hepatocellular and cholangiocarcinoma morphologies, in order to closely examine Miz-1, c-Myc and Zeb-1 interaction and expression across an adequate number of differently graded lesions to better test our hypothesis in epithelial derived human malignancies with frequently amplified 8q24 region where c-Myc interacts.

1022 Hepatoid Neuroendocrine Tumors: An Important Diagnostic Pitfall

Zongming (Eric) Chen[1], Karen Matsukuma[2], Dorina Gui[2], Saba Yasir[1], Michael Torbenson[1], Fan Lin[3]
[1]Mayo Clinic, Rochester, MN, [2]University of California, Davis, Sacramento, CA, [3]Geisinger Medical Center, Danville, PA

Disclosures: Zongming (Eric) Chen: None; Karen Matsukuma: *Advisory Board Member*, InCyte Corporation; *Consultant*, Diaceutics, Inc.; Dorina Gui: None; Saba Yasir: None; Michael Torbenson: None; Fan Lin: None

Background: Markers of hepatocellular differentiation such as HepPar and arginase are routinely used to identify hepatocellular carcinoma. In small biopsies, some metastatic neuroendocrine tumor (NET)s, can be morphologically confused with hepatocellular carcinoma (HCC), particularly ones with abundant eosinophilic or oncocytic cytoplasm. These hepatoid NETs may also express hepatocyte markers, representing a real diagnostic challenge and an important pitfall.

Design: Three cases of hepatoid NET were encountered in our consultation service over a period of 3 years, all of which were HepPar positive, and one was arginase positive. To further explore hepatocyte marker expression in NET, a tissue microarray (TMA) composed of NETs from various sites was stained HepPar and arginase. The TMA contained 49 NETs (17 from pancreas, 12 from liver metastases with primaries in the gastrointestinal tract, and 20 from lung NET). The staining results were semi-quantified as 1+ (5-10%), 2+ (10-20%) and 3+ (20-50%), 4+ (>50%), respectively.

Results: All 3 cases were liver biopsies of mass lesions with a radiological differential that included HCC (Table 1). Morphologically, all tumors showed features mimicking HCC, including abundant eosinophilic/oncocytic cytoplasm with trabecular growth patterns (Figure 1A). One case also exhibited pseudoglandular formation (Figure 1B). All tumors were diffusely and strongly positive for synaptophysin, chromogranin, and HepPar 1 (Figure 1C). Arginase 1 (Figure 1D) was positive in 1 case. Ki-67 proliferative indexes varied between 5-15%. Subsequent correlation with clinical and imaging findings confirmed 2 of these NETs were from the pancreas and 1 was from the GI tract. To gain insights into staining of hepatocyte markers in NETs, the TMA composed of 49 NETs was examined for HepPar and arginase expression. The immunostains identified 3 cases that were arginase positive (one 1+ and two 3+), all from pancreas. These additional tumors also exhibited hapatoid morphology, but are negative for HepPar.

Case	Age	Gender	Primary Tumor Site	IHC Scores			
				HepPar1	Arginase	Chromogranin	Synaptophysin
1	58	Male	Pancreas	3+	negative	3+	3+
2	77	Male	GI	3+	negative	3+	2+
3	60	Male	Pancreas	3+	2+	3+	3+

Figure 1 - 1022

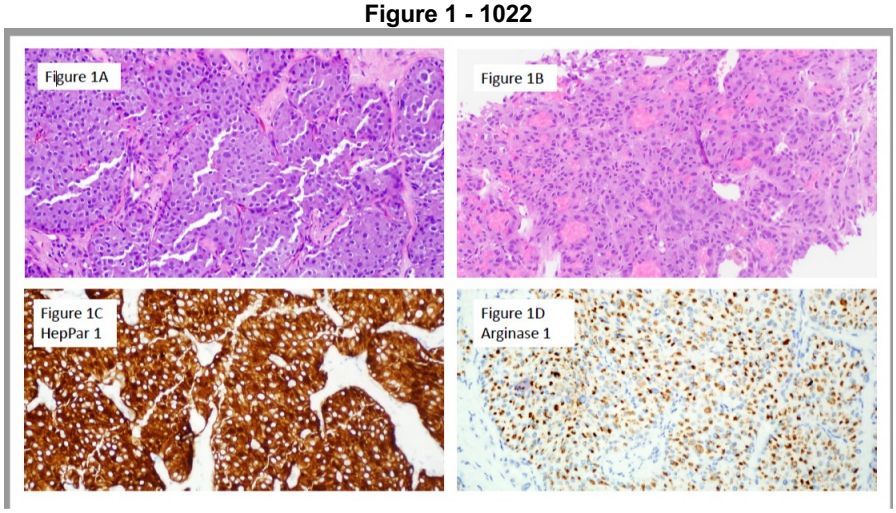

Conclusions: HepPar and arginase expression can be rarely seen in NETs that otherwise show typical neuroendocrine immunostaining profiles. Some of these tumors can mimic HCC on morphology. These hepatoid NETs represent an important diagnostic pitfall, particularly, when present as liver metastasis. Interestingly, arginase 1 immunostaining positivity seems to be restricted to pancreatic NETs.

1023 Incidence of Parenchymal Rejection in Liver Allograft Biopsies: One Institution's Experience

Andreas Ciscato[1], Alex Placek[2], Homayoun Mostaghni[3], Mojgan Hosseini-Varnamkhasti[1]
[1]University of California, San Diego, La Jolla, CA, [2]UCSD Medical Center, La Jolla, CA, [3]UCSD Medical Center, San Diego, CA

Disclosures: Andreas Ciscato: None; Alex Placek: None; Homayoun Mostaghni: None; Mojgan Hosseini-Varnamkhasti: None

Background: Parenchymal rejection (PR) is a rare and underdiagnosed form of atypical allograft liver rejection which can occur independently or in association with acute cellular rejection (ACR). In this study, we review clinicopathological features of PR +/- ACR and report our institution's experience with the diagnosis of PR.

Design: Following IRB approval, a retrospective review of archives from 2015-2021 identified 190 allograft liver biopsies. The cases were reviewed and information including date of birth, age at diagnosis, sex, final diagnosis, Information on Rejection Activity Index (RAI), parenchymal rejection and atypical rejection diagnosis were collected and compared.

Results: Of the 190 allograft liver biopsies 53 (28%) had ACR only, 39 (20%) with mild ACR, 13 (7%) with moderate ACR and 1 (0.5%) with severe ACR (See table 1). 22 (11%) had a diagnosis of PR. The overall age range was 23-77 years (average 53.5). In cases with a diagnosis of PR: 22 had a diagnosis of PR: 12 with ACR and PR, 10 with PR only. Of the cases with ACR and PCR: 9 (41%) had mild ACR, 2 (9%) moderate ACR and 1 (5%) severe ACR. Focal centrizonal necrosis was present in 4 (18%) confluent necrosis in 2 (9%). Among cases with PR, Donor Specific Antigen (DSA) was available in 9 cases: 4 positive DSA, 4 negative, and one reported as undetermined. C4D was performed only on one (3.8%) case and was reported as inconclusive. See table 1 for details.

ALL ALLOGRAFT LIVER BIOPSIES 2015-2021	N	PERCENTAGE	ALLOGRAFT LIVER BIOPSIES WITH PR	N	PERCENTAGE
TOTAL CASES	190		TOTAL CASES	22	
AGE RANGE		23-77	AGE RANGE		26-77
AGE AVERAGE		53.5	AGE AVERAGE		52.5
FEMALE	74	38%	FEMALE	10	45%
MALE	116	62%	MALE	12	55%
RAI SCORE/ CLASSIFICATION			RAI SCORE/ CLASSIFICATION		
NO REJECTION (0-2)	105	55%	NO REJECTION (0-2)	4	18%
INDETERMINATE (3)	32	17%	INDETERMINATE (3)	6	27%
MILD REJECTION (4-5)	39	20%	MILD REJECTION (4-5)	9	41%
MODERATE REJECTION (6-7)	13	7%	MODERATE REJECTION (6-7)	2	9%
SEVERE REJECTION (8)	1	0.5%	SEVERE REJECTION (8-9)	1	5%
					0%
PARENCHYMAL REJECTION (PR)	22	11%	PARENCHYMAL REJECTION ONLY	10	45%
PLASMA CELL RICH REJECTION	4	2%	PARENCHYMAL REJECTION+ ACR	12	55%
PARENCHYMAL REJECTION ONLY	10	5%	DONOR SPECIFIC ANTIGEN (DSA)		
PARENCHYMAL REJECTION+ ACR	12	6%	TOTAL PATIENTS TESTED	9	
VASCULAR REJECTION	4	2%	POSITIVE	4	
FOCAL NECROSIS	14	7%	NEGATIVE	4	
PERIPORTAL NECROSIS	11	6%	INDETERMINATE	1	
CONFLUENT NECROSIS	6	3%	C4D STAINING	1	Inconclusive
FIBROSIS	12	6%			

Conclusions: PR is a distinct and under recognized form of acute cellular rejection with distinct histological features affecting a slightly younger population. Awareness of this entity, defining histologic criteria of PR can help in recognition and reporting this entity to ensure appropriate treatment

1024 Loss of SMARCA2 is an Adverse Prognostic Finding for Patients with Hepatocellular Carcinoma and Correlates with Early Disease Recurrence After Hepatectomy

Nathan Cook[1], Simmi Patel[2], Michael Nalesnik, Aatur Singhi[1]
[1]University of Pittsburgh Medical Center, Pittsburgh, PA, [2]University of Pittsburgh Medical Center Presbyterian Shadyside, PA, [3]UPMC Montefiore, Pittsburgh

Disclosures: Nathan Cook: None; Simmi Patel: None; Michael Nalesnik: None; Aatur Singhi: None

Background: The SWItch/Sucrose Non-Fermentable (SWI/SNF) chromatin remodeling complex regulates a wide variety of cellular processes including gene expression and chromosomal stability. In addition, mutations in the SWI/SNF core components (ARID1A, SMARCA2, SMARCA4, and SMARCB1) occur in up to 20% of cancers and are often associated with adverse clinical outcomes. However, the status and clinical significance of the SWI/SNF core components in hepatocellular carcinoma (HCC) remains relatively unknown. The aim of this study was to evaluate the clinicopathologic features associated with SWI/SNF-deficient HCC.

Design: A total of 445 surgically resected, non-metastatic HCCs were collected between 2007 and 2019, and immunohistochemically stained for ARID1A, SMARCA2, SMARCA4, and SMARCB1. The status of each of the four proteins was assessed in conjunction with patient age, gender, tumor location, tumor size, multifocality, small and large vessel invasion, perineural invasion, T- and N-stage, disease recurrence, and relapse free-survival (RFS). Each HCC was also evaluated for HepPar-1, arginase-1, glypican-3, glutamine synthetase, and nuclear beta-catenin expression.

Results: Loss of ARID1A, SMARCA2, and both proteins were detected in 17 (4%), 10 (2%), and 1 (<1%) case, respectively. None of the 445 HCCs exhibited loss of expression for SMARCA4 or SMARCB1. No statistically significant correlation was identified between ARID1A status and associated clinicopathologic findings; however, loss of SMARCA2 did correlate with large tumor size, high histologic grade, small vessel invasion, large vessel invasion, and disease recurrence ($p<0.03$). Additionally, the 3-year RFS for HCC patients with SMARCA2 loss was 39% as compared to 70% for HCC patients with preserved expression for SMARCA2 ($p<0.03$). Immunohistochemical stains also revealed SMARCA2 loss correlated with negative expression for HepPar-1 and arginase-1, but strong and diffuse expression for glypican-3 ($p<0.01$).

Conclusions: Among the four SWI/SNF factors evaluated, ARID1A and SMARCA2 were the only proteins found to exhibit loss of expression in HCC. Further, SMARCA2 loss was a poor prognostic factor for resectable HCC patients and correlated with early recurrence of disease.

1025 Validation of a Point-based Histologic Scoring System for Hepatocellular Carcinoma (HCC): Application of the Recurrence Risk Assessment Score (RRAS) at a Single Institution

Brian Cox[1], Brent Larson[1], Kevin Waters[1], Danielle Hutchings[1], Stacey Kim[1], Kenechukwu Ojukwu[1], Maha Guindi[1]
[1]Cedars-Sinai Medical Center, Los Angeles, CA

Disclosures: Brian Cox: None; Brent Larson: None; Kevin Waters: None; Danielle Hutchings: None; Stacey Kim: None; Kenechukwu Ojukwu: None; Maha Guindi: None

Background: The RRAS is a histological score to predict post-transplant HCC recurrence risk (PMID: 29649017). It is a point-based system examining tumor architecture, nuclear pleomorphism, cytoplasmic amphophilia, and nuclear-to-cytoplasmic ratio (N:C ratio) to stratify HCC into low, intermediate, and high risk: 0, 1-3, and 4 points, respectively. This study attempted validating of the RRAS outside of the originating institution.

Design: Liver explants with HCC from 2011-2019 were identified in the Institutional pathology database. Cases with 100% tumor necrosis, <0.5 cm of viable residual HCC, or <1 year of follow-up were excluded. A representative slide from the most poorly-differentiated, largest viable tumor was simultaneously examined by 2 hepatopathologists and scored. After a washout period, 50% of cases were re-scored. A third hepatologist independently scored 25 HCCs for interobserver concordance. Multiple binomial logistic regression analyses were performed on SPSS v28.

Results: A final cohort of 107 cases comprising 15 recurrences (14%) were identified. Six of the 15 recurrences had high-risk RRAS scores of 4. Median follow-up was 51 months and median time to recurrence was 13 months. Patients with HCC recurrence had significantly more tumors ($p=0.004$), more poorly differentiated HCCs ($p=0.002$), a history of prior locoregional therapy ($p=0.019$), higher T stage ($p<0.001$), and a higher incidence of lymph-vascular invasion ($p<0.001$). The mean aggregate tumor bed size was significantly larger in the recurrence cohort ($p=0.018$), but the size of the largest single focus and aggregate viable tumor

were not significantly different. Inter- and intra-observer agreement of the RRAS was moderate (Kappa 0.48, p<0.001) and very good (Kappa 0.72, p<0.001), respectively. Multivariate regressions confirmed vascular invasion as the strongest predictor of recurrence (OR: 30.9, p<0.001). In a univariate analysis of the RRAS, HCCs with an RRAS of 4 were associated with recurrence (OR 10.6, p=0.001). The area under the ROC curve was 0.828 (p<0.001): an excellent level of discrimination. Additionally, high-risk scores were significantly associated with vascular invasion (p=0.001, OR: 12.2).

Recurrence Risk Assessment Score	
Architecture	Score
Trabecular or Acinar	0
Scirrhous or Solid	1
Nuclear to Cytoplasmic Ratio	
<50	0
≥50	1
Nuclear Pleomorphism	
Absent	0
Present	1
Cytoplasm	
Eosinophilic	0
Amphophilic	1

Cohort Demographics and Simple Contrasts

	Male		Female		T-Test
	N	Mean	N	Mean	p-value
Age at Explant	80	59.76	27	62.07	0.131

	No Recurrence		Recurrence		T-Test
	Mean	Median	Mean	Median	p-value
Size of Largest HCC (cm)	2.5	2.0	3.7	3.0	0.138
Aggregate Tumor Bed (cm)	5.0	4.0	11.0	7.0	0.018
Aggregative Viable Tumor (cm)	3.1	2.7	7.3	3.5	0.076

	No Recurrence		Recurrence		Chi-Squared p-value
Total Number of HCCs	N	%	N	%	0.004
1	30	32.6	2	13.3	
2	26	28.3	1	6.7	
3	15	16.3	4	26.7	
4	9	9.8	1	6.7	
5+	12	13.0	7	46.7	

Tumor Differentiation	N	%	N	%	0.002
Well	12	13.0	0	0.0	
Mod	72	81.5	9	60.0	
Poor	8	8.0	6	40.0	

Locoregional Therapy	N	%	N	%	0.019
None	34	37.0	1	6.7	
Present	58	63.0	14	93.3	

T-stage	N	%	N	%	<0.001
T1	30	32.6	1	6.7	
T2	58	63.0	8	53.3	
T3	4	4.3	3	20.0	
T4	0	0.0	3	20.0	

Vascular Invasion	N	%	N	%	<0.001
None	84	91.3	3	20.0	
Present	8	8.7	12	80.0	

Recurrence Score	N	%	N	%	0.001
0	13	14.1	1	6.7	
1	31	33.7	1	6.7	
2	27	29.3	3	20.0	
3	15	16.3	4	26.7	
4	6	6.5	6	40.0	

Risk Stratification	N	%	N	%	0.001
Low	13	14.1	1	6.7	
Intermediate	73	79.3	8	53.3	
High	6	6.5	6	40.0	

Conclusions: This is the first study to validate the RRAS at an outside Institution. It confirms that vascular invasion remains the most significant predictor of recurrence of post-transplant HCC. However, in cases where limited HCC sampling is performed, a high-risk RRAS may serve as an adjunct tool to predict recurrence.

1026 Clinico-Pathological Correlation of Porto-sinusoidal Vascular Disease in Post-Liver Transplant Patients

Tony El Jabbour[1], Thomas Schiano[2], Stephen Ward[3], Swan Thung[3], Maria Isabel Fiel[3]
[1]Mount Sinai Hospital, New York, NY, [2]Mount Sinai Medical Center, New York, NY, [3]Icahn School of Medicine at Mount Sinai, New York, NY

Disclosures: Tony El Jabbour: None; Thomas Schiano: None; Stephen Ward: None; Swan Thung: None; Maria Isabel Fiel: None

Background: Non-cirrhotic portal hypertension (NCPH) is characterized by portal hypertension (PH) without cirrhosis. NCPH could manifest histologically by obliterative portal venopathy (OPV), characterized microscopically by portal vein dystrophy (dilatation, herniation or shunting) and/or phlebosclerosis. The recently coined term “Porto-sinusoidal vascular disease” (PSVD) broadens the spectrum of these hepatic vascular pathological changes to include patients without PH who are found to have OPV features on liver needle biopsies. The significance of PSVD features in post liver transplantation (LT) biopsies has not yet been elucidated. We aim to describe the clinical and histological features of PSVD occurring in the post-transplant setting.

Design: We used the Mount Sinai pathology database to search for the key terms “liver allograft” and OPV for liver biopsies over the last 10 years and obtained clinical data from the medical record for the patients.

Results: Our study consisted of 10 patients (mean age: 33, range: 5–62 years, 3 males and 7 females). The average time from LT to the biopsy was 12 years. Microscopically, 40% of our cases showed mixed features of portal venous dystrophy and phlebosclerosis. The remaining cases showed only one end of the histologic spectrum (40% portal venous dystrophy only; 20% phlebosclerosis only). Nodular regenerative hyperplasia (consistent of alternation of thick and thin hepatocytes plates with sinusoidal dilatation) occurred concurrently in 50% of cases. Bile duct loss was confirmed by CK7 in 50% of cases. However, in 2 cases only (20%), the degree of ductopenia exceeded 50% and a diagnosis of chronic ductopenic rejection was ultimately rendered. C4d staining was performed in 5 cases, and was positive in 2 cases (20%) supporting the diagnosis of antibody-mediated rejection (AMR). Features of acute cellular rejection (ACR) were not seen in any case. Clinically, 80% of cases presented

with elevated alkaline phosphatase (with only 2 cases having concurrent elevations of aminotransferases). Seventy percent of our cases had associated thrombocytopenia at the time of the biopsy.

Conclusions: PSVD can be found on post-LT biopsies and always has other associated histopathology. It is associated with thrombocytopenia and in some patients bile duct loss and alkaline phosphatase elevation. These are all features of AMR, thus the potential association of PSVD with the ultimate development of AMR should be established with a larger cohort.

1027 Clinicopathologic Characteristics of Hematologic Malignancies of the Liver

David Escobar[1], Anika Nerella[2], Jennifer Rytych[3], Rebecca Obeng[1], Juehua Gao[4], Guang-Yu Yang[2], Maryam Shirazi[5], Yi-Hua Chen[4], Yue Xue[1]

[1]Northwestern University Feinberg School of Medicine, Chicago, IL, [2]Northwestern University, Chicago, IL, [3]McGaw Medical Center of Northwestern University, Chicago, IL, [4]Northwestern Memorial Hospital, Chicago, IL, [5]Tempus Labs, Chicago, IL

Disclosures: David Escobar: None; Anika Nerella: None; Jennifer Rytych: None; Rebecca Obeng: None; Juehua Gao: None; Guang-Yu Yang: None; Maryam Shirazi: None; Yi-Hua Chen: None; Yue Xue: None

Background: Diagnosis of hepatic hematologic malignancy may be challenging, especially in core biopsy specimens. Correct diagnosis of liver involvement by hematologic malignancies is important for adequate clinical staging and appropriate treatment selection. In this study, we report the clinicopathologic characteristics of a single-institution cohort of hepatic hematologic malignancies, with special emphasis on core biopsy specimens.

Design: Forty-two cases of hepatic hematologic malignancies were retrieved from the pathology database. H&E slides were reviewed for the morphologic patterns of involvement. Demographic, clinical and radiologic data were extracted from the electronic medical record.

Results: The clinical characteristics and spectrum of hematologic malignancies are shown in Table 1. Three cases (7.1%) were primary to liver and 39 (92.9%) showed secondary involvement. Most patients presented with non-specific symptoms, but with elevated liver enzymes (38/42, 90%). Morphologically, the cases were categorized as “Non-Subtle” (29 cases) and “Subtle” patterns (13 cases). Among the cases with “Non-subtle” pattern, 20 (69%) showed mass-like growth or effacement of liver, mimicking carcinoma, melanoma, small cell carcinoma, malignant spindle cell neoplasm, or inflammatory pseudotumor/IgG4-associated disease (Figure 1). Nine (31%) cases showed a diffuse, infiltrative pattern, which could be misdiagnosed as acute liver injury secondary to viral infection, medication or autoimmune hepatitis (Figure 2). Thirteen cases were classified as “Subtle” on histology, including portal/peri-portal infiltrates (6), sinusoidal infiltrates (5), or non-zonal infiltrates (2). These patterns could be easily interpreted as medical liver diseases (viral/autoimmune/medication, biliary process and granulomas hepatitis) or even considered as normal (Figure 2). Fifty-six percent of the cases (23/41) were missed on the imaging. As expected, “Subtle” patterns were associated with a much lower rate of detection on radiographic imaging compared to “Non-subtle” patterns (33% vs. 48%).

Cohort Characteristics		Total (n=42)	Primary (n=3)	Secondary (n=39)
Age (mean, years)		62	60	62
Male:Female Ratio		1.2	2.0	1.2
Clinical Presentation	***Fatigue***	16	0	16
	Abdominal Pain	8	1	7
	Fever	8	0	8
	Cough	6	0	6
	Weight Loss	5	0	5
	Dyspnea	3	0	3
Liver Enzymes (AST, ALT, Alk. Phos.)	***Normal***	4	1	3
	Abnormal	38	2	36
Underlying liver disease	***Normal***	23	0	23
	Fatty Liver	5	0	5
	Hepatitis B	2	0	2
	Hepatitis C	2	1	1
	Cirrhosis	2	0	2
Radiology Findings	***Mass Lesions detected***	18	2	16
	Undetected	23	1	22

Survival (median, months)		16	1	16
Spectrum of Hematologic Malignancies				
Large B cell lymphoma	DLBCL	20	3	17
Small B-cell lymphoma	CLL/SLL	3	-	3
	MZL	1	-	1
	MCL	1	-	1
T-cell lymphoma	Peripheral T cell lymphoma, NOS	2	-	2
	AITL	1	-	1
	ALCL	1	-	1
	Cutaneous gamma-delta T cell lymphoma	1	-	1
	LGL	1	-	1
Burkitt Lymphoma		1	-	1
Hodgkin lymphoma		2	-	2
Acute Leukemia	AML	4	-	4
	B-ALL	1	-	1
Plasma cell myeloma		2	-	2
Immune deficiency lymphoproliferative disorder	Clonal T cell lymphoproliferative disorder	1	-	1

Table Legend: AST=aspartate transaminase, ALT=Alanine transaminase, Alk. Phos.=Alkaline Phosphatase, DLBCL=diffuse large B cell lymphoma, CLL/SLL=chronic lymphocytic leukemia/small lymphocytic lymphoma, MZL=marginal zone lymphoma, MCL=mantle cell lymphoma, AITL=angioimmunoblastic T-cell lymphoma, ALCL=anaplastic large cell lymphoma, LGL=large granular lymphocytic lymphoma, AML=acute myeloid leukemia, B-ALL=B-acute lymphoblastic leukemia

Figure 1 - 1027

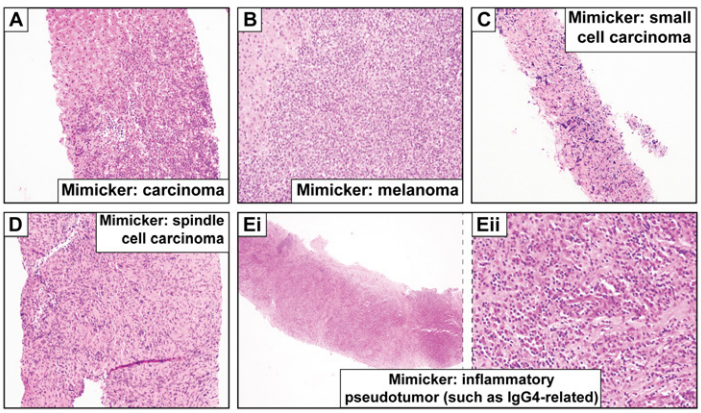

Figure 1. Non-Subtle patterns of liver involvement by hematologic malignancy

Figure 2 - 1027

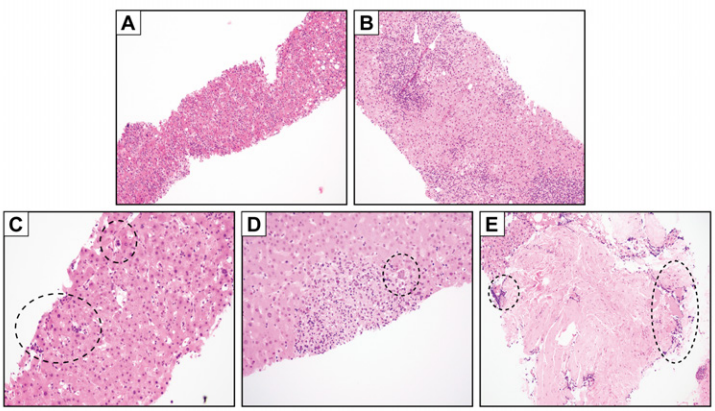

Figure 2. Subtle patterns of liver involvement by hematologic malignancy. Mimicking medical liver disease (viral, medicationinduced, or autoimmune hepatitis) (A-B). Easily missed lesions (C-E).

Conclusions: Secondary involvement of the liver by hematologic malignancies are more common. However, rates of (pre-biopsy) detection on radiographic imaging are very low. Pathologists must be familiar with the spectrum of the morphologic patterns, particularly subtle histologic patterns, in combination with the patients' clinical history, and have a high index of suspicion for hematologic malignancy workup to avoid misdiagnosis.

1028 pTEN Loss of Expression: A Novel Molecular Mechanism in Cryptogenic Hepatocellular Carcinoma in Elderly

Sayak Ghatak[1], Dauod Arif[1], Harmeet Kharoud[1], Oyedele Adeyi[1]
[1]University of Minnesota, Minneapolis, MN

Disclosures: Sayak Ghatak: None; Dauod Arif: None; Harmeet Kharoud: None; Oyedele Adeyi: None

Background: Cryptogenic hepatocellular carcinoma (cHCC) is defined as HCC arising in a patient with no history of known risk factors (Hepatitis B, Hepatitis C, alcoholic or non-alcoholic cirrhosis or adenoma) other than older age. The molecular pathways of HCC in from an infective or cirrhotic etiology has been well characterized and the activation of WNT and hTERT pathways play a major role. However, the molecular pathogenesis of cHCC in elderly population is poorly understood. Phosphatase and tensin homolog (pTEN) is a negative regulator of nuclear translocation of β-catenin and WNT activation, is altered in 30-50% of all HCC. Based on our clinical observations, we hypothesize that in this specific cohort, loss of pTEN is the major pathway for cHCC in the elderly.

Design: After obtaining IRB approval, we identified 27 consecutive cases of cHCC diagnosed in patients >60 years of age at our tertiary care center from 2011-2020. Representative blocks from each case were tested for pTEN expression using immunohistochemistry with proper controls and analyzed using the German semi-quantitative scoring system. Statistical analysis is done using two-tailed Student's t-test (α=0.05).

Results: Out of the 27 patients, 18 patients had adequate tumor tissue for analysis. pTEN immunoreactivity (nuclear and cytoplasmic) was lost in 8 of 18 (44.5%) cases of cHCC (Figure 1). Although there is a trend towards larger tumor, female gender, and slightly younger age at presentation for pTEN- tumors; the only significant difference noticed is absence of poorly differentiated histology (p= 0.05) and better overall 5-year survival (p=0.02) in pTEN- tumors (Table 1). In the pTEN- group, 7/8 (87.5%) patients achieved remission post therapy, with 3/7 (42.8%) developing recurrence, whereas in pTEN+ group, 5/10 (50%) patients achieved initial remission, and subsequently 4/5 patients (80%) developed recurrence.

Table 1: Patient Demographics	pTEN +	pTEN -	p-value
Percentage (%)	55.5	44.5	
Male: Female	4:1	3:5	0.08
Median age at diagnosis	72	68	0.12
Median tumor size (cm)	6.4	8.5	0.4
Grade 3 tumor %	40	0	0.05
Definitive therapy %	70	87.5	0.38
Median Survival (year)	2	5	0.19
Survival %	20	75	0.02

Figure 1 - 1028

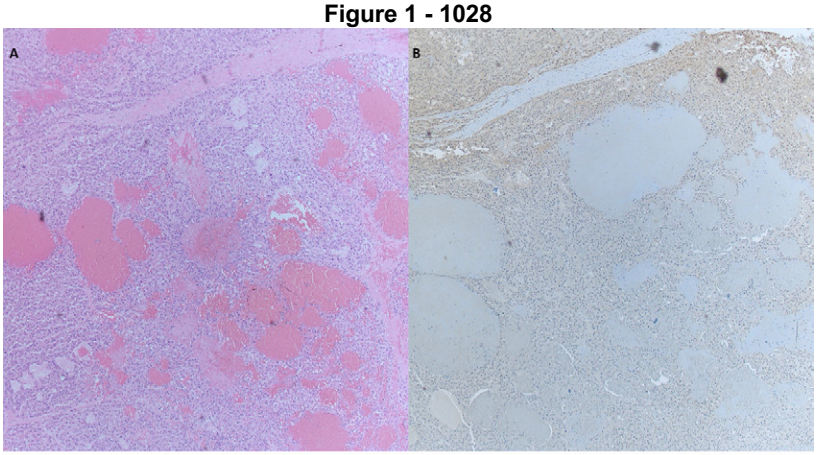

Figure 1 shows loss of pTEN expression in areas of cHCC, compared to retained expression in neighboring non-neoplastic tissue (A- hematoxylin and eosin, B- pTEN immunohistochemistry with DAB and hematoxylin)

Conclusions: Our study demonstrates pTEN loss as a novel molecular event in cHCC in elderly population. Overall, pTEN- seems to be associated with earlier presentation and likely more female patients, as well as better survival and better tumor grade. If confirmed this study provides many opportunities to uncover a novel HCC mechanism in this group, as well as explore screening and treatment options that could include mTOR inhibitors. Additional molecular studies are ongoing to better understand this mechanism.

1029 Immunohistochemical Characterization of Small and Large Duct Cholangiocarcinomas in a Western Cohort

Raymond Gong[1], Karen Matsukuma[1]
[1]*University of California, Davis, Sacramento, CA*

Disclosures: Raymond Gong: None; Karen Matsukuma: *Advisory Board Member*, InCyte Corporation; *Consultant*, Diaceutics, Inc.

Background: Two subtypes of intrahepatic cholangiocarcinoma (iCCA) are now recognized based on morphology. Large duct iCCAs, similar to extrahepatic cholangiocarcinomas (eCCAs), demonstrate abundant desmoplasia, columnar cells, haphazard glands, and mucin, whereas small duct iCCAs are characterized by cuboidal cells, anastomosing or cribriform architecture, dense stroma, and a “replacement growth" pattern. Because these subtypes are associated with distinct molecular pathways and therapeutic options, subtyping them at biopsy or resection could facilitate efficient patient triage. Initial studies have helped characterize the immunoprofile of the two subtypes (particularly important for cases with morphologic features that overlap with both small and large duct types); however, few studies have been undertaken in Western countries where incidence of these subtypes is likely distinct from that in the East.

Design: Cholangiocarcinomas, both intra- and extrahepatic, with available slides and paraffin blocks were used to create a tissue microarray. Original H&E slides were reviewed, and tumors were classified as large or small duct or deemed indeterminate. Stains for CRP, EMA, N-cadherin, mCEA, pCEA, and mucicarmine were performed using standard protocols. Albumin in situ hybridization (ALB-ISH) was performed with RNAscope.

Results: 56 tumors, including 30 iCCAs, 23 eCCAs, and 3 tumors for which the primary site was unclear (either iCCA or hilar eCCA growing into liver), were identified. Thirteen of 30 iCCAs were small duct, 4 were large duct, and 13 were indeterminate. Twenty-one of 23 eCCAs were large duct, 1 was small duct (a 10-cm hilar tumor found to be *IDH2* mutated), and 1 was indeterminate. Expression of N-cadherin, CRP, and ALB-ISH was independently associated with small duct morphology (P<.003). EMA, pCEA, mCEA, and mucicarmine expression was independently associated with large duct morphology (P<.01). Two of the 3 tumors of unclear primary site were small duct and positive for CRP, N-cadherin, and/or ALB-ISH; the third tumor was large duct type and lacked expression of all 3 markers. Eleven of the 13 indeterminate iCCAs were positive for CRP, N-cadherin, and/or ALB-ISH; none of these markers was expressed in the single indeterminate eCCA.

Conclusions: Large duct iCCAs were uncommon in our cohort, limiting conclusions on the immunoprofile of large versus small duct iCCAs. However, small duct iCCAs have an immunoprofile distinct from (large duct type) eCCAs. Thus, in cases in which the primary site is unclear, presence of small duct morphology and/or its immunoprofile may be useful in distinguishing iCCA from eCCA. CRP, N-cadherin, and/or ALB-ISH may be sufficiently specific to identify small duct iCCAs in cases in which morphology is indeterminate. Testing of this hypothesis in a greater number of large duct iCCAs as well as correlation of findings with background liver changes, clinical history, and outcome is underway.

1030 Hepatic Hyaline Globules in Post-Reperfusion Liver Biopsies: Incidence and Lack of Association with Ischemic/Reperfusion Injury

Linh Ho[1], Lindsey Westbrook[1], Patrick Henn[1]
[1]*University of Colorado Anschutz Medical Campus, Aurora, CO*

Disclosures: Linh Ho: None; Lindsey Westbrook: None; Patrick Henn: None

Background: The presence of prominent intracytoplasmic, PAS-positive, diastase-resistant (PASD-positive) hyaline globules in the liver is a characteristic histopathologic finding of alpha-1-antitrypsin (AAT) deficiency; however, they have also been reported in acute and chronic hepatitis, inflammatory liver diseases, as well as in autopsy and cirrhotic livers. We aim to describe the incidence

of PASD-positive globules in the immediate post-reperfusion liver biopsy and assess its association with ischemic/reperfusion injury.

Design: We retrospectively searched the department's anatomic pathology database from January 2017 to June 2021 for patients 18-years-old or older having undergone liver transplantation for conditions unrelated to AAT deficiency and identified those with a post-reperfusion liver biopsy (n=168). The biopsies were categorized into the following degrees of ischemic/reperfusion injury: none (n= 86), minimal (n=35), mild (n=36), moderate (n=7), and severe (n=4). The presence of PASD-positive globules and the result of AAT immunohistochemistry (IHC), if performed, were collected and subsequently correlated using Fisher's exact test.

Results: Of the 168 cases, 6 had PASD-positive globules (3.5%). The presence of PASD-positive globules did not show a significant association with the presence of ischemic/reperfusion injury (p=0.43). Four of six cases had AAT IHC performed, of which three stained positively (75%). The AAT positivity highlighted in these three cases was observed in the presence of minimal to mild ischemic/reperfusion injury. One of the four cases had an absence of PASD-positive globules in the donor biopsy and a subsequent liver biopsy one month after their post-reperfusion biopsy. Additionally, one case had PASD-positive globules two weeks after their post-reperfusion biopsy, with subsequent clinical workup negative for AAT deficiency.

Table 1. Post-reperfusion liver biopsies with PAS-positive, diastase-resistant globules (n=6).

Pre-Transplant Primary Liver Diagnosis	Presence and Degree of Ischemic/Reperfusion Injury in Post-Reperfusion Liver Biopsy	AAT immunohistochemical stain performed (Y/N)	Results of AAT immunohistochemical stain, if performed.
Non-alcoholic steatohepatitis	None	N	-
Hepatocellular carcinoma	None	Y	Negative
Primary biliary cholangitis[1]	Minimal	Y	Positive
End-Stage Alcohol Liver Disease[2]	Minimal	Y	Positive
End-Stage Alcohol Liver Disease	Mild	N	-
Primary Biliary Cholangitis	Mild	Y	Positive

[1]: Donor biopsy with an absence of AAT globules. Subsequent post-1- month liver biopsy showed no alpha-1-antitrypsin globules on PAS-D special stain.

[2]: Subsequent post-2-week liver biopsy showed alpha-1-antitrypsin globules on PAS-D special stain. Clinical follow-up showed low serum AAT levels (80 mg/dL) and normal AAT phenotype (M2M2)

Conclusions: There is a low incidence of PASD-positive hyaline globules in the immediate post-reperfusion liver biopsy (3.5%). The presence of AAT IHC positivity in 1 case with minimal ischemic/reperfusion injury and subsequent biopsy without PASD-positive globules suggests transient AAT globules may occur rarely in the immediate post-reperfusion setting. No association between PASD-positive globules and the presence of ischemic/reperfusion injury was observed in this study. However, additional studies to include a larger cohort are needed to confirm these findings.

1031 Checkpoint Inhibitor Induced Hepatitis: Morphological Patterns and Clinicopathological Correlation

Nupur Jadhav[1], Deepa Patil[2], Stuti Shroff[3], Rahul Jawale[4], Vikram Deshpande[5]
[1]Baystate Medical Center, Springfield, MA, [2]Brigham and Women's Hospital, Harvard Medical School, Boston, MA, [3]Massachusetts General Hospital, Watertown, MA, [4]University of Massachusetts Medical School-Baystate, Springfield, MA, [5]Massachusetts General Hospital, Harvard Medical School, Boston, MA

Disclosures: Nupur Jadhav: None; Deepa Patil: None; Stuti Shroff: None; Rahul Jawale: None; Vikram Deshpande: None

Background: Immune checkpoint inhibitors (ICI) are associated with a spectrum of immune-related adverse events. Herein, we evaluate the morphological patterns and distribution of immune cells and checkpoint proteins in clinically confirmed checkpoint inhibitor-induced hepatitis (CPI-H) and correlate these with clinical and outcome data.

Design: This retrospective study included 25 consecutive patients with CPI-H. The histological features and immunohistochemical markers were evaluated by 3 pathologists. Immunohistochemistry for PD-L1, CD4, CD8, and CD163 was performed. CD4 and CD8

positive T cells were counted in the three most densely infiltrated portal tracts. The number of clusters of ≥5 CD163 and PD-L1-positive immune cells was counted in a 10x field.

Results: Our cohort included 13 male and 12 female patients with mean age of 63 years, and most cases were of melanoma (n=12). Checkpoint inhibitors were either used as monotherapy (n=14) or as a combination of CTLA-4 and PD-1/PD-L1 inhibitors (n=11). Three patterns of injury were identified: 1) predominantly histiocytic (n=11), 2) predominantly lymphocytic (n=11), 3) predominantly steatosis (n=3). Portal and lobular granulomas were exclusive to pattern 1 (n=5). Pattern 1 was associated with increased numbers of CD163 cells (p=0.002) while pattern 2 was associated with increased CD8 positive lymphocytes (p=0.035) cells. There was no statistically significant difference in the CD4:CD8 ratio (p=0.37). Pattern 1 showed higher numbers of PD-L1 positive histiocytes (p=0.001) with the majority of histiocytes positive for PD-L1. Central vein endothelitis was observed in 3 cases (2- pattern 2, 1- pattern 1). All 3 cases with grade 4 transaminitis showed pattern 1 injury. All patients responded to immunosuppressive therapy. There was no correlation between the pattern of injury and age, gender, type of drug, and duration of abnormal LFT after therapy.

Conclusions: Checkpoint inhibitor-induced hepatitis is characterized by 3 patterns of injury: histiocyte rich, lymphocyte-rich and macrovesicular steatosis. The increased density of CD8 and CD163-positive cells in inflammation-rich type 1 and 2 patterns, accompanied by endothelitis, supports an immune-mediated mechanism of injury. The histiocyte-rich pattern of injury raises the possibility of granulomatous hepatitis and appears to be an indicator of more severe parenchymal injury. The mechanistic significance of the PD-L1 positive histiocytes in CPI-H requires further study.

1032 Porto-Sinusoidal Vascular Disease: A Heretofore Unrecognized Manifestation of Sickle Cell Disease?

Pari Jafari[1], Xiaotang Du[2], Gertruda Evaristo[3], Victoria Marcus[4], Xiuli Liu[5], Lei Zhao[6], Maria Westerhoff[7], John Hart[8]
[1]University of Chicago Medicine, Chicago, IL, [2]Barnes-Jewish Hospital/Washington University, Saint Louis, MO, [3]McGill University, Montreal, Canada, [4]McGill University Health Centre, Montréal, Canada, [5]Washington University School of Medicine, St. Louis, MO, [6]Brigham and Women's Hospital, Harvard Medical School, Boston, MA, [7]University of Michigan, Ann Arbor, MI, [8]University of Chicago, Chicago, IL

Disclosures: Pari Jafari: None; Xiaotang Du: None; Gertruda Evaristo: None; Victoria Marcus: None; Xiuli Liu: None; Lei Zhao: None; Maria Westerhoff: None; John Hart: None

Background: Porto-sinusoidal vascular disease (PSVD), a recently proposed histopathologic entity that encompasses a spectrum of often-subtle abnormalities of the hepatic portal tracts and parenchymal architecture, is recognized in a disparate array of clinical conditions. To our knowledge, while various histopathologic findings in sickle cell disease (SCD), such as sinusoidal congestion, are well-delineated, PSVD in SCD has not yet been described. We present the first case series exploring the prevalence and pathophysiology of PSVD in SCD.

Design: The pathology archives of five tertiary medical centers were searched for native liver biopsies from patients with a history of SCD, and pertinent clinical parameters were extracted on chart review. Biopsies were systematically evaluated for features associated with PSVD (Table 1). Cases demonstrating cirrhosis or significant pathology due to chronic liver disease (e.g., hepatitis C infection) were excluded. To further characterize the range of vascular alterations, immunohistochemical (IHC) stains for von Willebrand factor (vWF), CD34, and glutamine synthetase (GS) were performed on selected cases.

Results: Diagnostically adequate liver biopsies from 42 SCD patients (7-67yo; 69% female) were identified. Biopsy indications are summarized in Fig. 1. All biopsies exhibited ≥1 feature associated with PSVD (mean 3.67 features/case; see Table 1). Concurrent hepatic venous pressure gradient elevation (>5 mm Hg) was present in 5 of 10 documented cases. Clinical evidence of portal hypertension (e.g., varices) was present in 23.8% of cases. IHC findings (Fig. 2) were notable for aberrant centrilobular sinusoidal CD34 and vWF staining in all tested samples (Table 1). GS exhibited decreased reactivity in zone 3 hepatocytes in 64.3% of cases, with marked loss in 35.7%.

Table 1. Features of PSVD in SCD: Histopathologic Findings and Immunohistochemical Stain Results.		
Results of Histologic Evaluation (H&E, trichrome, and reticulin stains) [N=42]		
PSVD features	Number of cases (%)	
Obliterative portal venopathy (phlebosclerosis)	26 (61.9)	
Portal vein herniation	23 (54.8)	
Portal tract remnant	17 (40.5)	
Increased number of portal vessels	8 (19.0)	
Portal vein dilatation	9 (21.4)	
Incomplete fibrous septa	17 (40.5)	
Nodular regeneration	11 (26.2)	
Increased number of parenchymal draining vessels	13 (31.0)	
Sinusoidal dilatation	17 (40.5)	
Perisinusoidal fibrosis	10 (23.8)	
Central vein dilatation	3 (7.1)	
Evaluation of IHC Stains [N=14]		
CD34 – aberrant centrilobular sinusoidal vessels	Number of cases (%)	
[score 0-3]	0 [no aberrancy]	0
	1	4 (28.6)
	2	3 (21.4)
	3 [marked aberrancy]	7 (50.0)
von Willebrand factor – aberrant centrilobular sinuosoidal vessels	Number of cases (%)	
[score 0-3]	0 [no aberrancy]	0
	1	8 (57.1)
	2	3 (21.4)
	3 [marked aberrancy]	3 (21.4)
Glutamine synthetase – reduction in zone 3 reactivity	Number of cases (%)	
[score 0-3]	0 [no reduction in reactivity]	5 (35.7)
	1	3 (21.4)
	2	1 (7.1)
	3 [marked reduction in reactivity]	5 (35.7)

Figure 1 - 1032

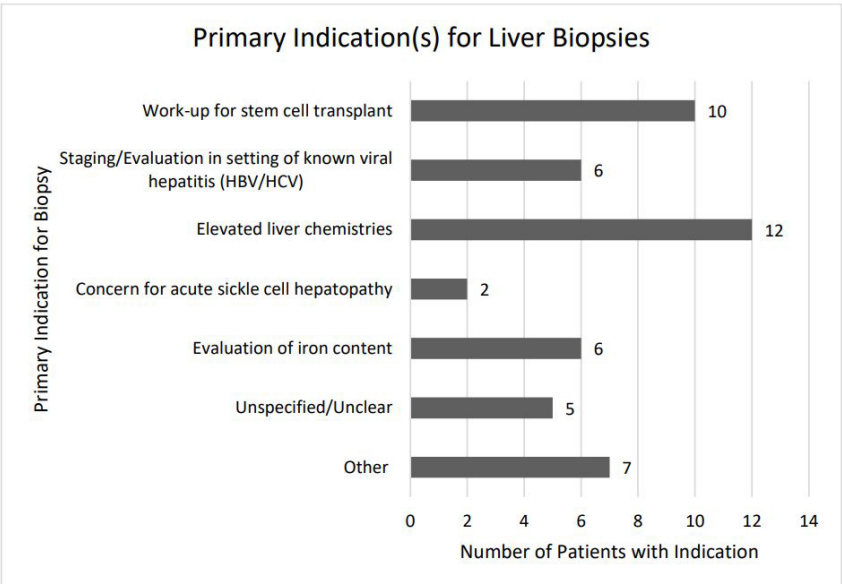

Figure 1. Most common primary indications for biopsy. Multiple overlapping indications occurred in five cases. "Other" included hepatosplenomegaly of unclear etiology and history of hepatic sarcoidosis.

Figure 2 - 1032

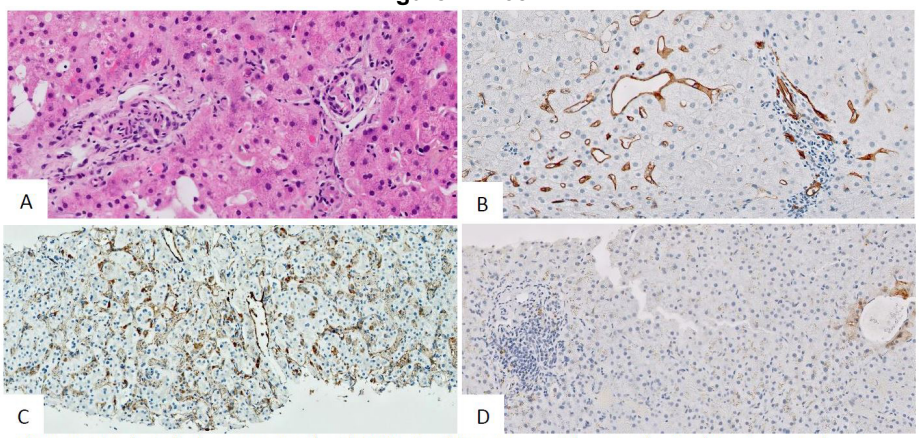

Figure 2. Histologic findings associated with PSVD. **A:** Obliterative portal venopathy involving two portal tracts (H&E). **B-C**: Immunohistochemical staining for CD34 **(B)** and von Willebrand factor **(C)** demonstrates aberrant centrilobular sinusoidal reactivity. **D:** Immunohistochemical staining for glutamine synthetase demonstrates markedly reduced reactivity in zone 3 hepatocytes.

Conclusions: Here, we show for the first time that findings associated with PSVD are highly prevalent in SCD liver biopsies. We posit that chronic erythrocyte sickling results in portal venous and sinusoidal microvascular compromise, with ultimate regression of zone 3 hepatocytes. Although no patient manifested clinically significant portal hypertension unequivocally attributable to these histologic findings, the presence of PSVD may explain, at least in part, the hepatic dysfunction and abnormal liver chemistries observed in this patient population. The histologic features of PSVD, while subtle and prone to over-diagnosis, should be considered when interpreting liver biopsies from SCD patients.

1033 Hepatoportal Sclerosis: A Clinicopathologic Review of 21 Cases

Nazia Khatoon[1], Murli Krishna[1], Jason Lewis[1], Raouf Nakhleh[1]
[1]Mayo Clinic, Jacksonville, FL

Disclosures: Nazia Khatoon: None; Murli Krishna: None; Jason Lewis: None; Raouf Nakhleh: None

Background: Hepatoportal sclerosis is a rare condition that leads to non-cirrhotic portal hypertension and is often unrecognized. Little is known regarding the diagnosis and outcome of such cases with current therapies.

Design: A 20 year retrospective search for the diagnosis of hepatoportal sclerosis was conducted in our surgical pathology files. Twenty one cases were identified and verified by review of the slides. Subsequently, the patients' charts were reviewed for the following: presentation, significant clinical history, liver function tests and other laboratory studies, radiographic studies, histology, treatment and outcome.

Results: The patients had a male predominance (13M; 8F). The majority of patients were in the 5th and 6th decade but had a wide age range (18-83). Only 2 patients were referred with the diagnosis of hepatoportal sclerosis. The remaining patients had signs or symptoms of portal hypertension including ascites, esophageal varices, and splenomegaly. 4 patients had evidence of hepatic encephalopathy, 2 had elevated liver function tests and 2 had no significant symptoms. Past relevant history included: 5 patients with malignancy treated with chemotherapy, 12 patients with autoimmune disorders, 4 patients with congenital vascular anomalies, and 2 with HIV. The only consistent finding in LFT's was elevation of alkaline phosphatase in 10 patients (138-417U/L). Hepatic venogram pressure measurement demonstrated elevated gap pressures in 12 of 15 patients (80%). Histologic diagnosis was made on biopsy in 13 patients. Initial diagnosis was made on the explanted livers in 6 cases (4 with prior biopsies). Additional histologic findings demonstrated mild portal fibrosis (20 patients) and steatohepatitis (1 patient). Nine patients were transplanted, five of whom remain alive and well. Two patients were treated with transjugular intrahepatic portosystemic shunting (TIPS). The remaining patients were treated symptomatically. Four patients were lost to follow up.

Conclusions: 1. Most patients had significant past medical history that may have contributed to the development of hepatoportal sclerosis, such as chemotherapy, autoimmune disorders, and vascular congenital conditions. 2. Although this series is small, transplantation appears to be a viable treatment in patients with advanced disease. 3. Hepatoportal sclerosis should be considered when evaluating liver specimens from patients with non-cirrhotic portal hypertension.

1034 Retinal Vasculopathy and Cerebral Leukoencephalopathy with Systemic Manifestations (RVCL-S): Vascular Disease Beyond Nodular Regenerative Hyperplasia (NRH) in the Liver

Pooja Khonde[1], Deyali Chatterjee[2], Elizabeth Brunt[3], John Atkinson[4], Jonathan Miner[5]
[1]Barnes-Jewish Hospital/Washington University, St. Louis, MO, [2]The University of Texas MD Anderson Cancer Center, Houston, TX, [3]Washington University School of Medicine, St. Louis, MO, [4]Washington University in St. Louis, St. Louis, MO, [5]Perelman School of Medicine, Hospital of the University of Pennsylvania, Pennsylvania, PA

Disclosures: Pooja Khonde: None; Deyali Chatterjee: None; Elizabeth Brunt: *Consultant*, Cymabay, Arrowhead, Perspectum Diagnostics; *Advisory Board Member*, Pfizer; *Consultant*, Histoindex, Intercept Pharmaceuticals; John Atkinson: None; Jonathan Miner: None

Background: RVCL-S is caused by frame-shift mutations in the approximately 80 amino acid carboxy-tail of the major mammalian intracellular 3'-5' exonuclease 1 (*TREX-1*). Hepatic lesions are almost always a part of the clinical pathologic findings with elevated alkaline phosphatase (ALP). Several cases describe NRH.

Design: Eleven autopsy liver specimens from 3 families with the most common mutation in *TREX-1* (V235Gfs*6) were reviewed. Histochemical (Hematoxylin and eosin; trichrome, reticulin, PAS-d) stains were augmented with IHC: CD34, Glutamine Synthetase (GS), K7. Five were selected for additional IHC CD31 and aSMA and compared to livers from similar years post-mortem.

Results: The 5 men and 6 women died at median age of 50 years, all with progressive neurologic and retinal disease. 7/11 had elevated ALP, one had alcoholic use disorder (AUD), and one disseminated cryptococcal infection. The gross descriptions documented liver atrophy in four. No portal vein thrombosis was observed. Liver histologic features were noted for their inhomogeneity; all vascular structures were affected. No thrombi were present. Portal veins (PV) were fibrosed or extruded; portal tracts (PT) were rounded or elongated; some were only small dyads of bile duct and artery. Hepatic veins (HV) were eccentrically fibrosed; GS highlighted approximation or adherence to PT. Sinusoids were enlarged, fibrotic or ruptured in areas of cord atrophy or loss. Hepatic artery branches were thickened by acellular mural deposits. Acellular fibrous bands extended haphazardly from many PT. Sclerotic nodules were present along some, and around some fibrotic CV's. CD31 was present within one. Nine cases had foci of NRH; 2 cases had dysplastic-like clonal proliferations. Lesions of AUD were not appreciated. Bile ducts were unremarkable. Periportal K7 positive single cells or doublets were noted in all cases. CD34 expression varied from normal to all of zone 1 to confluent foci within approximated structures. CD31 was present in all sinusoids but in regions of collapse was condensed, granular and filled the sinusoids. aSMA similarly was overly condensed in collapse and showed abundant HSC nuclear reactivity. HE, trichrome, reticulin, PASd, K7, CD31, CD34, aSMA were unremarkable in the controls.

Conclusions: The extensive changes in livers with *TREX-1* mutation involve all vascular structures. The findings of this study validate inclusion of vascular liver involvement in RVCL-S beyond NRH.

1035 Genomic Analysis in the Categorization of Poorly Differentiated Primary Liver Carcinomas

Alexander Kikuchi[1], Nancy Joseph[1], Sanjay Kakar[1]
[1]University of California, San Francisco, San Francisco, CA

Disclosures: Alexander Kikuchi: None; Nancy Joseph: None; Sanjay Kakar: None

Background: A subset of primary liver carcinomas (PLC) cannot be classified within existing categories of hepatocellular carcinoma (HCC), intrahepatic cholangiocarcinoma (iCCA) or combined HCC-iCCA based on morphology and immunohistochemistry (IHC). Tumors that fall in these categories often include those with morphologic resemblance to HCC but lacking hepatocellular marker expression, tumors with ambiguous morphology that co-express hepatocellular and cholangiocytic markers, and undifferentiated carcinomas with no discernible line of differentiation on morphology or IHC. Characteristic mutational profiles have been reported in HCC (*TERT* promoter/*CTNNB1* mutations) and iCCA (*IDH1/IDH2/PBRM1* mutations, *FGFR2* fusion). This study examines the role of genomic analysis in categorization of these tumors.

Design: Genomic analysis using a capture-based NGS assay was done in 11 PLCs that could not be definitely classified as HCC or iCCA based on morphology and IHC.

Results: The genomic profile provided information for better categorization of 9/11 (82%) cases. Mutations in *TERT* promoter were seen in 5 (46%) cases and strongly favored HCC. *IDH1* mutation and *PBRM1* mutation was observed in 1 case each and strongly favored iCCA. *BRCA1* mutation and *ERBB2* mutation was seen in 1 case each; while not characteristic of either HCC or ICCA,

these are more common in iCCA. Genomic changes in 2 cases (*MYC* amplification, *CDKN2A* deletion) did not help in pointing towards HCC or iCCA.

Case	Morphology/IHC	Diagnostic difficulty	Mutations	Conclusion
1	H&E: PDC with indeterminate features; Hep, Arg neg, GPC+; CK7+	GPC3+ suggests HCC but overall findings not diagnostic	*TERT* promoter, *TP53*, *RB1*	Strongly favors HCC
2	H&E: hepatoid features, no glands; Arg, Hep, GPC neg; CK7/CK19+	Morphology suggests HCC but hepatocellular markers negative	*TERT* promoter, *TP53*, *MET* (amplification)	Strongly favors HCC
3	H&E: PDC with sarcomatoid areas; Arg, GPC neg, Hep focal+; CK7/CK19+	No definite differentiation; Hep too focal for definite HCC diagnosis	*TERT* promoter, *TP53,* CCND1, FGF19 amplification	Strongly favors HCC
4	H&E: PDC with indeterminate features; Arg, Hep, GPC neg; CK19+, CK7 neg	No definite differentiation	*TERT* promoter, *TP53*	Strongly favors HCC
5	H&E: PDC with indeterminate features; Arg, GPC neg; CK19+	No definite differentiation	*TERT* promoter	Strongly favors HCC
6	H&E: PDC with indeterminate features; Arg, GPC neg, Hep+; CK7/CK19+	Hep+ and CK7/19+, morphology not typical of HCC, no glands	*IDH1*	Strongly favors iCCA
7	HE: Hepatoid with vague gland-like features; Hep/Arg/GPC neg; CK7/CK19+	Suggestive of HCC, but vague glands and negative hepatocellular markers	*PBRM1*	Strongly favors iCCA
8	HE: Undifferentiated high grade carcinoma; Hep/Arg/GPC neg; CK7/CK19+	No definite differentiation	*TP53*, *BRCA1*	Not characteristic; favors iCCA
9	H&E: Hepatoid features, no glands; Hep/Arg/GPC neg; CK7/CK19+	Morphology suggests HCC but hepatocellular markers negative	*ERBB2*; *CDKN2A/2B* (deep deletion)	Not characteristic; favors iCCA
10	H&E: PDC with indeterminate features; Hep neg; CK7+	No definite differentiation	*MYC* amplification	Indeterminate for HCC vs iCCA
11	H&E: PDC with indeterminate features; Hep, Arg, GPC neg; CK7/CK19+	No definite differentiation	*ERFF1*; *CDKN2A/2B* (deep deletion)	Indeterminate for HCC vs iCCA

Conclusions: Genomic changes were helpful in classifying 82% of poorly differentiated/undifferentiated primary liver carcinomas providing strong evidence for HCC (46%;5 cases) and iCCA (18%; 2 cases), and changes suggestive of ICCA in an additional 18% (2 cases). Genomic changes are not specific, but can provide valuable diagnostic clues in selected morphologically and immunohistochemically unclassifiable cases. Given the immense treatment implications of HCC vs iCCA, routine use of genomic analysis in diagnostically challenging settings should be considered.

1036 Neovascular PSMA Expression Is More Specific than CD34 for Differentiating Hepatocellular Carcinoma from Benign and Precursor Hepatic Lesions

Michel Kmeid[1], Young Nyun Park[2], Taek Chung[2], Georgi Lukose[3], Rupinder Brar[1], Luz Sullivan[1], Hwajeong Lee[1]
[1]Albany Medical Center, Albany, NY, [2]Yonsei University College of Medicine, Seoul, South Korea, [3]Weill Cornell Medicine, New York, NY

Disclosures: Michel Kmeid: None; Young Nyun Park: None; Taek Chung: None; Georgi Lukose: None; Rupinder Brar: None; Luz Sullivan: None; Hwajeong Lee: None

Background: Accurate classification of well-differentiated hepatocellular neoplasms can be challenging especially in core biopsies. CD34, a vascular marker, has been used to differentiate hepatocellular carcinoma (HCC) from benign hepatic mimickers but with suboptimal specificity. Prostate-specific membrane antigen (PSMA) has been shown to highlight tumor-associated neovasculature in many non-prostatic solid tumors including HCC. We assessed the specificity and accuracy of PSMA in identifying HCC by comparing its staining pattern to that of CD34.

Design: Archived 121 hepatectomy/explant specimens (68 HCC, 31 hepatocellular adenoma (HA), 24 dysplastic nodule (DN, 4-low grade, 20-high grade)) were retrieved and H&E slides were reviewed. CD34 and PSMA immunostains were performed on representative FFPE tissue blocks showing tumor/liver interface. For CD34, the staining was classified as negative (exclusive staining in portal/periportal vasculature), incomplete (staining <70% of lesional sinusoidal endothelium) and complete (≥70% of lesional sinusoids staining). Only complete CD34 staining was considered positive. For PSMA, capillarized sinusoidal staining

involving >5% of tumor area was considered positive. Sensitivity, specificity, accuracy and positive (PPV) and negative (NPV) predictive values were calculated for both antibodies. Staining in each subgroup was compared using appropriate tests with significance defined as p<0.05.

Results: 22.1% of HCC were grade 1. CD34 and PSMA staining was significantly higher in HCC compared to HA and DN (p<0.001). In 23.5% of HCC, CD34 staining was absent at the periphery of the tumor (rim sparing). 58.1% of HA and 4.2% of DN were positive for CD34. CD34 had a 98.5% sensitivity but a 64.8% specificity in identifying HCC. PSMA was less sensitive (80.9%) but had a 100% specificity and 100% PPV. PSMA was negative in all HA and DN. When grade 1 HCC were only considered, the sensitivity of CD34 and PSMA remained high (93.3% and 80.0% respectively) in diagnosing HCC. PSMA was also more accurate than CD34 (accuracy 89.4%). In all lesions, PSMA staining correlated with that of CD34 (p<0.05). **Table 1**

	CD34		PSMA	
	%	95% CI	%	95% CI
Sensitivity	98.53	92.08-99.96	80.88	69.53-89.41
Specificity	65.45	51.42-77.76	100	93.51-100
Positive Predictive Value	77.91	71.00-83.55	100	-
Negative Predictive Value	97.30	83.60-99.61	80.88	72.18-87.34
Accuracy	83.74	76.01-89.78	89.43	82.60-94.25

CI: Confidence Interval

Conclusions: Neovascular PSMA expression is more specific and accurate than CD34 for differentiating HCC from benign and precursor hepatic lesions. Negative PSMA staining, however, does not exclude the diagnosis of HCC especially in core biopsies. Likewise, rim sparing in CD34 stain can be a diagnostic pitfall in HCC core biopsies.

1037 SEPT9 Expression in Hepatocellular Neoplasm: an Immunohistochemical Study of Hepatocellular Adenoma, Dysplastic Nodule and Hepatocellular Carcinoma

Michel Kmeid[1], Young Nyun Park[2], Taek Chung[2], Richard Pacheco[1], Mustafa E Arslan[1], Hwajeong Lee[1]
[1]Albany Medical Center, Albany, NY, [2]Yonsei University College of Medicine, Seoul, South Korea

Disclosures: Michel Kmeid: None; Young Nyun Park: None; Taek Chung: None; Richard Pacheco: None; Mustafa E Arslan: None; Hwajeong Lee: None

Background: SEPT9, a member of the septin family, is overexpressed in variable human malignancies, possibly via impaired methylation of the SEPT9 gene promoter. Methylated SEPT9 (mSEPT9) in plasma is a promising biomarker for colorectal cancer (CRC) screening, but its application in hepatocellular carcinoma (HCC) has been limited. Also, SEPT9 expression in liver tumors by immunohistochemistry (IHC) has not been extensively studied.

Design: 164 hepatectomies and explants with 68 HCCs, 31 hepatocellular adenoma (HA)s, 24 dysplastic nodule (DN, 4 low grade, 20 high grade)s and 41 metastasis were retrieved. Archived H&E and IHC (SATB2, CK19, CDX2 and CDH17 for HCC) slides were reviewed for pathological parameters. SEPT9 stain was performed on representative FFPE tissue blocks showing tumor/liver interface. The extent of membranous/cytoplasmic staining was recorded and >5% tumor staining was considered positive. Electronic medical records were reviewed for demographics, risk factors, tumor size, AFP levels at diagnosis, T stage and oncologic outcomes (mean follow up 55.7 (4 – 210) months). SEPT9 expression was assessed in each tumor type and the association of staining with clinicopathological parameters and outcomes was evaluated with significance defined as p<0.05.

Results: Percentage of SEPT9 positivity differed significantly among HA (3%), DN (0%), HCC (32%) and metastasis (83%, p<0.001). Compared to patients with SEPT9- HCC, those with SEPT9+ HCC were older (70.3 vs. 62.5 years, p=0.01), had lower AFP levels at diagnosis (1861 vs 2297 ng/mL, p=0.04), and had a higher percentage of T2 tumors at diagnosis (45% vs. 20%, p=0.026). The extent of SEPT9 staining correlated with tumor grade (r_s=0.30, p=0.013) and extent of SATB2 staining (r_s=0.28, p=0.021). Patients with SEPT9+ HCC had shorter metastasis free survival compared to their SEPT9- counterparts (p=0.028). No associations were found between SEPT9 staining and tumor size, risk factors, CK19, CDX2 and or CDH17 expression, METAVIR fibrosis stage and overall survival in the HCC cohort.

Conclusions: Similar to CRC, SEPT9 is likely implicated in liver carcinogenesis. Its expression in benign and precursor liver lesions is virtually absent. SEPT9 staining by IHC may prove helpful as a diagnostic marker when evaluating primary hepatocellular

neoplasms with prognostic ramifications. Likewise, mSEPT9 measurement in liquid biopsies may be used as a potential biomarker to identify new and recurrent HCC in a subset.

1038 A Novel Digital Zonation Tool Based on the Voronoi Theory of the Classic Lobular Architecture of the Liver

Chun Lau[1], Bahman Kalantari[1], Kenneth Batts[2], Linda Ferrell[3], Scott Nyberg[4], Christopher Hartley[4], Rondell Graham[4], Roger Moreira[4]

[1]Rutgers University, New Brunswick, NJ, [2]Allina Health Laboratories, Minneapolis, MN, [3]University of California, San Francisco, San Francisco, CA, [4]Mayo Clinic, Rochester, MN

Disclosures: Chun Lau: None; Bahman Kalantari: None; Kenneth Batts: None; Linda Ferrell: None; Scott Nyberg: None; Christopher Hartley: None; Rondell Graham: None; Roger Moreira: None

Background: The precise characterization of the lobular architecture of the liver has been subject of investigation since the earliest historical publications, with regular hexagons serving as the quintessential representation of the basic histologic unit in the classic lobule model. In practice, the two-dimensional liver lobular microstructure is known to be significantly more variable and complex, and a more comprehensive theory to describe the hepatic microanatomy is yet to be proposed. Our aim was to evaluate whether the mathematical/geometric concept of Voronoi diagrams can be used to describe the classic lobular architecture.

Design: We examined tissue samples of normal porcine (n=10) and human (n=10) livers with histochemical stains and glutamine synthetase (GS) immunostain. Whole slide images were used for histologic annotations of portal tracts and GS-positive central zones and for digital image analysis, using QuPath v-.2.0-m12 and Fiji ImageJ 1.52p. Voronoi diagram were generated using four different methods. Histologic images with superimposed Voronoi diagrams were analyzed using Apache Groovy 3.0 / Java 14.

Results: The Voronoi model described the two-dimensional organization of the hepatic classic lobules with overall accuracy of nearly 90% in both porcine and human livers (Figure 1, A-C). We have also designed a Voronoi-based algorithm that divides human lobules into three concentric zones, analogous to the acinar model of Rappaport, which showed an overall zonal accuracy of nearly 90%. This digital lobulation and zonation tool has then been adapted to be used in QuPath, an open-source software. While a glutamine synthetase immunostain is needed for the initial acquisition of the algorithm, the resulting lobulation/zonation digital framework can automatically be superimposed onto any stains performed on sequential levels (H&E, trichrome, or immunostains) utilizing homotopy matrices for zonal analysis of various histologic features (Figure D-I).

Figure 1 - 1038

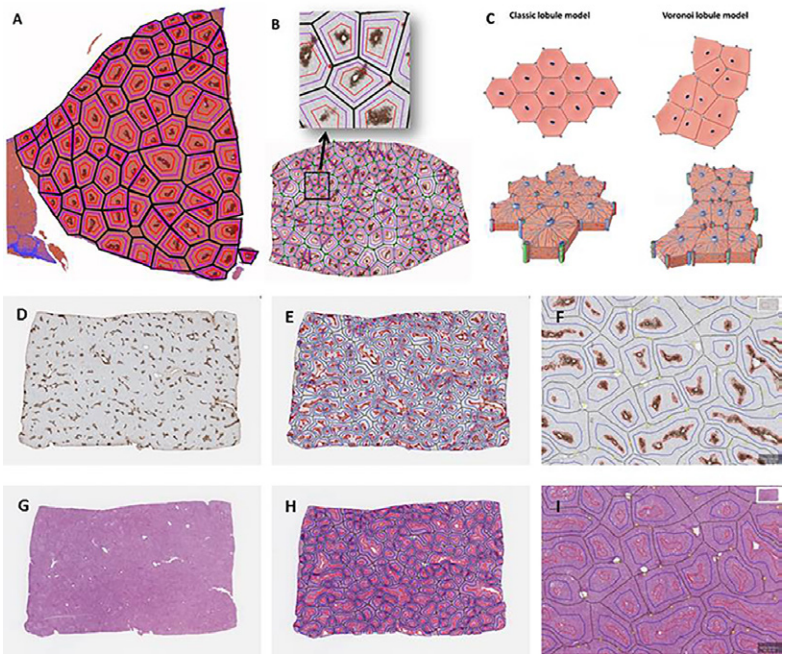

Conclusions: We have presented histologic and mathematical evidence that Voronoi diagrams are the basis of the two-dimensional organization of the normal hepatic micro-architecture. Utilizing this principle, we have designed a digital tool that allows for quantitative assessment of various histologic features based on precisely defined, customizable zonal delineation. Our findings represent a novel concept in our understanding of the histologic structure of the liver, with potential applicability in both diagnostic pathology and research.

1039 The Role of Routine Biopsy of the Background Liver in the Management of Hepatocellular Carcinoma

Seohyuk Lee[1], Muhammad Ahmed[2], Tamar Taddei[1], Dhanpat Jain[1]
[1]Yale School of Medicine, New Haven, CT, [2]Yale New Haven Hospital, New Haven, CT

Disclosures: Seohyuk Lee: None; Muhammad Ahmed: None; Tamar Taddei: None; Dhanpat Jain: None

Background: Hepatocellular carcinoma (HCC) treatment options depend not only on tumor characteristics, but also on the status of the background liver – the presence of cirrhosis often limits the potential for resection or necessitates liver transplantation listing. However, assessment of liver disease and the associated decisions on management are typically made solely using clinical parameters despite the lack of reliability in some cases. To date, the role of biopsy of the non-tumoral parenchyma in the evaluation of liver masses has not been assessed. The objective of this study was to determine the influence of background liver biopsies on HCC management.

Design: The pathology database at a large university hospital was searched between 2013 and 2018 for all instances of when a separate biopsy of the background non-tumoral liver was performed concurrently with or within 6 months of the HCC biopsy. Patients were evaluated for demographics, tumor staging at diagnosis, presence of background chronic liver disease, treatment proposed prior to biopsy, and impact of biopsy results on management.

Results: A total of 127 paired liver biopsies were identified of which the relevant clinical information was available in 104 cases. In the study group, 22% were female; the median age was 64 years; and most were of earlier HCC stages at diagnosis (Barcelona clinic liver cancer [BCLC] stages 0-A: 70%) than of intermediate (BCLC B: 17%) or later stages (BCLC C-D: 13%). 10 of 11 patients for whom cirrhosis status was clinically unclear were confirmed to have cirrhosis on biopsy; 1 patient who was not clinically suspected was discovered to have cirrhosis, and 1 patient did not have cirrhosis despite clinical suspicion. Treatment was altered by the background parenchymal findings for 6 patients (6%): management was more aggressive for 2 patients in whom surgical resection was precipitated and was less aggressive for 4 patients, 3 of whom were de-escalated from undergoing chemoembolization planned prior to biopsy findings.

Conclusions: A background liver biopsy can significantly impact the management of a small subset of HCC patients, especially those with early disease. It is particularly important since resection and transplant are the only curative options in such patients, and the number of donors are limited. In a select population of HCC patients, background liver biopsy should be considered concurrently with the biopsy of the mass, especially if no recent biopsies of the background liver are available.

1040 Rejection Treatment Before Liver Biopsy Decreases Portal Inflammation but Does Not Impact Bile Duct Injury

Nicole Leonard[1], Gillian Hale[1], Katie Boylan[2], Zachary Dong[1], Kimberley Evason[1]
[1]The University of Utah, Salt Lake City, UT, [2]University of Utah / ARUP, Salt Lake City, UT

Disclosures: Nicole Leonard: None; Gillian Hale: None; Katie Boylan: None; Zachary Dong: None; Kimberley Evason: None

Background: Liver biopsy is essential for management in liver transplant patients with rising transaminases, low tacrolimus troughs, and other features suspicious for acute cellular rejection (ACR). As more patients are transplanted for non-infectious indications, it has become increasingly common for them to receive immunosuppression treatment for presumed ACR pre-biopsy. Treatment may alter the classic histologic triad of ACR's mixed portal inflammation, endothelialitis, and bile duct damage, but this effect remains poorly described. The purpose of this study was to compare allograft liver biopsies in pre-treated versus non-treated patients.

Design: This retrospective study included electronic medical record review and histologic slide evaluation for 71 liver transplant biopsies performed for suspected ACR from 2018-2021. In 40 cases, the patient was pre-treated for presumed ACR with steroids, thymoglobulin, or other increased immunosuppression; no treatment was given prior to biopsy in the remaining 31 control cases. A representative H&E-stained slide from each case was reviewed independently in a blinded fashion by three attending hepatic pathologists. Cases were graded according to the Banff system and assigned a Rejection Activity Index (RAI) score. Cholestasis, ductular reaction, lobular activity, steatosis and predominance of eosinophils, neutrophils, and plasma cells were assessed semi-quantitatively. For each histologic feature, mean and median scores were calculated among the three pathologists and the statistical differences between the pre-treated and non-treated groups were determined. Kappa values for interobserver variability were assessed for each feature.

Results: Patients who were not pre-treated had significantly more portal inflammation (p=0.0022), more prominent eosinophils (p=0.0170), and higher RAI (p=0.0406). Endothelialitis tended to be more severe in untreated patients (p=0.0931). There was no significant difference between pre-treated and treated patients for the other examined variables, including the bile duct damage component of the RAI (p=0.3743).

Conclusions: Our findings suggest that portal inflammation, particularly eosinophils, become less prominent with pre-treatment, while bile duct damage may take longer to resolve. When evaluating biopsies for suspected ACR, the finding of bile duct damage should raise the possibility of partially treated ACR, even in the absence of significant mixed portal inflammation.

1041 Patterns of Targeted Hepatic Injury in Patients with Hepatocellular Carcinoma Treated with Ablative Y-90 Radioembolization

Jason Lewis[1], Beau Toskich[1], Raouf Nakhleh[1], Seyed Ali Montazeri[1], Cynthia De la Garza-Ramos[1], Murli Krishna[1]
[1]Mayo Clinic, Jacksonville, FL

Disclosures: Jason Lewis: None; Beau Toskich: *Consultant*, Boston Scientific, Sirtex Medical, Johnson and Johnson, AstraZeneca, Genentech, Eisai, HistoSonics, Turnstone Biologics; Raouf Nakhleh: None; Seyed Ali Montazeri: None; Cynthia De la Garza-Ramos: None; Murli Krishna: None

Background: Ablative radioembolization with Yttrium-90 (Y90) has become a first line therapy as a bridge to liver transplantation in patients with hepatocellular carcinoma (HCC). While there have been descriptions of the histologic changes that occur in HCC treated with Y-90, there are no detailed analyses of the spectrum of findings within the adjacent, non-neoplastic liver.

Design: We utilized a database of patients who underwent liver transplantation after ablative Y90 therapy for HCC. Regions around untreated tumors were excluded. All slides containing non-neoplastic tissue adjacent to treated HCC were evaluated for the following histologic changes: necrosis, cytologic atypia within benign hepatocytes or ductules, fibrosis, ductular proliferation, chronic inflammation, hemosiderin, hemorrhage, and number of microspheres/10x field (highest concentration). Each of these variables (except for the sphere quantitation) was qualitatively scored as absent, mild, moderate, or severe by two GI/liver pathologists.

Results: Forty-seven liver explants containing 57 treated HCCs were evaluated. The patients consisted of 38 males and 9 females, ranging in age from 37 to 74 (median 65) at the time of transplantation. Interval from treatment with Y90 to transplantation ranged from 59 to 551 days (median 207 days). Table 1 contains details of the histologic changes assessed. The number of spheres/10x field within the adjacent, non-neoplastic liver ranged from 0 to 104 (median 6.5). Sections from the periphery of the liver, remote from the tumor and not associated with Y90 beads, demonstrated no specific histologic changes.

Table 1 Histologic changes in non-neoplastic liver

Histologic Change	None n(%)	Mild n(%)	Moderate n(%)	Severe n(%)
Necrosis	25 (44)	6 (10)	9 (16)	17 (30)
Fibrosis	3 (5)	26 (46)	19 (33)	9 (16)
Atypia	29 (51)	20 (35)	5 (9)	3 (5)
Ductular Proliferation	1 (2)	16 (28)	14 (25)	26 (45)
Hemosiderin	26 (46)	13 (23)	10 (17)	8 (14)
Chronic Inflammation	18 (31)	34 (60)	5 (9)	0 (0)
Hemorrhage	35 (61)	7 (12)	10 (18)	5 (9)

Conclusions: 1. Injury produced by Y90 spheres in non-neoplastic liver is characterized by a prominent ductular proliferation (severe in 45% of cases) associated with variable degrees of fibrosis (severe in 16% of cases) and necrosis (severe in 30% of cases). This reaction is typically not associated with a prominent inflammatory infiltrate. The presence of hemosiderin is closely

associated with the finding of hemorrhage in the adjacent liver. 2. Atypia may be seen in benign hepatocytes or ductules, but when present is typically focal (35% of cases) and should not be interpreted as a neoplastic process. 3. Peritumoral changes, particularly necrosis and fibrosis, should not be included in post-treatment tumor size. Identification of portal structures or cirrhotic nodules in zones of necrosis is helpful in this regard.

1042 Benign and Malignant Incidental Findings During Routine Pathology Evaluation of Explanted Livers: Review of 266 Cases in a Single Center

Ning Li[1], Kusum Sharma[2], Yongjun Liu[3], Xiaofei Zhang[2]
[1]University of Wisconsin Hospital and Clinics, Madison, WI, [2]University of Wisconsin, Madison, WI, [3]University of Wisconsin School of Medicine and Public Health, Madison, WI

Disclosures: Ning Li: None; Kusum Sharma: None; Yongjun Liu: None; Xiaofei Zhang: None

Background: Explant liver pathology is important for confirming the pre-transplantation clinical diagnosis and for post-transplantation management as well as prognosis. The purpose of this study was to systematically review the liver explant pathology and correlate the incidental findings with outcomes of transplantation.

Design: Liver transplantation cases performed from August 2019 to August 2021 at our institution were identified. Retrospective review was conducted, and the following information was retrieved: age, gender, background liver disease, presurgical clinical diagnosis and imaging findings, explant liver pathology findings, and post-transplantation clinical management and follow-up information including complications, rejection, and disease recurrence. Incidental pathologic findings were defined as benign and/or malignant conditions that were not detected before liver transplantation.

Results: A total of 266 patients (76 females and 188 males) were identified, including 260 adults (24-73 years) and 6 children (2 months to 15 years). Most common causes of end-stage liver disease for adults were alcohol (33.2%), non-alcoholic steatohepatitis (NASH) (21.8%), and viral hepatitis (18.5%). For children, acute liver failure due to viral infection and congenital hepatobiliary disease are the common etiologies. Seventy-three explant livers (27.4%) demonstrated a wide variety of incidental findings. Malignant findings include hepatocellular carcinoma (HCC) (5/266, 1.8%), cholangiocarcinoma (1/266, 0.4%), combined HCC-cholangiocarcinoma (1/266, 0.4%), lymphoma (1/266, 0.4%), and well-differentiated neuroendocrine tumor (1/266, 0.4%). In 5 cases (1.8%) transplanted for HCC, addition HCC nodules were identified. Common benign findings include bile duct adenoma, von Meyenburg complex, hemangioma, and macroregenerative nodules. The underlying causes of cirrhosis were changed for six cases (5 from NASH to alpha-1 antitrypsin deficiency, and 1 from cryptogenic cirrhosis to hemochromatosis). Overstaged fibrosis and overgraded steatosis diagnosed on pre-transplantation MRI/CT were also noted. These patients did not experience early graft failure or disease recurrence.

Conclusions: Incidental or misdiagnosed malignancy is relatively rare in explanted livers. Benign incidental findings are common. The correlation between imaging and histology is not optimal, especially in assessment of fibrosis and steatosis. Thorough pathologic examination is critical for revealing the etiology of cirrhosis.

1043 Utility of Molecular Profiling in Distinguishing Poorly-Differentiated Primary Liver Carcinomas

Tom Liang[1], Shefali Chopra[2]
[1]University of Southern California, Keck School of Medicine of USC, Los Angeles, CA, [2]Keck School of Medicine of USC, Los Angeles, CA

Disclosures: Tom Liang: None; Shefali Chopra: None

Background: Hepatocellular carcinomas (HCC) and intrahepatic cholangiocarcinomas (ICC) both can arise in the setting of chronic liver disease and distinguishing the two is important for treatment and prognosis as ICC is a contraindication to liver transplantation in most centers. Although most cases can be diagnosed confidently on histology with help of IHC stains, a small subset of poorly differentiated (PD) primary liver carcinomas (PLC) cannot be reliably separated on H&E and IHC alone. Certain mutations like TERT promoter mutations which are exclusively associated with HCC while others are seen in ICC. This study was undertaken to determine the utility of molecular profiling in PD primary liver carcinomas (PLC)

Design: All cases of primary liver carcinomas on biopsies and resections which had molecular profiling performed were retrieved by a pathology database search and reviewed. Demographic, clinicopathologic data, IHC, molecular, and clinical follow-up were compiled.

Results: 32 cases of PLCs with molecular profiling were identified after carefully reviewing charts and excluding any possible metastasis. 17 of these cases (13 biopsies, 4 resections) were poorly differentiated (PD) and had no definitive morphological or IHC evidence of either HCC or ICC. 71% (12/17) of the PD cohort were ICCs, 4/17 were HCC, and 1 was a primary liver carcinoma with inhibin positivity. The PD cohort had an average age of 64 and tumor size of 8.1 cm. 53% (9/17) had cirrhosis and 94% (16/17) had metastatic disease. The molecular findings and IHCs of the PD PLC s are summarized in Table 1. In the PD cohort, Heppar1/arginase positivity should favor HCC though negative staining does not necessarily exclude HCC as illustrated by case 11 (Fig 1). Case 11 was initially favored to be ICC due to its negative Heppar1, arginase, strong diffuse CK7 and AE1/3 positivity. However, molecular showed a TERT promoter mutation suggesting HCC. There was a single case (#7) of PLC with inhibin positivity with GNAS mutation. The remaining 15 cases (7 biopsies, 8 resections) were easily recognizable on morphology and included 12 ICCs, 2 HCCs, and 1 combined HCC-ICC. The IHCs and molecular in these cases were concordant with the H&E.

Case	*Biopsy/resection*	*CK 7*	*CK AE1/3*	*RNA albumin ISH*	*HepPar1/ Arginase*	*Glyp-3*	*Molecular findings*	*Integrated Diagnosis*
1	biopsy	+, focal	+, patchy	n.p.	+, focal	+, patchy	ARID1A, TP53	HCC
2	biopsy	+, patchy	+, diffuse	n.p.	-	-	BRCA2	ICC
3	resection	+, diffuse	+	-	-	n.p.	FGFR2/INA fusion, EGFR, TP53	ICC
4	biopsy	+, patchy	weak +	+, patchy	-	n.p.	ARID2, TP53, PIK3CA	ICC
5	biopsy	+	n.p.	+	-	+, patchy	CDKN2A, TP53, CRKL	HCC
6	biopsy	+, patchy	n.p.	n.p.	-	n.p.	KRAS	ICC
7	biopsy	+, patchy	+, patchy	+	-	n.p.	GNAS	Primary liver carcinoma with inhibin positivity
8	biopsy	+, focal	+, diffuse	+, patchy	+, focal	+	TERT promoter, TP53	HCC
9	resection	+, patchy	n.p.	n.p.	-	-	FGFR2-BICC1 fusion	ICC
10	biopsy	+	+	n.p.	-	n.p.	KRAS, TP53	ICC
11	biopsy	+, diffuse	+	+, focal	-	+, focal	TERT promoter, MET amplification, P53	HCC
12	biopsy	-	+	+	-	n.p.	PIK3CA, TP53	ICC
13	biopsy	+	n.p.	n.p.	n.p.	n.p.	IDH1, BAP1, CDKN2A	ICC
14	resection	+	+	n.p.	-	n.p.	IDH1	ICC
15	resection	+	n.p.	n.p.	-	n.p.	IDH1, MUTYH	ICC
16	resection	+, diffuse	+	+, focal	-	n.p.	ARID2, MDM2	ICC
17	biopsy	+	n.p.	n.p.	n.p.	n.p.	TP53, CDKN2A, ARID1A, NF1	ICC

Figure 1 - 1043

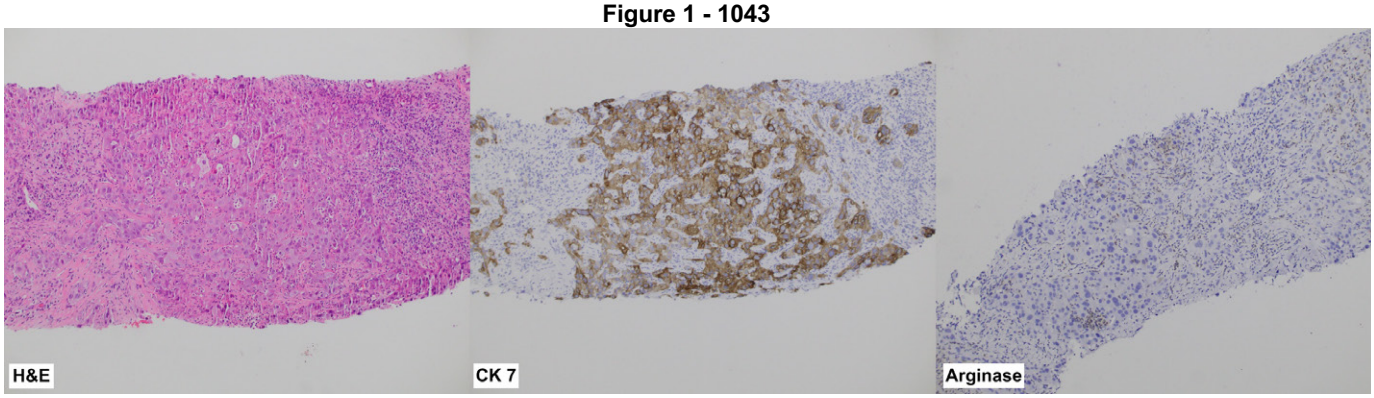

Conclusions: Morphology and IHCs in a small subset of PD PLCs cannot reliably separate HCC from ICC. As certain mutations are very specific for either HCC and ICC, integration of molecular data can help differentiate the two, lending more credibility to the diagnosis in PD PLCs and can guide therapy.

1044 HHLA2 Immune Checkpoint Is a Novel Prognostic Predictor in Hepatocellular Carcinoma

Xiaoyan Liao[1], Dongwei Zhang[1]
[1]*University of Rochester Medical Center, Rochester, NY*

Disclosures: Xiaoyan Liao: None; Dongwei Zhang: None

Background: Immunotherapy with antibodies against PD-1 and PD-L1 had low response rates and limited overall survival benefits in patients with hepatocellular carcinoma (HCC). The aim of this study was to characterize the expression pattern and clinical significance of B7 family immune checkpoint proteins HHLA2, PD-L1 and B7-H4 in HCC.

Design: Immunohistochemical stains for HHLA2, PD-L1, B7-H4, CD3, and CD8 were performed on tissue microarray slides from 103 surgically resected HCC specimens.

Results: Positive HHLA2 was detected in 63 (61.2%) cases, with 50 (48.5%) cases showing low expression and 13 (12.6%) cases showing high expression. Positive PD-L1 (Combined Positive Score [CPS] ≥1) was detected in 27 (26.2%) cases, with the majority showing low expression (CPS<10) (n=25, 24.3%) and only 2 (1.9%) cases showing high expression (CPS≥10). The coexpression of PD-L1 and HHLA2 was observed in 17 (16.5%) cases. B7-H4 expression was only detected in 1 (1.0%) case. HHLA2 positive cases had significantly better survival than HHLA2 negative cases (*P*=0.042). Positive HHLA2 expression correlated with high $CD8^+$ cell density (*P*=0.015). The subgroup with both HHLA2 expression and high $CD8^+$ cell density e*xhibited* the most *favorable prognosis (P*=0.036).

Conclusions: HHLA2 is frequently expressed in HCC. Positive HHLA2 correlates with high density of $CD8^+$ intratumoral lymphocytes and favorable prognosis. HHLA2 may be considered potential therapeutic immune target in HCC.

1045 Pan-TRK Protein Expression and NTRK Gene Fusions in Primary Malignant Tumors of the Liver

Xiaoyan Liao[1], Dongwei Zhang[1]
[1]*University of Rochester Medical Center, Rochester, NY*

Disclosures: Xiaoyan Liao: None; Dongwei Zhang: None

Background: Gene fusions involving the neurotrophic tyrosine receptor kinases (*NTRK1, NTRK2, NTRK3*) have been identified in up to 1% of all solid tumors. TRK inhibitors such as larotrectinib and entrectinib have shown anti-tumor activity regardless of tumor types. The aim of this study was to investigate the expression of TRK proteins and molecular characteristics of *NTRK* gene fusions in primary liver malignancies.

Design: A total of 179 surgically resected liver tumors, including 110 hepatocellular carcinomas (HCC) and 69 intrahepatic cholangiocarcinomas (ICC), were retrieved from our institution between 2009 and 2019. Immunohistochemistry for pan-TRK (clone EPR17341, AbCam) was performed on tissue microarray slides. Staining intensity (negative, equivocal/weak, moderate, strong) and localization (cytoplasmic or nuclear) were evaluated. Cases with at least equivocal staining were further tested by RNA sequencing (RNA-seq) using next generating sequencing technique to identify *NTRK* gene fusions and determine RNA expression levels. Statistical analysis was performed using SPSS Statistics 27.

Results: By immunohistochemistry, 12 (10.9%) of 110 HCC showed diffuse but equivocal/weak pan-TRK cytoplasmic staining. All others, including 69 ICC, were negative for pan-TRK. Kaplan–Meier analysis did not reveal survival difference between pan-TRK-positive HCC and pan-TRK-negative HCC. The expression of pan-TRK did not correlate with age, gender, tumor differentiation, or tumor stage. RNA-seq analysis did not detect any *NTRK* gene fusion in the 12 HCC that showed equivocal/weak pan-TRK expression. However, RNA-seq did identify many other gene fusions in the 12 HCC, including mitochondrial gene MT-ATP6/MT-ATP8 fusion (n=9, 75%), Ig κ light chain gene IGKV/IGKJ fusion (n=5, 41.7%), and histocompatibility complex gene HLA-C/HLA-B fusion (n=4, 33.3%).

Conclusions: *NTRK* gene fusion is extremely rare in primary liver tumors. Although equivocal/weak pan-TRK expression by immunohistochemistry can be seen in some HCC, no *NTRK* gene fusion was detected by RNA-seq confirmatory test, suggesting that equivocal/weak pan-TRK expression may not be used as a surrogate for *NTRK* gene fusion. Nevertheless, RNA-seq detected many other gene fusions in HCC, the function of which warrant further studies.

1046 Correlation of LI-RADS LR3 or LR4 Observations with Histopathologic Diagnosis of Hepatocellular Carcinoma in Liver Transplant Patients

Bo Lin[1], Colin Dunn[1], Travis Browning[1], Nicole Rich[1], Parsia Vagefi[1], Takeshi Yokoo[1], Hao Zhu[1], Amit Singal[1], Purva Gopal[1]
[1]UT Southwestern Medical Center, Dallas, TX

Disclosures: Bo Lin: None; Colin Dunn: *Stock Ownership*, Catalyst Pharmaceuticals; Travis Browning: *Consultant*, Change Healthcare; Nicole Rich: None; Parsia Vagefi: None; Takeshi Yokoo: *Grant or Research Support*, Siemens, Bayer, GE, Bracco, Guerbet; Hao Zhu: *Grant or Research Support*, Alnylam; *Stock Ownership*, ionis; Amit Singal: *Consultant*, Exact sciences, Glycotest, Fujifilm medical sciences, Bayer, Genentech, Eisai, Exelixis, BMS, AstraZeneca, Grail; Purva Gopal: None

Background: Hepatocellular carcinoma (HCC) is the third leading cause of cancer death worldwide and leading cause of cancer death in patients with cirrhosis. The Liver Imaging Reporting and Data System (LI-RADS) system is an evidence-based system to classify liver lesions in at-risk patients. LI-RADS categories progress from LR1 (definite benign) to LR5 (definite HCC), with LR3 and LR4 lesions being intermediate risk for being HCC. However, the histopathologic nature of LR3 and LR4 lesions have not been well studied. We correlated explant gross examination, histopathology and imaging findings from liver transplant patients with at least one LR3 or LR4 lesion on CT or MRI imaging within 6 months prior to transplantation.

Design: We conducted a retrospective cohort study of patients with cirrhosis and at least one LR3 or LR4 observation on contrast CT or MRI imaging who underwent liver transplantation between January 2014 and October 2020. Imaging findings were abstracted from radiology reports and pathology reports and nodule slides reviewed.

Results: We identified 90 eligible patients (median age 63 years, 74.4% male), with a total of 81 LR3 and 37 LR4 observations (15 patients had both LR3 and LR4 observations). The median size of the observations was 1.1 cm, with 72 (61%) being ³1 cm. On gross evaluation, 38 (46.9%) LR3 and 7 (18.9%) LR4 observations had no pathologic correlate (p=0.04). HCC was identified in 32 (39.5%) LR3 and 25 (67.6%) LR4 observations (p=0.005), and dysplastic nodules were identified in 8(9.9%) and 3 (8.1%), respectively. Of 52 LR3/4 lesions that were ≤ 1 cm, 25 were HCC (48%). Of these 25, 11 (44%) had no concurrent HCC. 12/45 LR3 HCC were ≤1.0 cm while 4/7 LR4 HCC were ≤ 1.0 cm (p>0.05). One LR3 < 1.0 cm was angiosarcoma on explant. There was no significant difference in tumor differentiation or vascular invasion between LR3 and LR4 (p>0.05). The presence of HCC or dysplastic nodules was significantly more common in men than women (92.5% vs. 60.9%, p<0.001).

Diagnosis	LR3 (n=81)	LR4 (n=37)	p-value
HCC	32 (39.5%)	25 (67.6%)	0.005
Dysplastic nodule	8 (9.9%)	3 (8.1%)	>0.05
Benign	2 (2.5%)	2 (5.4%)	>0.05
Not found grossly	38 (46.9%)	7 (18.9%)	0.04
Other	1 (1.2%) angiosarcoma		

Figure 1 – 1046

Figure 1. Diagnosis of LR3 and LR4 lesions

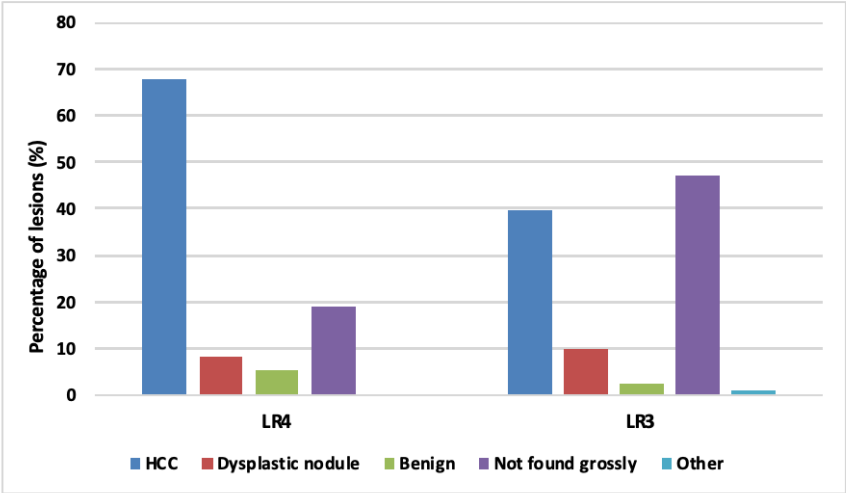

Conclusions: Over one-third of LR3 or LR4 observations were not found on gross examination, however, one-third of LR3 observations and over two-thirds of LR4 observations were HCC on histopathology, highlighting the importance of gross-radiologic correlation and sampling of these nodules, including those ≤ 1 cm when grossly identified. Also, better risk stratification tools for LR3 and LR4 observations are needed.

1047 An International Survey of Commonly Used Immunohistochemistry Practices for the Diagnosis of Hepatocellular Carcinoma

Xulei Liu[1], Elizabeth Brunt[2], Maria Isabel Fiel[3]
[1]Mount Sinai Health System, New York, NY, [2]Washington University School of Medicine, St. Louis, MO, [3]Icahn School of Medicine at Mount Sinai, New York, NY

Disclosures: Xulei Liu: None; Elizabeth Brunt: *Consultant*, Cymabay, Arrowhead, Perspectum Diagnostics, Histoindex, Intercept Pharmaceuticals; *Advisory Board Member*, Pfizer; Maria Isabel Fiel: None

Background: The diagnosis of hepatocellular carcinoma (HCC) is often straightforward. Sometimes though, pathologists are faced with a challenging case in which there is uncertainty in the diagnosis, especially when the tumor is outside the liver requiring confirmation by immunohistochemical stains (IHCs). With limited amount of tissue in needle biopsies and the realistic limitations of laboratories, selection of IHCs is critical. This study was a survey of pathologists in the USA and abroad on the most likely used IHCs for HCC diagnosis.

Design: The survey included 11 IHCs (Hepar-1, ARG-1, GPC-3, CK7, pankeratin, polyclonal CEA (pCEA), CK19, CD10, CD34, glutamine synthetase (GS) and TTF-1) with four choices of frequency, “Always”, “Occasionally”, “Rarely”, or “Never”. The survey was sent to liver pathologists throughout the USA and 23 countries in Europe and Asia to determine the frequency of different IHCs being used to aid in the definitive diagnosis of HCC.

Results: 190 out of 227 responded (84% response rate). Eighty percent of the respondents always used Hepar-1; 72% always used ARG-1; 61% always used both HEPAR-1 and ARG-1. Fewer than half consistently used GPC-3. Neither pCEA nor CD10 was always used, however the majority indicated that both IHCs were occasionally used. There was a significant difference in the use of CK19 ($P < 0.001$) and CD34 ($P = 0.038$) between US and international pathologists, respectively. No other IHCs such as CK7, TTF-1 GS, and pankeratin were always used by all the respondents.

Table. Immunohistochemistry for the Diagnosis of HCC among American and International Pathologists

Immunohistochemistry (N)	Frequency	International N (%)	USA N (%)	Total N (%)	P value
HEPAR-1 (188)	Always	47 (78%)	103 (80%)	150 (80%)	0.17
	Occasionally	9 (15%)	23 (18%)	32 (17%)	
	Rarely	4 (7%)	2 (2%)	6 (3%)	
	Never	0 (0%)	0 (0%)	0 (0%)	
ARG-1 (182)	Always	40 (70%)	91 (73%)	131 (72%)	0.054
	Occasionally	5 (9%)	23 (18%)	28 (15%)	
	Rarely	5 (9%)	3 (2%)	8 (5%)	
	Never	7 (12%)	8 (6%)	15 (8%)	
GPC-3 (181)	Always	19 (34%)	55 (44%)	74 (41%)	0.32
	Occasionally	20 (36%)	46 (37%)	66 (36%)	
	Rarely	8 (14%)	15 (12%)	23 (13%)	
	Never	9 (16%)	9 (7%)	18 (10%)	
CK7 (182)	Always	19 (32%)	29 (24%)	48 (26%)	0.287
	Occasionally	27 (46%)	50 (41%)	77 (42%)	
	Rarely	7 (12%)	24 (20%)	31 (17%)	
	Never	6 (10%)	20 (16%)	26 (15%)	
PAN-KERATIN (177)	Always	5 (9%)	27 (22%)	32 (18%)	0.107
	Occasionally	20 (35%)	40 (33%)	60 (34%)	
	Rarely	23(40%)	33 (28%)	56 (32%)	
	Never	9 (16%)	20 (17%)	29 (16%)	
pCEA (183)	Always	12 (21%)	21 (17%)	33 (18%)	0.916
	Occasionally	19 (33%)	43 (34%)	62 (34%)	
	Rarely	19 (33%)	45 (36%)	64 (35%)	
	Never	8 (14%)	16 (13%)	24 (13%)	
CK19 (181)	Always	19 (32%)	12 (10%)	31 (17%)	<0.001
	Occasionally	24 (41%)	46 (38%)	70 (39%)	
	Rarely	9 (15%)	29 (24%)	38 (21%)	
	Never	7 (12%)	35 (29%)	42 (23%)	
CD10 (186)	Always	14 (23%)	14 (11%)	28 (15.1%)	0.063
	Occasionally	21 (34%)	42 (34%)	63 (33.9%)	
	Rarely	20 (33%)	41 (33%)	61 (32.8%)	
	Never	6 (10%)	28 (22%)	34 (18.3%)	
CD34 (180)	Always	9 (16%)	10 (8%)	19 (11%)	0.038
	Occasionally	20 (35%)	33 (27%)	53 (29%)	
	Rarely	16 (28%)	28 (23%)	44 (24%)	
	Never	12 (21%)	52 (42%)	64 (36%)	
GLUTAMINE	Always	9 (17%)	9 (7%)	18 (11%)	0.204
SYNTHETASE (174)	Occasionally	14 (26%)	36 (30%)	50 (29%)	
	Rarely	13 (25%)	25 (21%)	38 (21%)	
	Never	17 (32%)	51 (42%)	68 (39%)	
TTF-1 (180)	Always	7 (12%)	8 (7%)	15 (9%)	0.567
	Occasionally	14 (24%)	28 (23%)	42 (23%)	
	Rarely	14 (24%)	28 (23%)	42 (23%)	
	Never	23 (40%)	58 (48%)	81 (45%)	
HEPAR-1 and ARG-1 (181)	Always	33 (59%)	78 (62%)	111 (61%)	0.658
	Not Always	23 (41%)	47 (38%)	70 (39%)	

N: Number of responses

Conclusions: Hepar-1 and ARG-1 are the most commonly used IHCs for HCC diagnosis worldwide. There were no significant differences in the use of IHCs for HCC diagnosis between US and international pathologists. As half of the surveyed IHCs are infrequently used, pathologists may reconsider their inclusion in an initial IHC panel, if Hepar-1 and ARG-1 are available.

1048 Fibrosis Regresses and Inflammation Persists in HCV Liver Transplant Cases Following Sustained Virological Response Post-Direct-Acting Antiviral Treatment

Bella Liu[1], Shengjie Cui[1], Joshua Onuiri[1], Yuanxin Liang[2], Stephen Ward[1], Swan Thung[1], Maria Isabel Fiel[1]
[1]Icahn School of Medicine at Mount Sinai, New York, NY, [2]Yale School of Medicine, New Haven, CT

Disclosures: Bella Liu: None; Shengjie Cui: None; Joshua Onuiri: None; Yuanxin Liang: None; Stephen Ward: None; Swan Thung: None; Maria Isabel Fiel: None

Background: Direct-acting antiviral agents (DAA) are effective against hepatitis C virus (HCV) infection, achieving sustained virologic response (SVR) in > 95% of patients, and are associated with a reduced, but not eliminated, risk of developing hepatocellular carcinoma (HCC). We aimed to evaluate the clinico-pathological features in DAA-SVR with and without HCC in liver transplantation (LT) cases and determined features of regression.

Design: HCV LT explants (2018-2020) achieving DAA-SVR were included:18 with HCC (Grp 1), 12 without HCC (Grp 2). Histologic evaluation was performed. Laennec cirrhosis (4A, 4B, 4C), which is based on increasing degrees of fibrosis and micronodule formation, and the Beijing Classification (BC), which pertains to predominantly progressive (P), predominantly regressive (R), and indeterminate (I) features of cirrhosis, were assessed. The Histological Activity Index (HAI) was calculated. Demographic and clinical information were gathered.

Results: Grp 1 patients were significantly older compared to Grp 2 patients (62.8 ± 5.15 vs. 58.0 ± 7.45; p=.0361), more often associated with HCV genotypes other than 1a (82.4% vs. 33.3%; p=.0277), and lower T bilirubin (1.9 ± 1.5 vs. 9.5 ± 12.7; p=.0104) and INR (1.4 ± 0.3 vs. 1.8 ± 0.7; p=.0117) at the time of LT. There were no significant differences between the two groups in terms of gender, time interval between DAA and LT, BMI, diabetes mellitus, platelet count, ALT, AST, AFP, albumin, MELD score, and liver weight. Histological examination of Laennec sub-stages and BC showed Grp 1 with 11 (61%) 4C (8 BC-P and 3 BC-I), 6 (33%) 4B (5 BC-I and 1 BC-R), and 1 (6%) 4A (1 BC-R), while there were 8 (67%) 4C (7 BC-P and 1 BC-I), 4 (33%) 4B (4 BC-I), and 0 4A (0 BC-R) in Grp 2. Features of fibrosis regression, including floating and interrupted septa, were present in 13 (72%) Grp 1 and 6 (50%) Grp 2 cases, and were noted even in those having Laennec 4C and BC-P pattern, indicating heterogeneity in fibrous tissue deposition. Both groups showed persistent inflammation with the majority (89%) having low HAI of 1-4.

Conclusions: Despite SVR, HCC may still develop in HCV cirrhosis. Age and HCV genotypes were significantly different between HCC and non-HCC groups in this patient population. Features of fibrosis regression, even in those having advanced cirrhosis as demonstrated in Laennec 4C and BC-P pattern may be seen, possibly an effect of DAA-SVR. Persistent inflammation was noted indicating ongoing immunologically-driven events despite SVR.

1049 Liver Biopsy of Poorly Differentiated Neuroendocrine Carcinoma: A Single Institutional Study of 117 Cases

Xiaoqin Liu[1], Irene Chen[1], Xiaoyan Liao[1]
[1]University of Rochester Medical Center, Rochester, NY

Disclosures: Xiaoqin Liu: None; Irene Chen: None; Xiaoyan Liao: None

Background: Neuroendocrine carcinomas (NECs) are highly aggressive malignant neoplasms that can occur in many organ systems and frequently metastasize to the liver. We undertook this study to characterize the clinicopathologic features of liver NECs.

Design: Liver biopsies carrying a diagnosis of NEC at our institution between 2005 and 2021 were reviewed. Relevant clinical information was retrieved and analyzed.

Results: The cohort included 61 M and 56 F with a median age of 67 years. The median tumor size was 3.8 (range: 0.5-24.3) cm. Besides liver, tumor also frequently metastasized to the bone (n=44, 37.6%), brain (n=24, 20.5%), lung (n=22, 18.8%) and/or adrenal gland (n=10, 8.5%). Histologically, 51 (43.5%) were classified as small cell (SCNEC), 36 (30.7%) as large cell (LCNEC), and 30 (25.6%) as unspecified (NEC-US). The most common primary site was lung (n=60, 51.2%), followed by gastrointestinal tract (GI, n= 27, 23.1%), pancreas and bile ducts (n=10, 8.5%), gynecologic tract (n=5, 4.3%), prostate (n=3, 2.6%), and tongue (n=1, 0.9%). Two (1.7%) were liver primary and 9 (7.7%) had unknown origin. Immunohistochemically, all NECs were positive for at least one neuroendocrine marker. Ki67 ranged from 20% to 100% (mean 71.5%). The majority of SCNEC were lung origin (n=36/48, 75%), while the majority of LCNEC and NEC-US were GI tract origin (n=22/60, 37%, p<0.01). SCNEC had significantly

higher ki67 mitotic index than LCNEC and NEC-US (85% vs. 68.5% vs. 67.5%, p<0.01). Seventy (59.8%) patients received treatment, among which 54 (46.2%) had chemotherapy only, 14 (12.0%) had resection plus chemotherapy, and 2 (1.7%) received resection only. Majority (n=107, 91.5%) died of disease after a median follow-up of 6.4 (range 0-50) months. Univariate and multivariate analysis revealed that chemotherapy and resection improved overall survival (OS, p<0.01); specifically, chemotherapy improved OS in patients with SCNEC (p<0.01), whereas resection and less organ metastasis correlated with better OS in patients with LCNEC (p<0.05). Metastasis from lung origin had worse outcome than metastasis from other primary sites (p=0.011) in patients with LCNEC.

Conclusions: NECs metastatic to liver occur in elderly patient with an aggressive clinical course. Lung and GI tract are the most common primary sites. Tumor origin, resection, and chemotherapy affect patient outcomes. Accurate NEC classification is critical as different NEC types demonstrate distinct clinicopathologic features and therapeutic response.

1050 Hepatocellular Carcinoma (HCC) Nuclear Density & Size Measured by Automated Image Analysis Software: Correlations with Patient Survival

Shu Kwun Lui[1], Zaid Mahdi[1], Shelley Caltharp[2], Jason Wang[3], Cynthia Cohen[4], Alton B. (Brad) Farris[4]
[1]Emory University Hospital, Atlanta, GA, [2]Children's Healthcare of Atlanta, GA, [3]Cook Children's Medical Center, Fort Worth, TX, [4]Emory University, Atlanta, GA

Disclosures: Shu Kwun Lui: None; Zaid Mahdi: None; Shelley Caltharp: None; Jason Wang: None; Cynthia Cohen: None; Alton B. (Brad) Farris: None

Background: Hepatocellular carcinoma (HCC) prognostication can be important in guiding patient care. With advancements in whole slide imaging (WSI) & artificial intelligence (AI) as aids for pathologists, this study investigates the utility of a nuclear image analysis algorithm in analyzing and predicting survival in HCC.

Design: HCC cases (n = 140) were sampled & combined into tissue microarrays (TMAs). TMA slides with a hematoxylin counterstain were digitally scanned into WSIs for analysis. A commercially available nuclear algorithm was optimized to detect & measure the nuclei (e.g., compactness, roundness, elongation, nuclear color, & curvature threshold). Clinical data (including survival data) was retrospectively collected for statistical analysis.

Results: The nuclear analysis algorithm effectively delineated nuclei on both qualitative & quantitative analysis, showing a mean area of 45.9 mm^2 (median = 45.6, standard deviation [S.D.] = 4.8) & mean density of 1,561 nuclei/mm^2 (median = 1,587, S.D. = 518) (Figure 1). Results were divided into 2 groups by median nuclear density (high & low) and survival was compared (months alive with no disease). Survival curve analysis showed a statistically significant survival difference between the 2 groups (Log-Rank p=0.0246, Wilcoxon p=0.0377) (Figure 2). Results were also divided into 2 groups by the nuclear area and compared to months of survival. Survival curve analysis was statistically significant with only the Wilcoxon test (p=0.0279) using the median as the high/low cutoff, but was statistically significant using the 75th percentile as the cutoff (Log-Rank p=0.0472, Wilcoxon p=0.0122).

Figure 1 - 1050

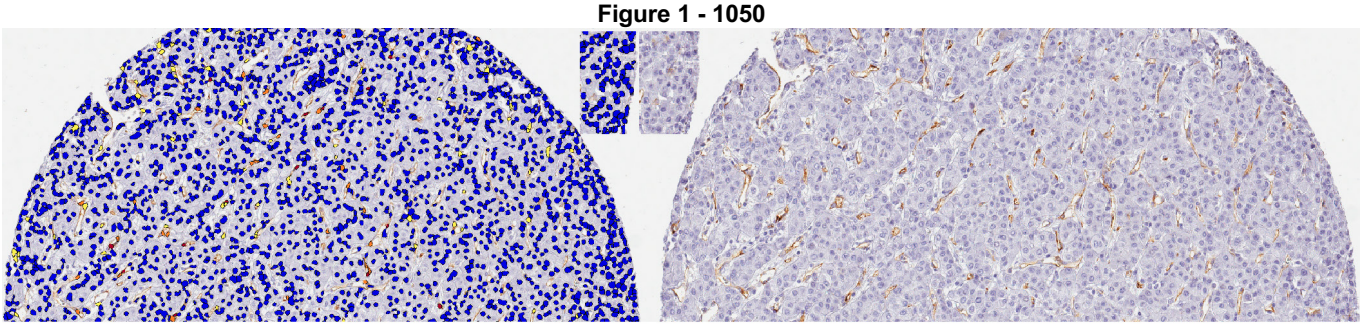

Figure 1: Nuclei detection after adjusting commerically available nuclear algorithmn.

Figure 2 - 1050

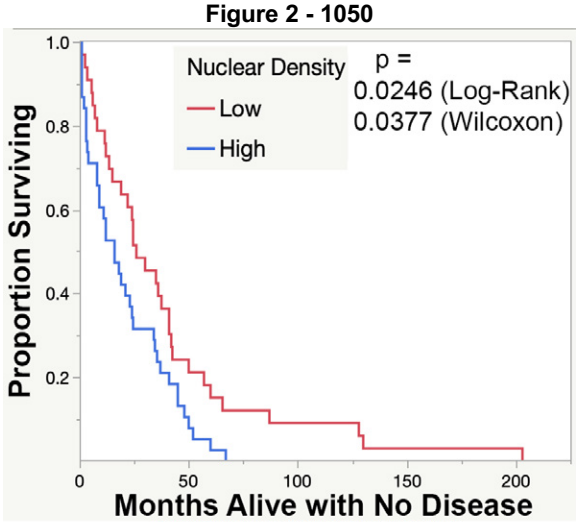

Figure 2: Survival curve comparing high and low nuclear density (separated by median)

Conclusions: It is important to identify predictive factors available from new emerging technology to assess tumors & outcome. This study proposes the use of nuclear size & density as complementary data to help categorize tumors as they show correlation with survival in our cohort. This data can also help inform future AI/machine learning efforts & illustrates how computational techniques can augment traditional histopathologic analysis.

1051 Differential miRNA Analysis of Combined Hepatocellular-Cholangiocarcinoma in Comparison to Hepatocellular Carcinoma and Intrahepatic Cholangiocarcinoma: Pilot Study

Preeti Malik[1], Yan Huang[1], Carlos Castrodad-Rodríguez[1], Juan Lin[1], Olivier Loudig[2], Amarpreet Bhalla[1]
[1]Albert Einstein College of Medicine, Montefiore Medical Center, Bronx, NY, [2]Hackensack Meridian Health, Nutley, NJ

Disclosures: Preeti Malik: None; Yan Huang: None; Carlos Castrodad-Rodríguez: None; Juan Lin: None; Olivier Loudig: None; Amarpreet Bhalla: None

Background: Combined hepatocellular cholangiocarcinoma (HCC-CC) is a rare type of primary intrahepatic malignancy with unequivocal histomorphological features of both Hepatocellular carcinoma and intrahepatic cholangiocarcinoma (iCC). The prognosis is intermediate with a high risk of recurrence and lymph node metastases. Molecular studies are not widely utilized in diagnostic decision-making or assessing the prognosis of this tumor. Hence, we aim to characterize any distinct miRNA profile and molecular pathway associated with HCC-CC in comparison to iCC and HCC in this pilot study.

Design: An electronic database search was carried for cases of HCC, iCC, and HCC-CC at the Montefiore Medical Center. The archived slides were reviewed, and a suitable section from each tumor was identified for miRNA analysis. Five 20-micron thick sections were cut from each selected block. The sections were utilized for RNA extraction. RNA was extracted from all the individual samples separately and incubated with a different 3' barcoded adapter. The RNA samples were then pooled together for the remainder of the molecular assays and sequenced in a single library. Biostatistical analysis was performed to evaluate the differential expression of miRNAs in the three tumor groups.

Results: 13 patients were included; HCC (4), iCC (4), and combined HCC-CC (5). The age ranges from 34-78 years and 9/13 (69%) were male. All five combined HCC-CC cases were confined to hepatic parenchyma and had an uninvolved surgical margin. 4/5 cases had HCV infection and cirrhosis (Table). Differential analysis revealed distinct miRNA profiles for the three tumor groups (Fig. 1). There was upregulation of miRNA-498, miRNA-105-1 and miRNA-551(b); while downregulation of miRNA-506 and miRNA-10b in combined HCC-CC compared to HCC and iCC. HCC and iCC also showed distinct miRNA profiles. HCC had upregulation of miRNA-483 and miRNA-204 while downregulation of miRNA-135b, miRNA-200a, and miRNA-31. There was upregulation of miRNA-934 and miRNA-141 and downregulation of miRNA-488, and miRNA-1269 in iCC (Table).

Demographics and histomorphological characteristics of three tumors groups			
	Combined HCC-CC	**Hepatocellular carcinoma (HCC)**	**Intrahepatic Cholangiocarcinoma (iCC)**
Number of cases	5	4	4
Age (years)	34-82	63-79	68-78
Sex (M, F)	M:4, F:1	M:3, F:1	M:2, F:2
Tumor site	Right lobe: 3, Left Lobe: 1 Live Biopsy:1	Right lobe:1 Right and left lobe: 1	Right lobe:2, Left lobe: 1 Right and left lobe: 1
Maximum tumor size (cm)	2.2-18	2.5-17.2	3.5-6.5
Tumor focality	Solitary:2, Multiple: 2 Not sure:1	Solitary:1, Multiple: 3	Solitary: 4
Satellite Nodules	No: 5	Yes: 2 No: 2	No: 4
Tumor growth	Mass forming: 2	Mass: 4	Mass forming: 4
Tumor Grade	Grade 2: 3, Mod-poorly differentiated: 1	Grade 2: 4	Grade 3: 2 Grade 2: 1 Grade 2: 3, Mod-poorly differentiated: 1
Hepatic Parenchymal margin	Uninvolved: 5	Uninvolved: 4	Uninvolved: 4
Local Invasion	Hepatic parenchyma: 5	Hepatic parenchyma: 2; involve vessels:2	Hepatic parenchyma: 2; involve adjacent organs:2
Vascular Invasion	Yes: 1, No: 4	Yes: 2, No: 2	Yes: 1, Not identified: 3
Perineural invasion	Yes: 1, Not identified: 3	Not identified: 4	Yes: 1, Not identified: 3
Lymphovascular invasion	Yes: 1, Not identified: 3	Not identified: 4	Yes: 3, Not identified: 1
Liver cirrhosis	Yes: 4	Yes: 3	Yes: 1
Viral Infection	HCV: 4	No: 4	HCV:1

Significant miRNA differential expression among three tumor groups				
miRNA	**HCC vs ICC Log2Fold change**	**HCC vs combined HCC-CC Log2Fold change**	**ICC vs combined HCC-CC Log2Fold change**	**adj p value**
	Upregulation combined HCC-CC			
miRNA-498	-3.39	-11.58	-8.19	<0.001
miRNA-105-1	-2.75	-9.1	-6.36	0.03
miRNA-551b	-2.40	-5.27	-2.87	<0.001
	Downregulation combined HCC-CC			
miRNA-506	1.36	3.73	2.36	0.04
miRNA-10b	1.60	2.3	0.7	0.03
	Upregulation HCC			
miRNA-204	5.13	3.69	-1.44	<0.001
miRNA-483	5.30	5.84	0.54	<0.001
	Downregulation HCC			
miRNA-31	-9.33	-5.09	4.24	<0.001
miRNA-135(b)	-8.32	-5.05	3.27	<0.001
miRNA-200a	-4.68	-1.64	3.04	<0.001
	Upregulation iCC			
miRNA-934	-10.22	-2.08	8.13	<0.001
miRNA-141	-8.85	-2.73	6.12	<0.001
	Downregulation iCC			
miRNA-1269	8.99	1.66	-7.33	<0.001
miRNA-488	3.35	-1.14	-4.49	0.02

Figure 1 - 1051

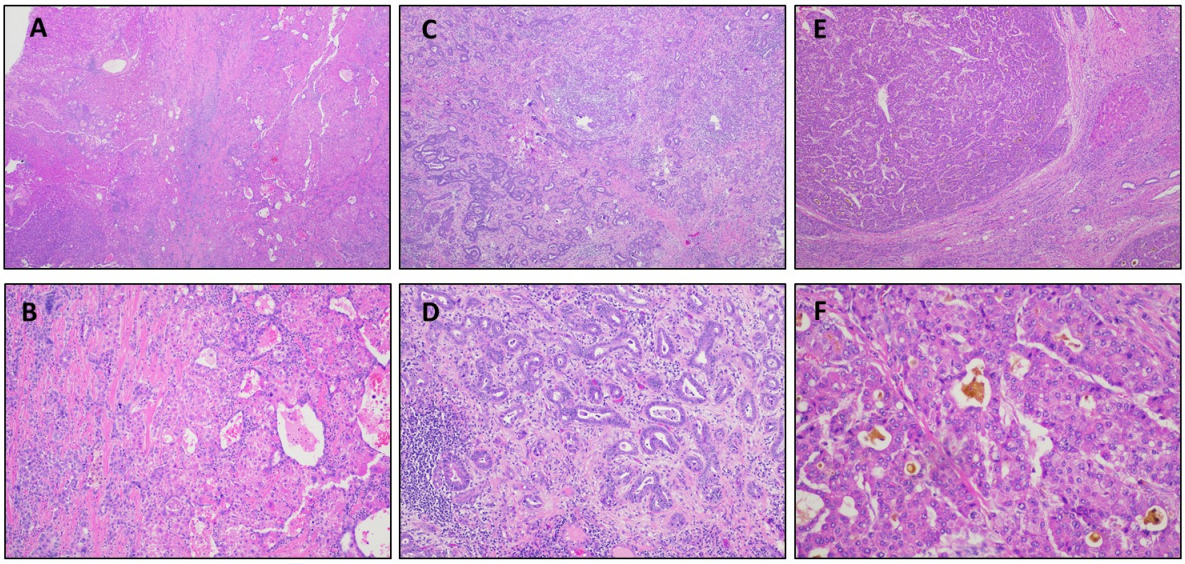

Fig 1. H&E stain. A-B: Combined Hepatocellular-cholangiocarcinoma (HCC-CC), C-D: Intrahepatic cholangiocarcinoma (iCC) E-F: Hepatocellular Carcinoma (HCC)

Figure 2 - 1051

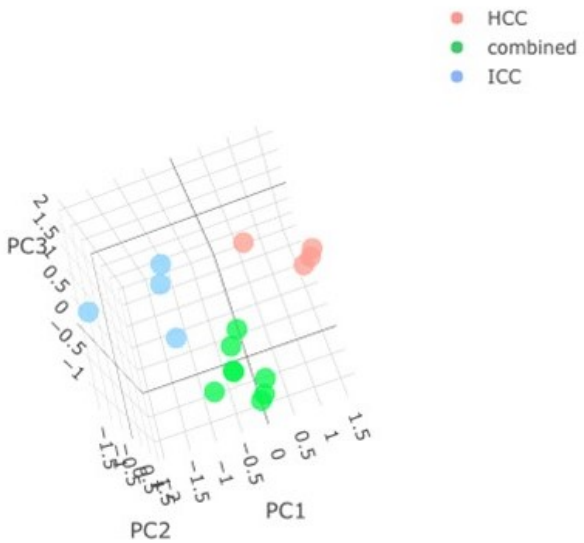

Fig 2. miRNA expression profiling reveals distinct miRNA signatures for the three tumor groups

Conclusions: The three tumor groups, HCC, iCC and HCC-CC have distinct miRNA profiles. Combined HCC-CC had significant expression of miRNA-551b, miRNA-498, miRNA-105-1 and miRNA-10b. These miRNAs have been reported to be associated with metastatic adenocarcinomas arising in other sites. Prospective validation studies and correlation with demographic, clinical and histologic variables will be performed on a larger cohort in the near future.

1052 Histologic Features of Hepatocellular Carcinomas with Atypical MRI Findings

Ilke Nalbantoglu[1], Kirsten Cooper[1], Xuchen Zhang[1], Jeffrey Weinreb[1], Dhanpat Jain[1]
[1]*Yale School of Medicine, New Haven, CT*

Disclosures: Ilke Nalbantoglu: None; Kirsten Cooper: None; Xuchen Zhang: None; Jeffrey Weinreb: *Advisory Board Member*, GE Healthcare; Dhanpat Jain: None

Background: Hepatocellular carcinoma (HCC) is the most common primary malignant hepatic tumor. On MRI, most HCCs are diagnosed based on their typical imaging features of arterial phase contrast enhancement and washout with pseudocapsule, without the need for a biopsy (bx). Some however, do not display typical imaging features and pose a diagnostic challenge. The goal of the study was to compare histologic correlates of resected HCCs with typical and atypical MRI findings.

Design: Available slides and MRI images of resections performed for untreated and unifocal HCC were blindly reviewed. Cases were categorized as typical (T-HCC) vs atypical (A-HCC) based on imaging characteristics. Histologic features of the tumor including subtype, growth pattern, pseudocapsule, tumor borders (well vs. ill-defined), intra-tumoral steatosis, hemorrhage, sclerosis, clear cells, necrosis, etc. were recorded and subjectively quantified by percentage (%). Background liver disease and fibrosis stage were recorded.

Results: Total of 25 cases were included (15 T-HCC, 10 A-HCC). Key features are shown in the table. Of various studied features, larger size (6.6 vs 3.8 cm, p=0.02), presence (50 vs 13%, p=0.08) and % amount of intra-tumoral hemorrhage (9.5 vs 1.33%, p=0.049), higher % amount of intra-tumoral necrosis (17 vs 5%, p=0.1) and clear cell change (18 vs 6.7%, p=0.3), and having ill-defined borders (42 vs 25%, p=0.2) were commonly associated with A- HCC on imaging. Of note, among A-HCC cases, having a prior bx didn't correlate with the presence of intra-tumoral hemorrhage (60 vs 80% respectively, p=0.4). HCV (80 vs 20%, p=0.01) and advanced fibrosis (60 vs 30%, p=0.04) were more common in T-HCC. More T-HCC cases had a psesudocapsule (100 vs 70%, p=0.05). Having a pseudocapsule on microscopy also correlated with the radiologic finding of a pesudocapsule (p=0.041, not shown on table). T-HCC showed a higher % of trabecular growth pattern (39 vs 20%, p=0.09). Of the above listed features, six were statistically significant. Tumor differentiation, nuclear grade, and other histologic parameters were similar between two groups.

	Atypical HCC N=10	**Typical HCC N=15**	**p value**
Age (years)	65 (37-83)	67 (58-84)	0.3
M:F	13:2	7:3	0.36
Background liver			
1. **Hepatitis C virus (HCV) infection**	2 cases (20%)	12 cases (80%)	**0.01**
2. **Advanced fibrosis**	3 cases (30%)	9 cases (60%)	**0.04**
HCC features			
3. **Tumor size (cm, mean)**	6.6 (±*3.3)* cm Median: 5.4 (3-12 cm)	3.8 (±*2.2)* cm Median: 3.3 (1.5-8.3) cm	**0.02**
4. **Presence of pseudocapsule on microscopy**	7 cases (70%)	15 cases (100%)	**0.05**
5. **Ill-defined tumor border (% circumference, mean)**	42 (± 41.3) % Median: 25 (0-100)	25 (± 19.6) % Median: 20 (0-70)	0.2
6. **Presence of intra-tumoral hemorrhage**	5 cases (50%)	2 cases (13%)	**0.08**
7. **% Intra-tumoral hemorrhage (mean)**	9.50 (±*11.17)* % Median: 5 (0-3) %	1.33 (±*3.52)* % Median: 0 (0-10) %	**0.049**
8. **Presence of intra-tumoral necrosis**	5 cases (50%)	6 cases (40%)	0.7
9. **% Intra-tumoral necrosis (mean)**	17 (±*21.1)* % Median: 10 (0-60) %	5 (±*7.56)* % Median: 0 (0-20) %	0.1
10. **% Intra-tumoral steatosis (mean)**	14.4 (±*26)%* Median: 0 (0-80)	14 (±*26)%* Median: 0 (0-70)	
11. **% Clear cell change (mean)**	18 (±*31.5)* % Median: 0 (0-80) %	6.7 (±*10.7)* % Median: 0 (0-30) %	0.3
12. **Trabecular growth pattern (overall % within tumor)**	20 (±*25.7)* % Median: 12.5 (0-80) %	39 (±*26*)% Median: 40 (0-75) %	0.09

Conclusions: Our study shows that A-HCC were larger tumors, had higher % intra-tumoral hemorrhage and ill-defined borders, and lacked pseudocapsule compared to T-HCC. Some of these features seen in A-HCC may provide explanations for etiopathogenesis. Better understanding of these microscopic features on a larger series may help improve imaging-pathologic correlation and help select cases for bx.

1053 Posttransplant Glycogenic Hepatopathy: A Retrospective Study

Tara Narasimhalu[1], Yipeng Geng[2], Hanlin Wang[1]
[1]David Geffen School of Medicine at UCLA, Los Angeles, CA, [2]University of California, Los Angeles, Los Angeles, CA

Disclosures: Tara Narasimhalu: None; Yipeng Geng: None; Hanlin Wang: *Advisory Board Member*, Astellas; *Grant or Research Support*, Bristol Meyers Squibb; *Consultant*, NGM BioPathAI

Background: Glycogenic hepatopathy refers to glycogen overload in hepatocytes, resulting in a swollen and pale or pseudoground glass appearance. It is typically associated with poorly controlled diabetes mellitus. Hyperglycemia is a well-documented complication post organ transplantation, but there has been little data on posttransplant glycogenic hepatopathy.

Design: A total of 33 patients were retrospectively identified based on their liver biopsies showing striking glycogen accumulation in hepatocytes demonstrated on H&E (Figure 1) and periodic acid-Schiff (Figure 2) stains. Pertinent patient data were collected, including transplant status, demographic data and medical history, medications at time of biopsy, blood glucose levels within one week prior to and after biopsy, results of liver tests, and viral status within one month of biopsy. Five cases were subsequently excluded from this study because an updated medication list could not be found at time of biopsy.

Results: There were 12 males and 16 females, ranging in age from 2 to 69 years (mean: 41.7; median: 50). All 28 patients were organ transplant recipients: 25 (89.3%) were liver transplant recipients, and 3 (10.7%) were small bowel or modified multivisceral transplant recipients. Twenty-four (85.7%) patients were on systemic corticosteroid therapy for the treatment of rejection. Among them, 20 (83.3%) were found to have elevated blood glucose levels, including 7 patients who also had preexisting diabetes. Four patients who were on steroids had blood glucose levels under the normal range. These included one patient with preexisting diabetes. The remaining 4 patients did not receive steroid therapy but 3 showed elevated blood glucose levels. None of these 4 patients had preexisting diabetes, but all were on multiple medications including those known to cause hyperglycemia such as cyclosporine, sirolimus, or tacrolimus. All patients had elevated liver tests at the time of liver biopsies, which were performed to primarily rule out rejection.

Figure 1 - 1053

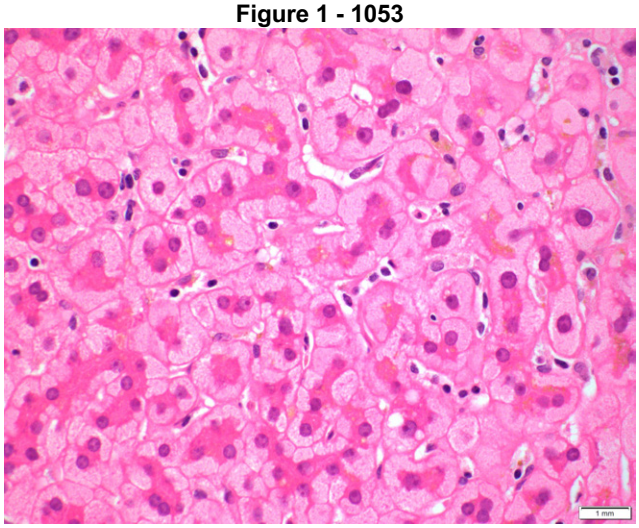

Figure 2 - 1053

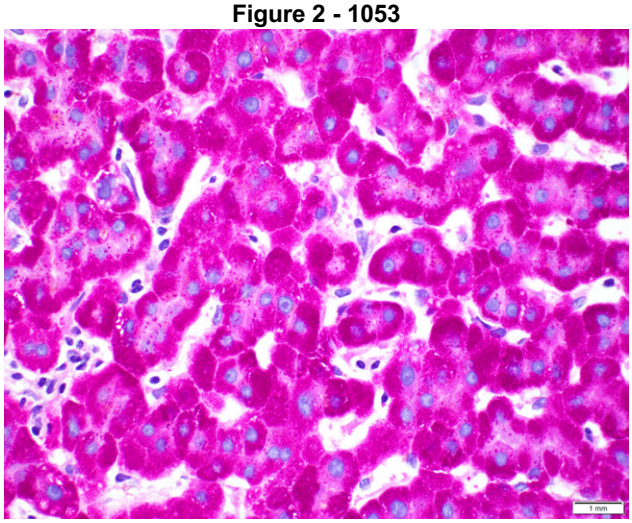

Conclusions: Posttransplant glycogenic hepatopathy is commonly seen in the setting of hyperglycemia, and is frequently associated with systemic corticosteroid therapy, the mainstay of treatment for rejection. Histologic recognition of this entity is important because it helps explain continued elevation in liver tests following successful treatment of rejection. Blood glucose monitoring and liver biopsy are necessary for the diagnosis to avoid confusion with other potential posttransplant complications.

1054 Prevalence of Periodic Acid Schiff Positive Diastase-Resistant (PASD) Globules Within Liver Allografts

Aqsa Nasir[1], Ashwin Akki[2], Xiuli Liu[3]
[1]University of Florida College of Medicine, Gainesville, FL, [2]University of Florida, Gainesville, FL, [3]Washington University School of Medicine, St. Louis, MO

Disclosures: Aqsa Nasir: None; Ashwin Akki: None; Xiuli Liu: *Consultant*, Arrowhead Pharmaceuticals, PathAI; *Advisory Board Member*, AbbVie

Background: Liver allograft biopsy protocol varies considerably among liver transplant centers. Biopsies taken within 1 week of transplantation not only provide baseline histology but may also reveal abnormalities. The frequency, distribution, and clinical significance of PASD positive globules in liver allografts have not been studied. This study aims to determine the frequency and distribution of PASD+ globules in liver allograft biopsies performed within 1 week of liver transplantation.

Design: All liver allografts biopsies within 1 week of transplantation during the study period of 2019-2021 were retrieved from Pathology database and reviewed. PASD positive globules were classified into periportal intrahepatocellular, centrilobular intrahepatocellular, and non-zonal. Other histologic features (necrosis, neutrophilic inflammation, ischemic/reperfusion (I/R) injury score, steatosis, hepatocyte ballooning, cholestasis, and fibrosis) were recorded. Histological features between biopsies with periportal and non-zonal globules and cases without this feature were compared.

Results: During the study period, a total of 128 biopsies from 85 allografts were performed within 1-week post-transplantation (85 with baseline/time 0 biopsy, 14 with two biopsies, 14 with three biopsies and 1 with four biopsies). PAS and PASD stains were performed in 117 (of 128, 91.4%) biopsies. PASD positive globules were identified in 30 biopsies (of 117, 25.6%) and in 24 (of 80 patients, 30%) [Table 1]. Eighteen biopsies from 13 allografts showed periportal or nonzonal PASD globules and immunohistochemistry for alpha-1-antitrypsin (A1AT) performed in five allografts and confirmed these globules to be A1AT [Figure 1]. These five allografts had no fibrosis in three, portal fibrosis in one, and periportal fibrosis in one. The presence of periportal and non-zonal PASD+ globules is not related with inflammation, necrosis, overall degree of I/R injury, sinusoidal dilatation, hepatocyte ballooning, steatosis, cholestasis or fibrosis (P>0.05 for all; data not shown).

Table 1: Frequency and distribution of PASD positive globules in liver allograft biopsy taken within 1-week post-transplantation

Number of cases with PASD positive globules	Total biopsies tested (N=117), N(%)	Total allografts with PAS and PASD stains (N=80), N(%)
Any positive globules	30 (25.6)	24 (30)
Periportal	13 (11.1)	10 (12.5)
Centrilobular	12 (10.2)	9 (11.2)
Non-zonal	5 (4.3)	3 (3.7)

Figure 1 - 1054

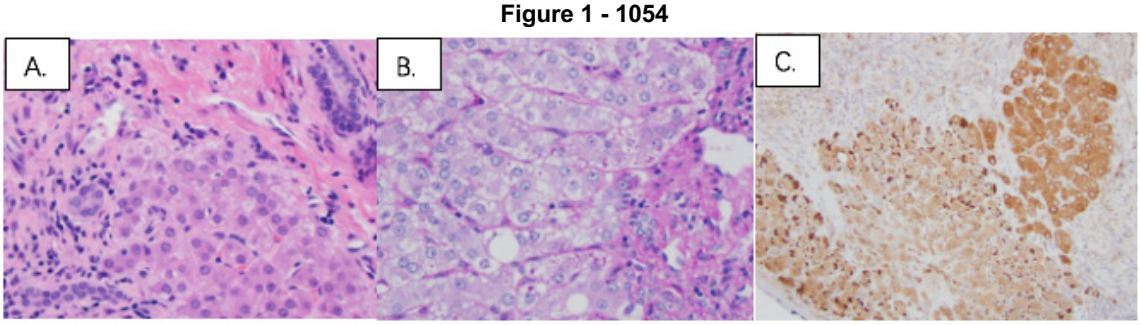

Figure 1. One example of periportal alpha 1 antitrypsin globules. A. H&E stain, 400x; B. PASD stain, 400x; C. Immunohistochemical stain for A1AT, 400x.

Conclusions: PASD positive globules were present in 30% of liver allografts and at least 6.3% (5 of 80) of liver allografts are likely A1AT deficient livers. Clinical significance of A1AT globules remains to be determined in large cohorts.

1055 Utility of Comparing Orcein and Trichrome Staining to Aid Evaluation of Cirrhosis Dynamics

Eric Nguyen[1], Chien-Kuang Cornelia Ding[1], Sarah Umetsu[1], Linda Ferrell[1], Kwun Wah Wen[1]
[1]*University of California, San Francisco, San Francisco, CA*

Disclosures: Eric Nguyen: *Stock Ownership*, Moderna, Inc.; Chien-Kuang Cornelia Ding: None; Sarah Umetsu: None; Linda Ferrell: None; Kwun Wah Wen: None

Background: Advanced liver fibrosis is a dynamic process that can regress following elimination of causative injury such as viral infection or alcohol, leading to improvement in clinical outcomes. Trichrome stain (T) has traditionally been used to evaluate the degree of fibrosis. Orcein stain (O) highlights established elastic fibers; its use in examining fibrosis is not well recognized, but has been previously described (PMID 17498254). Lack of longstanding fibrosis appears pale with lack of extensive staining for elastic fibers on O, and pale with less dense staining of collagen on T. In contrast, remote fibrosis appears dense on T, but shows compact elastic fibers in thin septa and/or extensive thick or broad scars with dark staining on O. This study assessed the utility of O and T staining patterns to evaluate the dynamics of regressed and progressed cirrhosis.

Design: We examined 26 liver resection specimens from 2018-2021 with cirrhosis from different etiologies (Table 1). Progressive and regressive features were determined per prior criteria by Wanless (PMID 11079009) and Beijing schemes (PMID 29700417). O and T stains were evaluated to compare the extent and pattern of pale vs. dense staining on a representative block of non-neoplastic liver per case.

Results: 26 cases were evaluated. 14 cases showed regression (R) on T by Beijing scheme. Among these cases, 9 cases showed equivalent T and O by extent and intensity. 7 cases showed indeterminate (I) on T. Interestingly, O stains demonstrated predominant regressive features, with a minor superimposed component of progression (P) (R>P) in 6 cases and only 1 case remained I. 5 cases showed progression (P) on T. O stains confirmed 4 cases and 1 case showed no obvious P or R ("stagnant"). When cases were classified by etiologies, ASH/NASH were split between R and mixed R/P, whereas viral etiologies were enriched for R. Pale staining on T also could represent dense elastic deposition.

Table 1A. Orcein vs. Trichrome staining on interpretation of Beijing scheme (R-I-P)

Beijing	O & T comparison	n	Interpretation based on O & T impression
R (14)	O=T	9	All R
	O~T, with focal O less than T	4	All mostly R
	O less than T	1	R>P
I (7)	O=T	2	1 mostly R; 1 with early R
	O~T, with focal O less than T	3	All R>P
	O less than T	2	1 R>P, 1 R~P
P (5)	O=T	1	Stagnant with no R or P
	O less than T	2	P
	O significantly less than T	2	Rapid P

Table 1B. Dynamics of cirrhosis by orcein & trichrome interpretation

	Viral*	Viral + NASH/ASH	ASH +/- NASH	AIH	n
R/mostly R	4	5	5		14
P	1		2		3
Mixed R/P		1	6	1	8
Stagnant			1		1
total					26

Viral*: HBV, HCV; ASH: Alcoholic steatohepatitis; NASH: Non-alcoholic steatohepatitis;
AIH: Autoimmune hepatitis;
R: predominantly regression; I: Indeterminate: P: predominantly progression as defined by Beijing criteria

Conclusions: O and T stains evaluated in combination are an effective method of assessing the dynamics of cirrhosis. O significantly less than T can suggest rapid progression. O=T or O~T can suggest absent/minimal progression.
3) O=T with thick bands suggests stagnant fibrosis.

4) O=T with thin, bridged septa suggest more linear (continuous) regression that is more common in treated viral hepatitis.
5) NASH/ASH cases showed more variable/nonlinear regression patterns.
6) Pale staining on T can also correlate with dense elastin fibers.

1056 Novel Benign Hepatocellular Lesions Lacking Alpha-1-antitrypsin Globules in Patients with Cirrhosis Due to Alpha-1-antitrypsin Deficiency

Andrea Olivas[1], Xuefeng Zhang[2], Lei Zhao[3], Lanisha Fuller[2], Jamile Wakim-Fleming[2], Maria Westerhoff[4], Rish Pai[5], Hanlin Wang[6], Namrata Setia[7], John Hart[7]
[1]University of Chicago Medical Center, Chicago, IL, [2]Cleveland Clinic, Cleveland, OH, [3]Brigham and Women's Hospital, Harvard Medical School, Boston, MA, [4]University of Michigan, Ann Arbor, MI, [5]Mayo Clinic, Scottsdale, AZ, [6]David Geffen School of Medicine at UCLA, Los Angeles, CA, [7]University of Chicago, Chicago, IL

Disclosures: Andrea Olivas: None; Xuefeng Zhang: None; Lei Zhao: None; Lanisha Fuller: None; Jamile Wakim-Fleming: None; Maria Westerhoff: None; Rish Pai: *Consultant*, Alimentiv Inc, Allergan, Verily, Eli Lilly, AbbVie, PathAI; Hanlin Wang: *Advisory Board Member*, Astellas; *Grant or Research Support*, Bristol Meyers Squibb; *Consultant*, NGM Bio, PathAI; Namrata Setia: None; John Hart: None

Background: Alpha-1-antitrypsin deficiency (A1AT) is a known cause of cirrhosis, particularly with the PiZZ or PiSZ phenotype, and therefore also carries an increased risk for the development of HCC. Current guidelines recommend ultrasound surveillance of patients with cirrhosis due to A1AT. When a lesion over 1 cm is detected, needle biopsy sampling may be performed for some lesions with indeterminant CT or MRI imaging characteristics (Li-RADS 4 lesions). Diagnosis at the time of liver transplantation also occurs in some patients.

Design: A cirrhotic native liver was examined following needle biopsy of a 4.8 cm mass with indeterminant features by imaging had yielded a diagnosis of “dysplastic nodule”. The hepatocellular lesion, which measured 5.6 cm in the explant, exhibited an unusual constellation of histologic findings not consistent with FNH, dysplastic nodule or HCC. A striking feature of the lesion was the total absence of cytoplasmic PAS/D+ A1AT globules, compared to their abundance in the surrounding cirrhotic parenchyma (also confirmed with A1AT immunostains). Additional examples of this novel phenomenon were sought through a search of the pathology files of 6 transplant centers for cirrhotic livers due to A1AT deficiency with mass lesions (both needle biopsy specimens and native liver explants).

Results: A total of 6 patients (including index patient) were identified with histologically similar lesions (Table 1). Each lesion is composed of cytologically bland hepatocytes arranged in trabecular cords of normal thickness. There are abortive fibrous septa traversing the lesions, but no regenerative nodules, in comparison to the fully cirrhotic surrounding parenchyma. Normal portal tracts are scattered throughout the lesions, but there are also portal tracts lacking normal bile ducts and scattered isolated arterioles. There is abnormal weak diffuse glutamine synthetase reactivity throughout the lesions. All lesions are devoid of PAS/D+ globules, and all of the surrounding regenerative nodules have abundant globules (Fig 2).

Table 1: Summary of Cases

Demographics	A1AT phenotype	Nodule size	Imaging	Procedure	Assoc. condition
66 F	PiMZ	5.6 cm (Fig 1)	LiRad 4	OLT	Steatohepatitis
66 M	PiZZ	3.6 cm (Fig 1)	LiRad 4	OLT	Steatohepatitis
69 F	PiMZ	2.5 cm (Fig 2)	LiRad 4	OLT	Steatohepatitis
62 M	PiZZ	2.2 cm	LiRad 4	Needle bx	Steatohepatitis
50 F	PiZZ	1.1 cm	no nodules seen	OLT	Steatohepatitis
69 M	PiZZ	1.7 cm	no nodules seen	OLT	Hemosiderosis

Figure 1 - 1056

Figure 2 - 1056

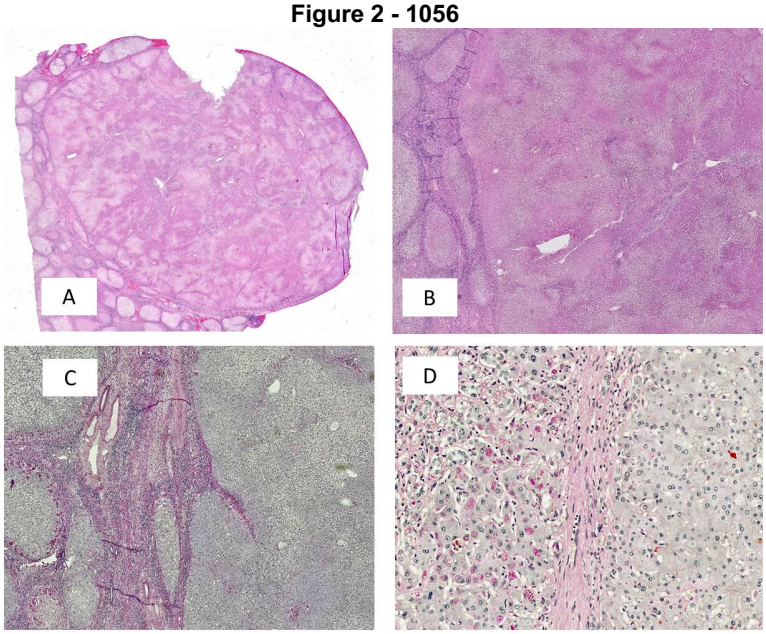

Figure 2: A&B A1AT-neg. nodule with surrounding cirrhotic parenchyma; note the fibrous septa and intact portal tracts
C & D PAS/D stain highlights complete absence within the nodule in contrast to conspicuous globules in surrounding parenchyma

Conclusions: In cirrhosis due to A1AT deficiency benign hepatocellular mass lesions with a striking lack of PAS/D+ globules can rarely develop. These nodules can have imaging characteristics that are worrisome but not diagnostic of HCC. The histologic features of these nodules are not typical of FNH, MRN, dysplastic nodule or HCC. It is possible that they form simply as a consequence of a growth advantage over the surrounding A1AT globule containing cirrhotic nodules.

1057 Comparison of Transient- Elastography, Shear Wave-Elastography and Biopsy in Liver Fibrosis Staging; Significant Discrepancies in Assessing Early Stages of Fibrosis

Byoung Uk Park[1], Michael Ching[1], Kathleen Nilles[1], Coleman Smith[1], Bhaskar Kallakury[2]
[1]MedStar Georgetown University Hospital, Washington, DC, [2]Georgetown University Hospital, Washington, DC

Disclosures: Byoung Uk Park: None; Michael Ching: None; Kathleen Nilles: None; Coleman Smith: None; Bhaskar Kallakury: None

Background: Liver fibrosis is a common endpoint for chronic liver insults of different etiologies. Its assessment is an integral part of patient evaluation as it is associated with overall/disease-specific mortality, prognosis and utilized to guide treatment decisions. Although liver biopsy has been considered the gold standard for its evaluation, other non-invasive methods such as serum biomarkers and imaging techniques such as transient- elastography (TE) and shear wave- elastography (SWE) have been widely used. Therefore, the present study is performed to assess the correlation between the degree of fibrosis evaluated by liver biopsy and the two elastography methods.

Design: Following approval (#STUDY2032), retrospectively, all patients who had undergone liver biopsy, TE (FibroScan; Echosens) and/or SWE (LOGIQ E9, GE HealthCare) from 2017/01/01, to 2020/09/30, were identified. The inclusion criteria were all patients who had undergone a liver biopsy and TE and/or SWE evaluation. The exclusion criteria were patients who did not have a liver biopsy. Statistical analysis was performed in Graphpad Prism (ver. 7.1). The Mann-Whitney U test was used to compare the fibrosis stage following D'Agostino and Pearson normality test. The Chi-square test was utilized to determine the statistical difference of the categorical variables. Confidence intervals were calculated at 95% on binomial distributions.

Results: A total of 91 patients who underwent liver biopsy and one or both elastography evaluations were identified. The mean age was 54, Female to Male ratio 47:44 with a mean BMI (kg/cm2) of 29.29. The percentage of patients with non-alcoholic fatty liver disease, Hepatitis B and C was 43%, 16%, and 19%, respectively. Mean length of the liver core biopsy was 1.54 cm (Table 1). Correlation between liver fibrosis assessment by biopsy and TE was as follows: Stage 0– 29.63%, Stage 1– 13.64%, Stage 2– 35.71%, Stage 3– 16.67%, and Stage 4– 72.73%. Moreover, correlation between biopsy and SWE was: Stage 0– 28.57%, Stage

1– 85.71%, and Stage 2– 0% (Table 1 and Figure 1). Stage 0 and 1 showed significant difference between stage assessment by biopsy and TE (p=<0.0001 and 0.002); by SWE, only Stage 0 revealed significant difference (p=0.013). The presence of steatosis was found to be a significant factor for discrepancy (p=0.02; odd ratio: 0.32).

Table 1.

Demographics and Overall Characteristics				
Demographics	Sex (Female:Male)		47:44	
	Age (years)		54 (2-85)	
	BMI (kg/cm^2)		29.3 (15.5 - 47.0)	
	Hepatitis B		13 (16%)	
	Hepatitis C		15 (19%)	
	Non-alcoholic fatty liver disease		35 (43%)	
Modalities Distribution	Biopsy + TE		71	
	Biopsy + SWE		10	
	Biopsy + TE + SWE		10	
Biopsy	Core length (cm)		1.54 (0.4 - 2.7)	
	Fibrosis Stage		1 (0 - 4)	
TE	Fibrosis Stage		2 (0 - 4)	
SWE	Fibrosis Stage		1 (0 - 3)	
BIOPSY and TE				
Biopsy (n)	**Transient Elastography (n)**	**% Correlation Biopsy - TE**	**Range of Fibrosis Stage by TE**	**p value**
Stage 0 (27)	Stage 0 (8)	29.6%	0 - 4	< 0.0001
Stage 1 (22)	Stage 1 (3)	13.6%	0 - 4	0.002
Stage 2 (14)	Stage 2 (5)	35.7%	0 - 3	
Stage 3 (6)	Stage 3 (1)	16.7%	0 - 4	
Stage 4 (11)	Stage 4 (8)	72.7%	0 - 8	
Not available (1)				
BIOPSY and SWE				
Biopsy (n)	**Shear Wave Elastography (n)**	**% Correlation Biopsy - SWE**	**Range of Fibrosis Stage by SWE**	**p value**
Stage 0 (7)	Stage 0 (2)	28.6%	0 - 3	0.013
Stage 1 (7)	Stage 1 (6)	85.7%	1 - 1	
Stage 2 (6)	Stage 2 (0)	0.0%	0 - 3	

Figure 1 - 1057

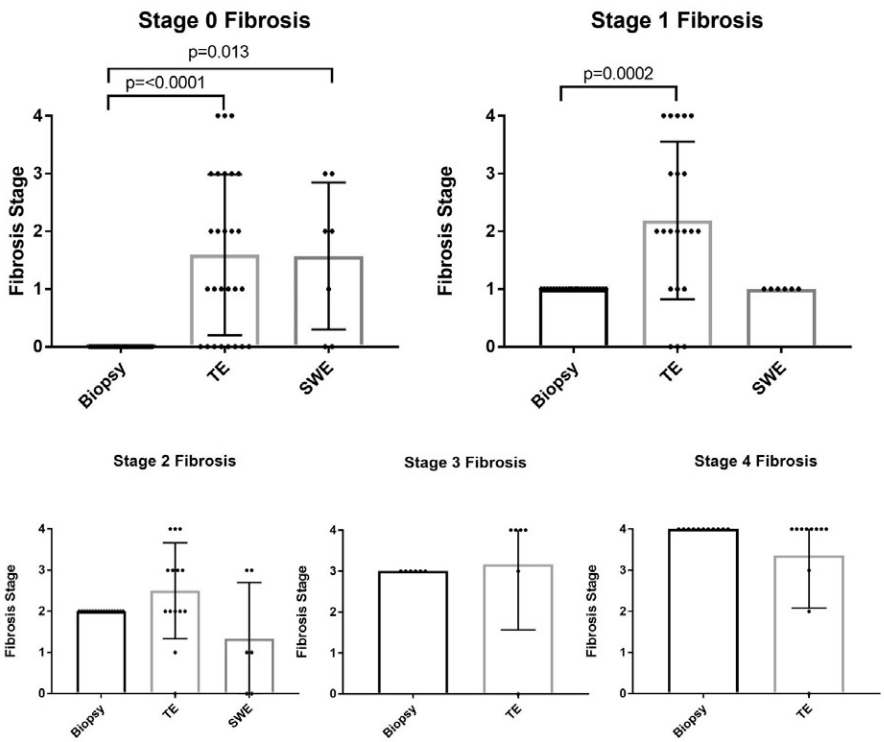

Conclusions: Although non-invasive methods for liver fibrosis assessment are available, it should be interpreted with caution. With the possibility of potential selection bias notwithstanding, these results indicate the low concordance with elastography, raising consideration of accurate stage confirmation by biopsy as clinically appropriate.

1058 Hepatocellular Carcinoma and the Imperative Role of Liver Biopsy versus Radiology Alone for the Milan Criteria and Liver Transplantation

Byoung Uk Park[1], Katherine Amarell[2], Benjamin Fisher[2], Kyungmin Ko[3], Bhaskar Kallakury[4]
[1]MedStar Georgetown University Hospital, Washington, DC, [2]Georgetown University School of Medicine, Washington, DC, [3]MedStar Georgetown University Hospital, Alexandria, VA, [4]Georgetown University Hospital, Washington, DC

Disclosures: Byoung Uk Park: None; Katherine Amarell: None; Benjamin Fisher: None; Kyungmin Ko: None; Bhaskar Kallakury: None

Background: Transplantation is considered an excellent option as it treats both hepatocellular carcinoma (HCC) and underlying liver disease. The Milan criteria are currently widely utilized to identify patients who qualify for liver transplantation following their diagnosis of HCC. Therefore, it is of interest that the Milan criteria do not require tissue diagnosis of HCC, but its diagnosis can be solely based on the radiologic assessment of the lesion. This study aims determine a discrepancy between radiology and pathology's diagnosis, number, and size of the tumor nodules.

Design: Retrospectively, all patients who underwent MRI and/or CT evaluation and available liver tissue for histologic analysis between January 2017 and July 2019 have been reviewed following approval by Institutional Review Board (#STUDY00001257). The following terms were utilized within the radiology and pathology reports to identify the patients of interest: hepatocellular carcinoma, HCC, and LI-RADS.

Results: The search revealed a total of 81 patients who were diagnosed with either high probability (LI-RADS 4; n=17 (21%)) or 100% certainty (LI-RADS 5; n=64 (79%)) of HCC by MRI and/or CT. The mean age was 64 (range: 20-80) with a male to female ratio of 3.5:1. The number of patients with pertinent history are as follows: alcoholism 13 (16%), non-alcoholic steatohepatitis 12 (15%), cirrhosis 70 (86%), Hepatitis B virus 16 (20%) and Hepatitis C virus 45 (56%). Of the 81 patients, only 72 patients (89%) correlated with the histologic diagnosis of HCC. In the remaining 9 cases (11%), the tissue diagnosis was either benign (5), cholangiocarcinoma (2), or hepatocholangiocarcinoma (2). The difference in the number of lesions between radiology and pathology reports ranged from -2 to 4, and the size difference ranged from -2.8 to 5.8 cm.

Table 1. Radiology and Pathology characteristics

		Frequency and Average
Radiology characteristics	MRI Only	60 (74%)
	CT Only	10 (12%)
	Both MRI and CT	11 (14%)
	LI-RAD 4	17 (21%)
	LI-RAD 5	64 (79%)
Pathology characteristics	HCC	72 (89%)
	Other*	9 (11%)
	Average histologic grade of HCC	2 (Range: 1 to 4)
	Lymphovascular invasion	9 (11%)
Average number of lesion by pathology		1.5 cm
Average difference in the number of lesions by Pathology and Radiology		- 0.1 cm (Range: -2 to 4 cm)
Average size of lesion by pathology**		3.8 cm
Average difference in the size of lesion by Pathology and Radiology		0.2 cm (Range: -2.8 to 5.8 cm)
*Pathology diagnosis other than HCC included: benign, cholangiocarcinoma, or hepatocholangiocarcinoma		
**In cases with multiple lesions, the largest lesion size was utilized to calculate the average/mean and the difference.		

Conclusions: Despite available non-invasive methods for diagnosing HCC, histologic confirmation via liver biopsy should be obtained before considering a critical and life-altering procedure such as liver transplantation. In addition to the accurate diagnosis for MELD scoring and organ allocation, the biopsy will allow assessment of proven prognostic factors such as histologic grading, detection of lymphovascular invasion, and molecular analysis for possible targeted molecular therapies. In summary, radiology alone may not be sufficient for global assessment of HCC, and liver biopsy should be obtained if there are no contraindications and be an integral part of the widely utilized Milan criteria.

1059 Histologic Features Can Help Suggest Site of Origin For Primary and Secondary Neuroendocrine Neoplasms Involving the Liver

Masa Peric[1], Simon Lamothe[2], Raul Gonzalez[1]
[1]Beth Israel Deaconess Medical Center, Harvard Medical School, Boston, MA, [2]Beth Israel Deaconess Medical Center, Boston, MA

Disclosures: Masa Peric: None; Simon Lamothe: None; Raul Gonzalez: None

Background: Neuroendocrine neoplasms (NENs) involving the liver are almost always metastatic. There exist limited data on primary hepatic neuroendocrine neoplasms (phNENs), which were recently added to the WHO classification of digestive system tumors. No morphologic or immunohistochemical markers have been established as indicating hepatic origin. This study aimed to characterize clinicopathologic features of primary and metastatic NENs involving the liver.

Design: We searched departmental archives for cases of NENs involving the liver with available slides. We classified cases as neuroendocrine tumor (NET) or neuroendocrine carcinoma (NEC) and recorded histologic and immunohistochemical features. We reviewed medical records for clinical features, including primary site for each case, then categorized cases by primary site and compared clinicopathologic features to establish correlations between histologic features and sites of origin, with statistical significance set at $P<0.05$.

Results: We identified 133 cases from 62 men and 71 women, with a mean age of 63 years. Clinical investigation yielded a confirmed extrahepatic site of origin for 115 (86%) cases (39 pancreas, 33 lung, 24 small bowel, 7 colorectal, 12 others). The remaining 18 (13%) included 15 clinically considered metastatic but with no identifiable primary site, and 3 considered likely phNEN (Table). Metastatic NEC in the liver were more likely to originate from the lung (P<0.0001), consistent with the known propensity of NEC to arise there. NEC arising in the pancreas were less likely to show necrosis in comparison to other sites (P=0.022, Fig 1A-1B). The most common primary site for metastatic NET was the pancreas (n=34). NETs showing nested architecture were more likely to originate in the small bowel (P=0.013, Fig 1C). Two phNET samples (1 NET, 1 NEC) showed an architecture of discohesive cells in a striking background of blood (Fig 2A) and demonstrated large cytoplasmic granules (Fig 2B).

Correlations between histologic features and sites of origin

Total cases (n = 133)	Lung (n =33, 24%)	Pancreas (n = 39, 29%)	Small bowel (n = 24, 18%)	Colorectum (n = 7, 5%)	Other sites (n = 12, 9%)	No primary found (n = 15, 11%)	PHNEN (n = 3, 2%)	*P*-value
Diagnosis								
NET	5 (15%)	34 (87%)	24 (100%)	6 (86%)	6 (50%)	12 (80%)	1 (33%)	***P* < 0.0001**
NEC	28 (85%)	5 (13%)	0 (0%)	1 (14%)	6 (50%)	3 (20%)	2 (67%)	
Architecture								
Nested	20 (61%)	15 (38%)	18 (75%)	3 (43%)	6 (50%)	6 (40%)	1 (33%)	***P* = 0.036**
Trabecular	8 (24%)	14 (36%)	6 (25%)	3 (43%)	3 (25%)	2 (13%)	0 (0%)	
Sheets	5 (15%)	10 (26%)	0 (0%)	1 (14%)	3 (25%)	7 (47%)	2 (67%)	
Chromatin								
Salt & pepper	1 (3%)	7 (18%)	5 (21%)	1 (14%)	3 (25%)	3 (20%)	0 (0%)	***P* = 0.033**
Prominent nucleoli	3 (9%)	11 (28%)	0 (0%)	5 (72%)	0 (0%)	1 (7%)	1 (33%)	
Bland / other	29 (88%)	21 (54%)	19 (79%)	1 (14%)	9 (75%)	11 (73%)	2 (67%)	
Mitotic rate								
Low (<2/10 HPF)	4 (12%)	17 (44%)	16 (67%)	2 (29%)	7 (58%)	7 (47%)	0 (0%)	***P* = 0.0001**
Intermediate (2-20/10 HPF)	9 (27%)	15 (38%)	8 (33%)	4 (57%)	2 (17%)	2 (13%)	1 (33%)	
High (>20/10 HPF)	20 (61%)	7 (18%)	0 (0%)	1 (14%)	3 (25%)	6 (40%)	2 (67%)	
Tumor necrosis								
None	5 (15%)	30 (76%)	18 (75%)	5 (71%)	4 (33%)	10 (67%)	1 (33%)	***P* <0.0001**
Focal	9 (27%)	8 (21%)	6 (25%)	1 (14%)	3 (25%)	2 (13%)	1 (33%)	
Diffuse	19 (58%)	1 (3%)	0 (0%)	1 (14%)	5 (42%)	3 (20%)	1 (33%)	

Figure 1 - 1059

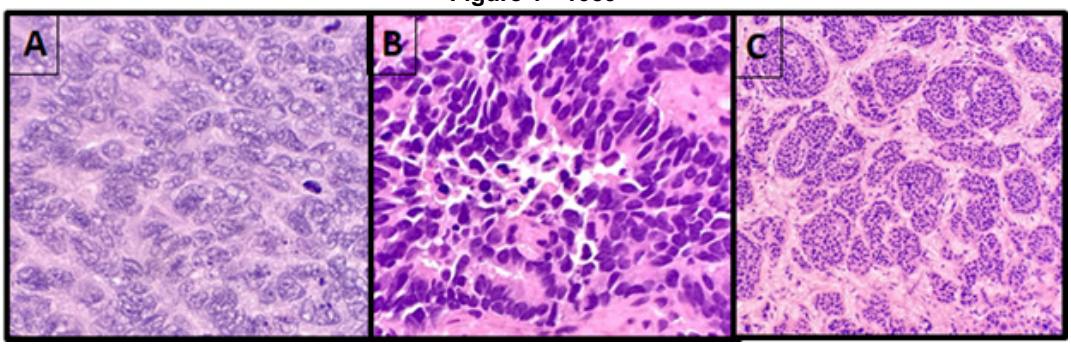

Figure 2 - 1059

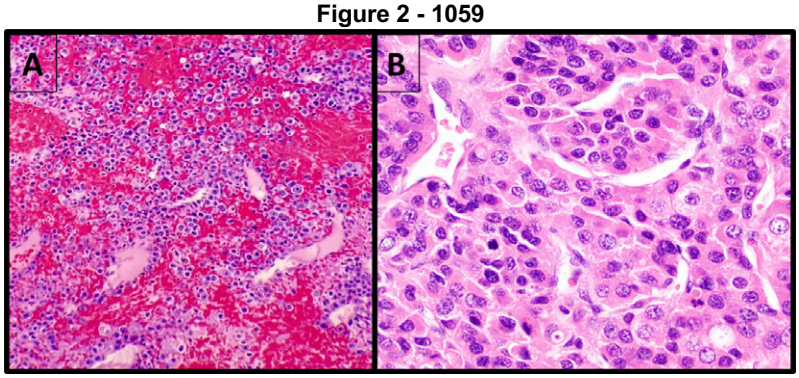

Conclusions: Our study suggests that hepatic NENs show histologic features that often correlate with site of origin, which could be a useful tool in the workup of NEN metastatic to the liver. While phNEN are indeed rare, we observed that sampling often yielded discohesive cells with large granules in a bloody background, which was rarely seen in confirmed metastatic cases. This is consistent with a prior report that phNENs show areas of liquefaction on CT scan and therefore should raise the possibility of phNEN when encountered.

1060 Nivolumab-Induced Liver Injury in the Post-Transplant Setting

Alex Placek[1], Gabriel Schnickel[1], Yuko Kono[1], Andreas Ciscato[2], Mojgan Hosseini-Varnamkhasti[2]
[1]UCSD Medical Center, La Jolla, CA, [2]University of California, San Diego, La Jolla, CA

Disclosures: Alex Placek: None; Gabriel Schnickel: None; Yuko Kono: None; Andreas Ciscato: None; Mojgan Hosseini-Varnamkhasti: None

Background: The utilization of immune checkpoint inhibitors continues to expand. There is limited data on the safety and consequences of checkpoint inhibitors in the post-transplant setting. Our study highlights our institution's experience with patients who received Nivolumab in the community prior to being referred to us for liver transplantation.

Design: Following IRB approval, a retrospective review of archives identified 5 patients who received Nivolumab for hepatocellular carcinoma (HCC) prior to liver transplantation from 2018-2021. The allograft liver biopsies and hepatectomy slides were reviewed and scored for acute cellular rejection, atypical rejection, steatosis (NAS), necrosis, and fibrosis. Immunohistochemical stains were used in evaluation of inflammatory infiltrate.

Results: We identified five patients who received Nivolumab for HCC and cirrhosis prior to liver transplantation (see table 1). Two of the 5 suffered hepatic necrosis within a few weeks of transplantation. Biopsies showed confluent to bridging centrizonal necrosis, severe obliterative endotheliitis of the central veins and mild endotheliitis of the portal veins. There was no bile duct injury or significant portal inflammation (Figure 1). One patient required urgent re-transplantation. Explanted allograft shows panacinar necrosis, severe venous endotheliitis and lymphocytic arteritis. IHC demonstrated predominance of CD4+ T lymphocytes in the endotheliitis and arteritis. PD-1 was positive in the lypmohocytes, PDL-1 in the surviving endothelial cells. The two patients with hepatic necrosis had received their last dose of Nivolumab 10 and 35 days prior to transplant, while the other 3 with better post-transplant outcomes, received their last dose greater than 3 months prior.

Figure 1: Marked centrizonal necrosis (Left), Severe centrizonal vaculitis with pericentral encrosis (Right).

	A	B	C	D	E
Age at transplant	61	65	71	65	68
Gender	Female	Male	Male	Female	Male
Etiology	HCV	HCV	HBV	HCV	HCV
Cirrhosis	Yes	Yes	Stage 2/4	Yes	Yes
Duration of Nivolumab	18 months	8 months	8 months	12 months	12 months
Time from last treatment to transplant	5 weeks	10 days	3 months	4 months	6 months
Time to rising AST/ALT	10 days	12 days	n/a	n/a	n/a
Induction IS	None	rATG	rATG	rATG	none
Time to first biopsy	12 days	14 days	n/a	n/a	7 days
First biopsy result	Acute cellular rejection (RAI 4/9) with 60% necrosis	Acute cellular rejection (RAI 5/9)	n/a	n/a	Cholestasis, No ACR
Treatment	rATG, steroid pulse, plasmapheresis, IVIG	rATG, steroid pulse, rituximab, IVIG	n/a	n/a	none
Subsequent pathology	Massive hepatic necrosis	20% hepatic necrosis	n/a	n/a	Cholestasis, No ACR
Graft outcome	Graft failure with Re-transplant	Salvaged	Stable graft function	Stable graft function	Stable graft function
Patient outcome	Alive	Alive	Alive	Alive	Deceased
Follow up time	33 months	10 months	11 months	8 months	2 months

rATG: anti-thymocyte globulin

Figure 1 - 1060

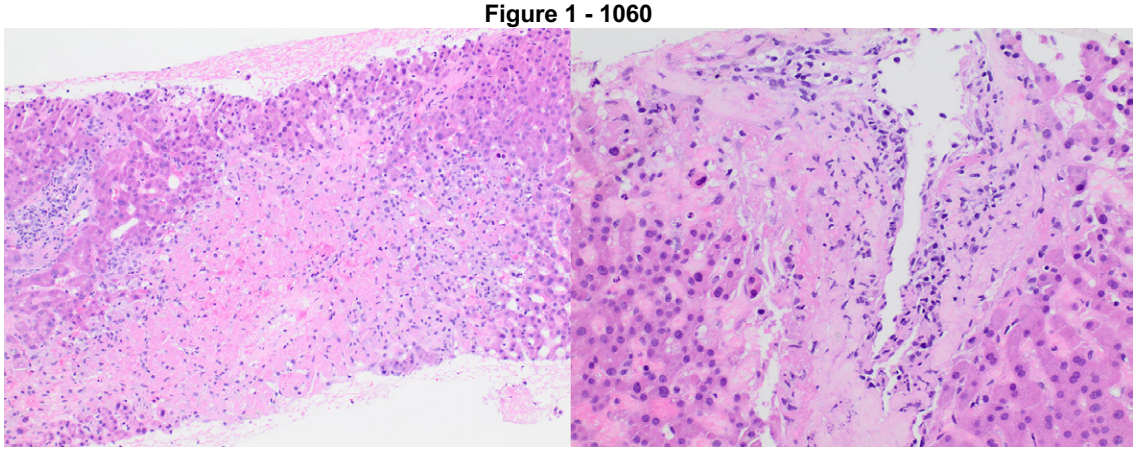

Conclusions: We identified two cases of allograft necrosis in patients who received Nivolumab for HCC prior to transplantation. In our patient's biopsies, the findings suggest an immune-mediated destruction of the central veins, while the portal veins and arteries were involved only in the more severe case. In the setting of liver transplantation, the time of last dose of Nivolumab should be considered.

1061 Prognostic Impact of FGFR2 Alterations in Biliary Tract Cancers Patients Receiving Systemic Chemotherapy: the BITCOIN Study

Mario Domenico Rizzato[1], Stefano Brignola[2], Giada Munari[1], Maura Gatti[1], Vincenzo Dadduzio[1], Chiara Borga[3], Francesca Bergamo[1], Antonio Pellino[1], Valentina Angerilli[3], Claudia Mescoli[4], Maria Guido[3], Enrico Gringeri[3], Cillo Umberto[3], Marta Sbaraglia[5], Angelo Dei Tos[6], Vittorina Zagonel[1], Fotios Loupakis[7], Sara Lonardi[1], Matteo Fassan[6]
[1]Istituto Oncologico Veneto IOV - IRCCS, Padova, Italy, [2]Treviso General Hospital, Treviso, Italy, [3]University of Padova, Padova, Italy, [4]University and Hospital Trust of Padova, Italy, [5]Azienda Ospedaliera Padova, Italy, [6]University of Padua, Padua, Italy, [7]AstraZeneca, Milano, Italy

Disclosures: Mario Domenico Rizzato: None; Stefano Brignola: None; Giada Munari: None; Maura Gatti: None; Vincenzo Dadduzio: *Consultant*, MSD, Bayer, Ipsen, Eisai; Chiara Borga: None; Francesca Bergamo: None; Antonio Pellino: None; Valentina Angerilli: None; Claudia Mescoli: None; Maria Guido: None; Enrico Gringeri: None; Cillo Umberto: None; Marta Sbaraglia: None; Angelo Dei Tos: None; Vittorina Zagonel: None; Fotios Loupakis: *Employee*, AstraZeneca; Sara Lonardi: *Consultant*, Amgen, Merck Serono, Lilly, Astra Zeneca, Incyte, Daiichi-Sankyo, Bristol-Myers Squibb, Servier, MSD; *Speaker*, Pierre-Fabre, GSK; Matteo Fassan: *Grant or Research Support*, Astellas Pharma, Macrophage pharma, QED Therapeutics; *Advisory Board Member*, Astellas Pharma; *Consultant*, Diaceutics, GSK, Roche, MSD

Background: *FGFR2* rearrangements have been identified as a novel therapeutic target of biliary tract cancer (BTC). However, reliable prevalence estimates of this molecular alteration and its prognostic role have not been fully elucidated.

Design: A retrospective mono-institutional series of 286 patients affected by locally advanced or metastatic BTC (183 intrahepatic cholangiocarcinomas, 67 extrahepatic cholangiocarcinomas, 36 gallbladder carcinomas) was profiled by means of targeted DNA/RNA NGS sequencing, immunohistochemistry, and FISH for *FGFR2/3*, *ERBB2*, *NTRK* alterations, *IDH1/2* and *BRAF* mutations and DNA mismatch repair complex proteins alterations/microsatellite instability (MMRd/MSI).

Results: *FGFR2* rearrangements, amplifications and point mutations were detected in 15 (5.2%), 1 and 3 cases, respectively. *FGFR3* alterations were observed in 5 (1.7%) cases. *IDH1/2* were mutated in 35/223 cases (15.7%). A total of 9/258 (3.5%) and 6/260 (2.3%) BTCs had *ERBB2* and *BRAF* gene alterations, respectively. Two cases (2/242; 0.8%) had *NTRK1* amplifications but no rearrangement was found. A deficit of mismatch repair protein expression was identified in 9/237 cases (3.8%). At multivariate analysis, age, ECOG performance status, number of metastatic sites, tumor stage, *FGFR2/3* alterations and *IDH1/2* mutations were prognostic factors of overall survival.

Conclusions: These data provide a strong proof - challenged with a robust and detailed multivariate model - that *FGFR2/3* aberrations (including *FGFR2* rearrangements) and *IDH1/2* mutations can be prognostic for better survival in BTC patients. The recognition and the measurement of their prognostic impact could be of primary importance for the correct interpretation of currently available data and in the design of new therapeutic trials.

1062 Portal Vascular Changes and Nodular Regenerative Hyperplasia in Common Variable Immunodeficiency and X-linked Agammaglobulinemia

Ryan Sappenfield[1], Kathleen Byrnes[1]
[1]Washington University in St. Louis, St. Louis, MO

Disclosures: Ryan Sappenfield: None; Kathleen Byrnes: None

Background: Common variable immunodeficiency (CVID) and X-linked agammaglobulinemia (XLA) encompass a broad spectrum of clinical manifestations and frequently involve the liver. Histologically, hepatic CVID has been associated with a wide variety of lesions, most notably nodular regenerative hyperplasia (NRH). In contrast, other histologic features associated with idiopathic non-cirrhotic portal hypertension (INCPH)/porto-sinusoidal vascular disease (PSVD) have not been well-characterized in patients with XLA and NRH.

Design: A retrospective review of all available archival cases of NRH was performed. Our cohort included cases with confirmed documentation of a primary hypogammaglobinemia. Histologic slides were examined, and demographic, clinical, and laboratory data were recorded from the electronic medical record.

Results: A total of 236 cases of NRH were identified at our institution between 1990 and 2021. From these, we reviewed five liver biopsies from four patients with an established diagnosis of CVID and one patient with XLA. The median age was 47 years, and the majority of patients were men (80%). Liver function tests were frequently abnormal, especially alkaline phosphatase (median: 286 IU/L), which was elevated in all five cases. All patients showed manifestations of portal hypertension, including ascites (*n* = 4), splenomegaly (*n* = 4), thrombocytopenia (*n* = 3), and esophageal varices (*n* = 2). All cases showed NRH-like changes, confirmed by reticulin stain. Four biopsies showed portal vascular changes associated with INCPH/PSVD characterized by portal vein sclerosis. Four cases displayed mild to moderate chronic portal inflammation. Plasma cells were generally absent. Additional findings included mild pericellular fibrosis (*n* = 2), macrovesicular steatosis (*n* = 1), and focal non-necrotizing granulomas (*n* = 1). Follow-up data was available for three patients with a median follow-up time of 6 months. Two patients with portal vascular changes associated with INCPH/PSVD showed progressive portal hypertension, while the one patient without these changes died with disease.

Case	Sex	Age (years)	Primary hypogammaglobinemia	Elevated LFTs	Portal hypertension	Portal vascular changes associated with INCPH/PSVD	Follow-up (months)	Outcomes
1	M	31	XLA	Yes	Yes	No	6	Deceased (invasive aspergillosis)
2	M	36	CVID	Yes	Yes	Mild portal vein sclerosis	0	N/A
3	M	60	CVID	Yes	Yes	Mild portal vein sclerosis	0	N/A
4	M	47	CVID	Yes	Yes	Mild portal vein sclerosis	60	Progressive portal hypertension
5	F	75	CVID	Yes	Yes	Moderate portal vein sclerosis	3	Progressive portal hypertension

Figure 1 - 1062

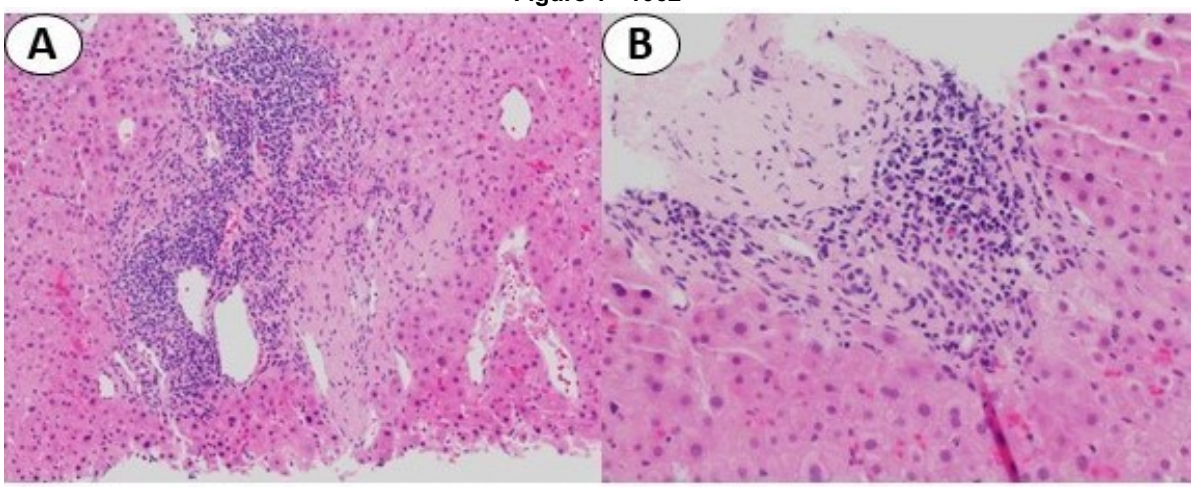

Figure 1. Portal vascular changes associated with INCPH/PSVD in the setting of CVID and NRH-like changes. (A) Portal vein sclerosis, 200x (B) Portal vein sclerosis, 400x

Conclusions: Portal vascular changes associated with INCPH/PSVD are common in patients with primary hypogammaglobinemia and NRH-like changes. It is unclear whether these findings coupled with NRH-like changes lead to faster disease progression and adverse outcomes. However, the presence of portal inflammation in conjunction with PSVD/NRH changes should prompt one to confirm a clinical history of CVID or XLA.

1063 Molecular Features of Hepatic Adenomas with Malignant Transformation

Nima Sharifai[1], Fahad Khan[2], Hsiang-Chih (Sean) Lu[3], Kathleen Byrnes[1]
[1]Washington University in St. Louis, St. Louis, MO, [2]Barnes-Jewish Hospital/Washington University, St. Louis, MO, [3]Diagnostic Pathology Medical Group, Inc, Sacramento, CA

Disclosures: Nima Sharifai: None; Fahad Khan: None; Hsiang-Chih (Sean) Lu: None; Kathleen Byrnes: None

Background: Hepatic adenomas (HCA) are benign neoplasms typically occurring in young women. Malignant transformation is rare, occurring in 5% of HCAs, with some cases being associated with *CTNNB1* and *TERT* promoter mutations. With expanding genetic sequencing panels, additional drivers of malignant transformation may be uncovered.

Design: A retrospective review of records and slides from 1990-2018 was performed to identify HCAs with malignant transformation. 7 cases with formalin fixed paraffin blocks (FFPE) and H&E slides were included. Reticulin, LFABP, beta-catenin, glutamine synthetase, serum amyloid A, and CRP were reviewed when available. FFPE tissue cores from paired HCAs/hepatocellular carcinomas (HCCs) were used for targeted hybridization capture-based next-generation sequencing using the MSK-IMPACT panel (498 genes).

Results: The majority of tumors occurred in women (n=5) with a mean age of 45 years (range: 26-69). All patients had a solitary mass identified prior to partial hepatectomy. The HCAs were subclassified as inflammatory (n=3), HNF1a-inactivated (n=1), and unclassified (n=3). The HCCs ranged from stage pT1 (n=5), pT2 (n=1), to ypT4 (n=1). Malignant transformation was multifocal in 3 cases (Table 1).

Molecular analysis showed multiple gene mutations including *TERT* promoter (n=2), *CTNNB1* (n=2), and *MRE11* (n=2). *TERT* promoter mutations were only seen in HCC, whereas *CTNNB1* and *MRE11* were seen in paired HCA/HCC. *CTNNB1* and *TERT* promoter mutations were identified in all multifocal HCCs. One I-HCA had a *KMTC2-HILPDA* fusion that was not noted in the paired HCC.

Copy number analysis showed amplification of *AR* (n=4), *CDK4* (n=1), and *GLI1* (n=1). One HCC gained amplifications in *CDK4* and *GLI1* and one gained an *AR* amplification. Mutations and copy number variations did not correlate to subtype of HCA. One patient developed metastatic HCC and recurrence after surgery (follow up range: 7-113 months).

		Age/ Gender	Number of Tumors	Subtype of HCA	Size of tumor	Gene Mutations/Fusions	Copy Number Alterations	Recurrence
Case 1	HCA	37 M	Single	Inflammatory with beta-catenin activation	18.5 cm		RECQL4, ZFHX3, ARID5B, NF2	No evidence of disease
	HCC		Single				RECQL4, ARID5B, NF2	
Case 2	HCA	55 F	Single	Unclassified	20 cm	KMT2C-HILPDA fusion		Metastatic HCC
	HCC		Single				AR, PRKN, PTPRT, POT1	
Case 3	HCA	38 F	Single	Unclassified	8.5 cm		AR, GATA3	No evidence of disease
	HCC		Single				AR, DAXX	
Case 4	HCA	26 F	Single	Inflammatory	10.1 cm	CTNNB1 N387K, MRE11 X36_splice	AR, BRD4, AKT2, AXL, PIK3R2, CCNE1, MEF2B, RUNX1, POT1, BBC3	No evidence of disease
	HCC		Multifocal			CTNNB1 N387K, MRE11 X36_splice, SOX9 C72Lfs*38	AR, BCL10	
Case 5	HCA	69 F	Single	HNF1A-mutated/pigmented adenoma	3.6 cm	RECQL S620*	AR, CDK4, GLI1, CBFB	No evidence of disease
	HCC		Single			RECQL S620*	AR, CDK4, GLI1, CYLD, IKZF1, HLA-A	
Case 6	HCA	40 M	Single	Unclassified	9.5 cm	MRE11 X36_splice	CYLD	No evidence of disease
	HCC		Multifocal			TERT Promoter 5'flank, MRE11 X36_splice	CYLD, MAPK3	
Case 7	HCA	48 F	Single	Inflammatory	7.2 cm	CTNNB1 S45P	AR	No evidence of disease
	HCC		Multifocal			CTNNB1 S45P, TERT Promoter 5'flank, PIK3CA H1047R, KMT2A T3069Rfs*9	AR, CDK4, ERBB3, GLI1	

Conclusions: The presence of *CTNNB1* and *TERT* promoter mutations confirms previously reported findings, and corresponded to cases with multifocal malignant transformation in our cohort. These cases did not portend a worse prognosis. Amplification of *AR* (androgen receptor) is a novel finding in paired HCA/HCC. *AR* has been previously implicated in hepatocarcinogenesis, but is not well described in HCAs. This raises the possibility that detection of *AR* amplification in HCAs could indicate a higher risk of transformation. Further analysis of benign HCAs could help further discern this risk.

1064 Clinical Implications of Liver Transplantation Associated with Preoperative HLA Antibody Status

Minqian (Jasmine) Shen[1], Maria Betinotti[2], Robert Anders[3], Ahmet Gurakar[3], Kiyoko Oshima[4]
[1]Johns Hopkins Hospital, Baltimore, MD, [2]Johns Hopkins Hospital School of Medicine, Baltimore, MD, [3]Johns Hopkins University, Baltimore, MD, [4]Johns Hopkins University School of Medicine, Baltimore, MD

Disclosures: Minqian (Jasmine) Shen: None; Maria Betinotti: None; Robert Anders: None; Ahmet Gurakar: None; Kiyoko Oshima: None

Background: Human leukocyte antigen (HLA) compatibility is important for successful liver transplantation, thus pre- and post-transplantation HLA cross-match is routinely recommended. The presence of donor-specific antibody (DSA) alerts for the increased risk of antibody-mediated rejection (AMR); however, HLA cross-match may also detect antibodies to non-donor antigen or DSA below reactivity levels. The aim of this study is to evaluate the risk of developing AMR or AMR overlapping acute cellular rejection (ACR) in the liver transplant patients with abnormal preoperatively HLA antibody status.

Design: All liver transplant recipients from 1/1/2017 to 5/6/2021 were included in the study (n=361). All pre- and post-transplant HLA cross-match compatibility results, post-transplant liver pathology reports and electric medical records were reviewed. In addition, C4d immunohistochemical staining was performed in all ACR with/without AMR. C4d score is based on the percentage of positive portal vascular staining (0: no staining; minimal: <10%; focal: 10%-50%, and diffuse: >50%).

Results: Total 77 liver transplants recipients received post-transplant liver biopsies for allograft dysfunction. Preoperatively, 10 patients (13.0%) had significant levels of DSA, 21 patients (27.3%) had presence of DSA below reactivity levels, 8 patients (10.4%) had non-donor antigen antibody, 32 patients (41.5%) had no antibody, 6 patients (7.8%) had no preoperative data. Three of 10 patients (30%) with significant positive DSA developed overlapping AMR/ACR and 6 of 10 patients (60%) developed ACR while C4d score was either negative or focal in both groups. One of 21 patients (4.8%) with DSA below reactivity levels developed AMR/ACR with focal C4d score. Ten of 21 patients (47.6%) developed ACR with negative or minimal C4d score. Three of those 10 patients that developed ACR also developed *de novo* DSA below reactivity levels with negative to minimal C4d score. Four of 8 patients (50%) with positive non-donor antigen antibody developed ACR, 1 with focal C4d score and 3 patients with negative C4d score; and 2 developed *de novo* non-donor antigen antibody with negative C4d score. None of the patients with negative DSA developed *de novo* DSA. [Table 1]

	Non-donor antibody (n=8)	DSA below reactivity levels (n=21)	Significant DSA (n=10)
ACR	4 (50%)	10 (47.6%)	6 (60%)
AMR/ACR	0	1 (4.8%)	3 (30%)
C4d Score	negative to focal (0%-14%)	negative to focal (0%-10%); Focal (40%) for AMR case	Negative to focal (0%-30%); same range for AMR
De novo antibody	2 (25%)	3 (14.3%)	N/A
Increased antibody level	0	0	2 (20%)

Conclusions: Although DSA below reactivity levels or positive for non-donor antibody usually indicates low risk of AMR, we found 14-25% of these patients developed *de novo* antibody after transplantation with 4.8% to develop combine AMR/ACR.

1065 Post-Infantile Giant Cell Hepatitis: A Histological and Etiological Perspective from a Single Center

Krithika Shenoy[1], Neal Andruska[1], Kathleen Byrnes[2]
[1]Barnes-Jewish Hospital/Washington University, St. Louis, MO, [2]Washington University in St. Louis, St. Louis, MO

Disclosures: Krithika Shenoy: None; Neal Andruska: None; Kathleen Byrnes: None

Background: Giant cell hepatitis (GCH) is a well-described pattern of liver injury in infants, but its occurrence in adults is exceedingly rare, with less than 100 documented cases. Histologically it is characterized by multinucleated hepatocytes associated with features of hepatitis including lobular/portal inflammation and, occasionally, hepatocyte dropout. We present our institutional experience with this rare entity, describing possible etiologies, associated histologic findings, and outcomes.

Design: A retrospective review of medical records and pathology database (1990-2020) was performed to identify cases of adult GCH. The hematoxylin-eosin slides, reticulin, and trichrome stains were reviewed. Hepatocyte giant cells were defined as multinucleated hepatocytes with ≥ 4 nuclei per cell. The zonal distribution of giant cells was noted and quantitatively scored (1= <5; 2= 5-10; 3= >10 giant cells; Figure 1). Histologic parameters were recorded including: portal/lobular inflammation, degree of hepatocyte necrosis (single-cell dropout; zone 3; bridging; submassive), cholestasis, steatosis, bile duct injury, and degree of fibrosis.

Results: Of the 62 cases (50 biopsies; 12 explants), 52 cases were from native livers and 10 from allograft livers. There were more women (male:female=1:1.7) with a mean age of 46 years (range: 19-71 years). The most common etiology was autoimmune (n=26), followed by drug induced liver injury (21%; n=13), and viral hepatitis (18%; n=11). In the autoimmune cases, 46% had overlap features (n=12). Giant cells were either azonal (n=36; 58.1%), centrilobular (n=15; 24.2%), or periportal (n=8; 12.9%). Giant cells were prominent (score 3; >10 giant cells) in 23 cases (37.1%). Bile duct injury, interface activity, and cholestasis were more commonly seen in autoimmune cases (Table 1). The presence of bile duct injury was significantly associated with autoimmune overlap when compared to autoimmune hepatitis cases (p = 0.019; 95%CI: 0.16-0.57). The presence of hepatocyte loss correlated to worse prognosis and overall survival (Figure 2).

Table 1: Histologic findings associated with etiology

Histologic findings	**Autoimmune etiology** **n (%)**	**Others** **n (%)**	***p* (95% CI: Upper; Lower)**
Giant cell distribution			**0.008*** (0.29; 0.64)
Azonal	21 (80.8)	15 (41.7)	
Periportal (Zone 1)	3 (11.5)	5 (13.9)	
Zone 2	1 (3.8)	2 (5.6)	
Centrilobular (Zone 3)	1 (3.8)	14 (38.9)	
Giant cell score			0.702 (0.03; 0.37)
Score 1 (<5 giant cells)	11 (42.3)	16 (44.4)	
Score 2 (5-10 giant cells)	4 (15.4)	8 (22.2)	
Score 3 (>5 giant cells)	11 (42.3)	12 (33.3)	0.416 (0.01-0.36)
Bile duct injury	15 (57.7)	17 (47.2)	0.130 (0.01, 0.39)
Portal inflammation	26 (100)	35 (97.2)	0.392 (0.09; 0.22)
Interface activity	26 (100)	20 (55)	**<0.001*** (0.36; 0.64)
Lobular inflammation	24 (92.3)	25 (69.4)	**0.029*** (0.04; 0.49)
Hepatocyte dropout			0.062 (0.25; 0.61)
Single cell dropout	12 (46.2)	11 (30.6)	
Bridging necrosis	5 (19.2)	2 (5.6)	
Zone 3 necrosis	1 (3.8)	7 (19.4)	
Submassive necrosis	6 (23.1)	7 (19.4)	
Cholestasis	24 (92.3)	20 (55.6)	**0.002*** (0.21; 0.59)
Steatosis	3 (11.5)	5 (13.9)	0.785 (0.01; 0.27)
Fibrosis			0.124 (0.24; 0.65)
No fibrosis	9 (45.0)	4 (14.3)	
Portal and periportal fibrosis	4 (20.0)	8 (28.6)	
Perivenular fibrosis	0 (0)	2 (7.1)	
Bridging fibrosis	3 (15.0)	9 (32.1)	
Cirrhosis	4 (20.0)	5 (17.9)	
* significant *p* value			

Figure 1 - 1065

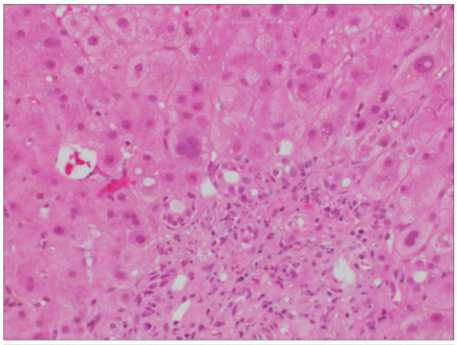

Figure 1A: A case of biliary obstruction with giant cell hepatocytes (score 1), distributed in zone 1 (40X)

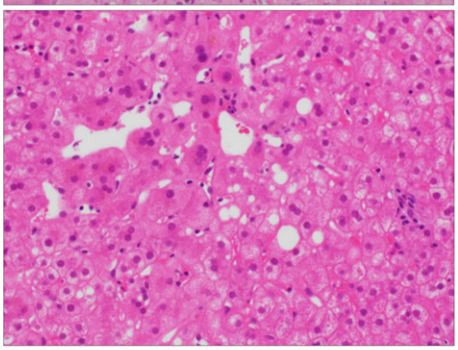

Figure 1B: A case of chronic hepatitis C with giant cell hepatocytes (score 2), distributed in zone 3 (40X)

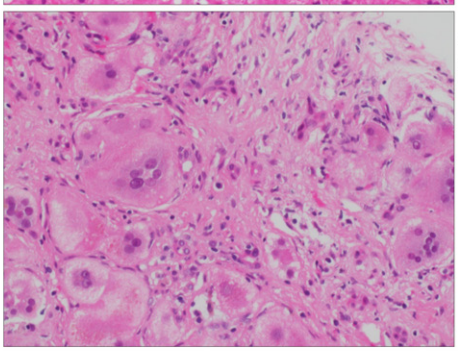

Figure 1C: A case of syncytial giant cell hepatitis from paramyxovirus infection, with giant hepatocytes (score 3) in an azonal distribution (40X)

Figure 2 - 1065

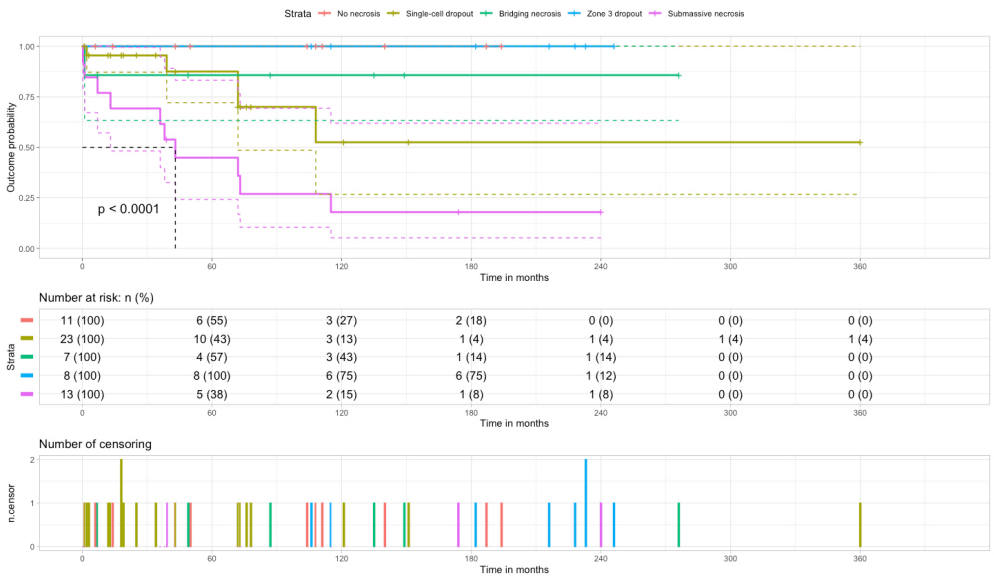

Conclusions: GCH in adults is an uncommon pattern of injury to a variety of etiologies, with autoimmune diseases representing more than a third of cases. Presence of bile duct injury should raise the possibility of an autoimmune overlap syndrome. The degree of necrosis in conjunction with GCH is associated with a poor prognosis and overall survival, regardless of the amount or distribution of giant cells or underlying etiology.

1066 Novel GPC-3 Targeted Therapies Require Hepatocellular Carcinoma Tissue Evaluation for GPC-3 Status: A Plea to Reinstitute Biopsy Procurement After Diagnostic Multiphase Imaging

Sindhuja Sivanandham[1], Shriram Jakate[1]
[1]Rush University Medical Center, Chicago, IL

Disclosures: Sindhuja Sivanandham: None; Shriram Jakate: None

Background: Prototypical hepatocellular carcinoma (HCC) cases that occur in the background of cirrhosis usually show elevated serum AFP and characteristic imaging features on triphasic CT and MRI. This presentation is so classical that biopsy confirmation of the mass is not currently practiced. Currently, an advanced HCC is subjected to trans-arterial chemo and/or radio embolization (TACE/TARE) without pretherapeutic tissue biopsy evaluation. Novel Glypican 3 (GPC-3) targeted molecular, gold nanocomplex gene silencing and photothermal therapies promise a more precise target and a better response rate. However, this would necessitate pretherapeutic procurement of HCC tissue to evaluate GPC-3 status. We studied the GPC-3 positivity in untreated HCC needle biopsies and in explanted livers with untreated and TACE/TARE treated residual HCCs. We also studied the success rate of TACE/TARE therapy.

Design: From our medical center's databases (2010-2021) we collected 75 explanted livers with HCCs. We reviewed the success rates of TACE/TARE therapies and GPC-3 status in untreated and selected partially treated HCCs. We also studied GPC-3 in 40 needle biopsies with HCC.

Results: At least moderate or greater intensity (Gr 2/3 or 3/3) cytoplasmic and/or membranous staining for GPC-3 was considered positive. Additionally, since the staining is patchy, 20% or more tumor cells in excised HCCs and 10% or more in needle biopsies qualified for positive GPC-3 status. 15/75 explanted livers had untreated HCC of which 14/15 (93%) were positive for GPC-3. 60/75 explanted livers with treated HCCs showed no residual tumor in 16 (27% complete response) and 44/60 showed 30-95% necrosis (73% partial response). 7/44 pretreated HCCs with residual tumors showed GPC-3 positivity in 6/7 (86%). 31/40 needle biopsies (78%) showed positive GPC-3 staining.

Conclusions: The overwhelming majority of HCC cases are positive for GPC-3 (ranging from 78% in needle biopsies and 93% in untreated explants). Thus, most patients with HCC would potentially benefit from GPC-3 targeted therapies which are likely to be superior to TACE/TARE therapies which show only 27% complete response. However, to recruit patients for GPC-3 targeted therapies, it is essential to evaluate the GPC-3 status on a needle biopsy. Hence, the practice of pretherapeutic HCC tissue procurement needs to be reinstituted.

1067 Is EBV-Associated Cholangiocarcinoma Uniformly of the Lymphoepithelial Type or Does It Exist with Other Phenotypes?

Andrew Stone[1], Oyedele Adeyi[1], Khalid Amin[1]
[1]University of Minnesota, Minneapolis, MN

Disclosures: Andrew Stone: None; Oyedele Adeyi: None; Khalid Amin: None

Background: Along with the more well-known association with post-transplant lymphoproliferative disorders (PTLD), Epstein-Barr virus (EBV) infection in the hepatobiliary system has been linked to a very rare variant of intrahepatic cholangiocarcinoma (CCC) with a lymphoepithelioma-like (LEL) morphology. While the association between EBV and LEL CCC has been established by previous case reports and small case series, a handful of EBV-positive CCC with conventional morphology have also been reported. As cholangiocarcinomas with conventional morphology are not routinely tested for EBV, the true prevalence of EBV infection in these cancers remains unknown, raising the question of the utility of testing CCC for EBV in the absence of an LEL phenotype. We set out to investigate rates of EBV infection among all CCC, and also determine other clinicopathological differences between EBV-positive versus EBV-negative tumors.

Design: After Institutional Review Board (IRB) approval, a systematic search of our institution's archival database of surgical pathology cases from 2002 to 2021 identified 40 resection specimens diagnosed as cholangiocarcinoma (22 intrahepatic/hilar, 18 extrahepatic) and 1 biopsy of an intrahepatic LEL cholangiocarcinoma with previously demonstrated EBV positivity that did not have a subsequent resection. The retrieved slides from these cases were examined, with two extrahepatic cases eliminated from consideration due to ambiguous diagnosis. To detect EBV, EBER in-situ hybridization (ISH) was performed on formalin fixed paraffin embedded sections of the 39 cases with appropriately reactive controls, utilizing kits and an automated stainer from Ventana Medical Systems.

Results: Of the 39 cases, only 2 (5.1%) showed positive intranuclear expression of EBV RNA by ISH. Both these cases demonstrated LEL morphology and occurred in Asian women. However, none of the EBV-negative CCC showed a LEL phenotype. Although limited by the small sample size, EBV-positive status did not appear to impact tumor size, stage, grade, or outcome in this cohort.

Conclusions: Our results suggest that EBV expression is rare in both intrahepatic and extrahepatic cholangiocarcinoma. When present, EBV expression appears limited to tumors with a lymphoepithelioma-like morphology, supporting the lack of a role for EBV testing in cholangiocarcinoma in general. Lastly, both patients with EBV-positive tumors in our cohort were of Asian heritage, consistent with observations from previous studies.

1068 Frequent Loss of BAP1 or ARID1A Expression Caused by Inactivating Mutations in Intrahepatic Cholangiocarcinoma (ICC) Can Help Distinguishing ICC from Metastatic Pancreatic Ductal Adenocarcinoma (PDAC) In Liver Biopsies

Tong Sun[1], Xuchen Zhang[1], Minghao Zhong[1]
[1]*Yale School of Medicine, New Haven, CT*

Disclosures: Tong Sun: None; Xuchen Zhang: None; Minghao Zhong: None

Background: Distinction between primary intrahepatic cholangiocarcinoma (ICC) and metastatic pancreatic ductal adenocarcinoma (PDAC) in a liver biopsy is often histologically impossible and immunophenotypically challenging but has important clinical implications. Previous studies of the molecular alterations in cholangiocarcinoma have focused on selected genes, which were known to be also altered in PDAC, including somatic mutations in *KRAS*, *PIK3CA*, *TP53*, *CDKN2A* and *SMAD4* (*DPC4*) genes. Recently the role of several chromatin-remodeling genes has emerged in ICC pathogenesis, such as *BAP1*, *ARID1A* and *PBRM1*. To further explore potential differentiating markers between ICC and PDAC, we conducted a comprehensive genetic sequencing and subsequent immunohistochemical (IHC) validation of BAP1 and AR1D1A.

Design: With IRB approval, a total of 116 ICC cases from liver biopsy or resection of our institute were recruited in current study. All cases underwent a comprehensive target cancer gene next generation sequencing (Oncomine Assay). Frequency of genetic alteration in PDAC was referred from The Cancer Genome Atlas (TCGA) program database. The protein expression status of BAP1 and ARID1A in ICC was subsequently evaluated by IHC.

Results: Somatic mutations in *BAP1*, which encodes a nuclear deubiquitinase involved in chromatin remodeling, occurred in 29 of 116 ICC cases (25.0%). We also identified that 22 of 116 ICC (18.9%) harbor somatic mutations in *ARID1A*, which encodes a subunit of the SWI/SNF chromatin-remodeling complexes. These two genes were significantly enriched for inactivating mutations in ICC, with nonsense, frameshift and splice-site mutations accounting for the majority of alterations. Forty-six of 116 (39.6%) ICC contained at least one somatic mutation in these two chromatin-remodeling genes. According to TCGA database, in PDACs, somatic mutations are rare in *BAP1* (1.1%) and much less frequent in *ARID1A* (5.7%) (*P* values for two-tailed unpaired t-test for both genes < 0.001). IHC demonstrated nuclear expression loss of BAP1 or ARID1A in 20 ICC tumor with inactivating mutations of these two genes, respectively.

Conclusions: The frequent alterations in *BAP1* and *ARID1A* indicated an essential role of chromatin remodeling in ICC development. Moreover, our data indicated that inactivating nuclear BAP1 or ARID1A loss is common in ICC but rare in PDAC, suggesting potential utility of these two IHC markers in distinguishing ICC from metastatic PDAC in liver biopsies.

1069 Primary Hepatic Malakoplakia: A Case Report and Analysis of the Literature

Callie Torres[1], Jana Hitgano[2], Michael Anreder[3], Samuel Ballentine[4]
[1]Barnes-Jewish Hospital/Washington University, Saint Louis, MO, [2]Kansas City University of Medicine and Biosciences, Joplin, MO, [3]Mercy Hospital, Joplin, MO, [4]Washington University in St. Louis, St. Louis, MO

Disclosures: Callie Torres: None; Jana Hitgano: None; Michael Anreder: None; Samuel Ballentine: None

Background: Malakoplakia is known as the great mimicker, often presenting as a large suspicious mass on imaging. Primary hepatic malakoplakia is exceedingly rare, with only nine previously published cases. Due to its infrequent nature, the presentation, means of diagnosis, and treatment have not been well established.

Design: Systematic literature searches were conducted for published articles of primary hepatic malakoplakia. Cases of non-primary hepatic malakoplakia or malakoplakia with hepatic extension were not included.

Results: Results are shown in Table 1. Cases were diagnosed at autopsy (n=4), via needle core biopsy (n=3), segmentectomy (n=2), and wedge biopsy (n=1). The age range was 16-82 (mean=46.3). The female (n=4) age range was 16-68 (mean=45.5). The male (n=6) age range was 19-82 (mean=50.2). Comorbid conditions included lupus (n=2), alcohol abuse (n=1), mucopolysaccharide disorder (n=1), AIDS (n=1), and chronic steroid use (n=2). The most prevalent infectious agent was *Escherichia coli* (n=4). Other organisms present in liver or blood cultures include *E. avium* (n=1), *E. faecium* (n=1), *A. calcoaceticus* (n=1), *B. thetaiotaomicrom, fragilis,* and *ovatus* (n=1), *S. Aureus* (n=1), and *S. maltophilia* (n=1). Imaging of the liver showed either a discrete mass (n=4) or no mass (n=1). When the mass was described, it was noted to be heterogenous and associated with surrounding fluid (n=2). On MRI, the lesion was noted to be hypointense on T1 and show locules of hyperintensity on T2 (n=2). Treatment was highly variable. If applicable, immunosuppressive medications were stopped. All patients were treated with antibiotics, although the drug class varied. Some patients were also treated with incision and drainage (n=1) or partial lobe resection (n=1). Of the non-autopsy cases, 2 patients had CT confirmed complete regression, 3 were discharged from the hospital, and 1 expired in the hospital.

Table 1: Previously published reports of primary hepatic malakoplakia including author and publication year, patient age and sex, underlying condition(s), bacterium(a) cultured, diagnostic material, presentation, imaging, management, and outcome.

Author(s)	Sex/ Age	Presentation	Underlying Condition(s)	Diagnostic Material	Culture Location/ Bacterium(a)	Imaging/Autopsy Findings	Management	Outcome
Moldavski & Rustamov	F/34	Unavailable	Miliary tuberculosis, hepatic pseudocyst	Autopsy	Unspecified: *M. tuberculosis*	Unavailable	Unavailable	Deceased
De Saint-Maur & Gallot	F/68	Unavailable	Infected polycystic liver	Segmentectomy	Liver Culture: *Escherichia coli*	Unavailable	Unavailable	Discharged
Robertson et al.	F/54	- 1st presentation: liver incidentally enlarged, asymptomatic - 2nd presentation: abscess with retroperitoneal tract	Lupus (treated with azanthioprine & steroids), autoimmune hemolytic anemia	Wedge Biopsy	-2nd presentation: Liver Culture: *E. coli, Acinetobacter calcoaceticus* and *E. cloacae*	Unspecified scan: hepatic lobe lesion, noted to possibly be an abscess or metastatic tumor	-1st presentation: discontinued steroids, unspecified antibiotics, drainage tube placed -2nd presentation: I&D of retroperitoneal tract, otherwise unspecified treatment	Discharged: expired 18 months after malakoplakia diagnosis due to sepsis post cholecystectomy
Boucher et al.	M/43	3 weeks of fever, anorexia, nausea, & diarrhea. 50lb weight loss over 2 months. 1 year history of RUQ pain	Psoriasis, gout, peptic ulcer disease, alcohol abuse, & perforated diverticulitis 3 months prior	Segmentectomy	-Initial Liver Culture: *E. coli & E. avium, B.thetaiotaomicron* -Hosp day 27: liver culture: *B. fragilis, B. ovatus, S. aureus, E. avium, & E. coli*	Unspecified scan: 8.0 x 8.0cm liver mass	-Drainage of initial liver mass and tobramycin, ampicillin/sulbactam, & metronidazole - Partial resection of right lobe of liver on day 27 -Overall hospital stay: vancomycin, ampicillin, gentamicin, cefizoxamine, streptomycin, amikacin, aztreonam	Discharged on hospital day 70. CT showed resolution of the lesion
Hartman et al.	M/19	Nausea, vomiting, diarrhea, & ascites, small bowel obstruction, pneumonia, and sepsis	Mucopolysaccharide disorder & neurodegenerative condition	Needle Core Biopsy	Pneumonia with unspecified *Klebsiella* species	CT: Liver cirrhosis	Spironolactone & furosemide for ascites, ampicillin & sulbactam for pneumonia	Deceased

Nouira et al.	F/16	Abdominal pain and fever lasting 21 days	Epilepsy and treated pulmonary tuberculosis	Needle core biopsy	N/A	CT: heterogenous mass with a hypodense rim MRI: hypointense mass with rim on T1, hyperintense with peripheral rim on T2	β-lactam antibiotic for 6 weeks	Discharged: CT scan performed 6 months later showed total regression of the hepatic lesion
Sim & Hsu	M/4 4	Weight loss, perianal & penile ulcerations, persistent diarrhea	HIV/AIDS, Cryptosporidium, Syphilis, Herpes, T Cell Lymphoma	Autopsy	Liver biopsy: gram positive cocci	Autopsy: 1.0 x 0.5 x 0.5 cm whitish firm hepatic nodule	N/A	Deceased
Botros et al.	M/5 3	Presented one week after renal biopsy with rigors & urinary urgency	Lupus treated with steroids, bacteremia, monoclonal gammopathy	Autopsy	Blood Culture: *Stenotrophomonas maltophilia* and *E. faecium*	Autopsy: liver grossly normal	Unspecified broad-spectrum antibiotics and repeated blood transfusions prior to death	Deceased: respiratory failure
Botros et al.	M/6 0	N/A	Tertiary syphilis with ocular involvement & adrenal abscess found at autopsy	Autopsy	Orbit Biopsy: *Treponema*organisms identified	Autopsy: liver grossly normal	N/A	Deceased: unexpectedly at home
Present Case	M/8 2	Diffuse abdominal pain	Cholecystectomy& temporal arteritis treated with steroids for 3 months	Needle core biopsy x2	Blood culture: *E. coli*	CT:heterogeneous mass measuring 8.8 x 4.8 x 8.8 cm MRI: 13.6 x 7.5 cm mass with extrahepatic extension	IV Ceftriaxone and Metronidazole for 2 weeks	Discharged to swing bed for 18 day stay

Conclusions: These results suggest that surgical management in addition to antibiotics may be useful in treatment hepatic malakoplakia and that when a mass lesion is present, it will appear heterogenous on imaging. Although treatment of malakoplakia in other locations is well established, treatment of hepatic malakoplakia should be further elucidated including investigation into the use of surgical management. Hepatic malakoplakia should be included in the differential diagnosis for a mass lesion after a surgical procedure or recent abdominal infection particularly in patients with an underlying immune disorder.

1070 Von Hippel-Lindau (VHL) Protein Immunostain Helps Classify Small Duct Type Intrahepatic Cholangiocarcinoma and Indicates A Good Prognosis

Yaohong Wang[1], Jun Yin[2], Tiffany Bainter[2], Taofic Mounajjed[3], Michael Torbenson[2], Saba Yasir[2], Fan Lin[4], Zongming (Eric) Chen[2]

[1]Vanderbilt University Medical Center, Nashville, TN, [2]Mayo Clinic, Rochester, MN, [3]Hospital Pathology Associates, Minneapolis, MN, [4]Geisinger Medical Center, Danville, PA

Disclosures: Yaohong Wang: None; Jun Yin: None; Tiffany Bainter: None; Taofic Mounajjed: None; Michael Torbenson: None; Saba Yasir: None; Fan Lin: None; Zongming (Eric) Chen: None

Background: According to the 2019 WHO recommendation, intrahepatic cholangiocarcinoma (ICC) should be classified into small duct and large duct subtypes based on tumor histomorphology to reflect distinct clinical features and molecular tumorigenesis. VHL immunostain is positive in small bile ducts and ductules of normal liver parenchyma. It is also positive in some ICCs but not in hepatocellular carcinoma and common metastatic adenocarcinoma involving the liver, a feature may be diagnostically useful. In this study, we focused on the association of VHL immunostaining status with ICC subtypes and overall survival (OS).

Design: 44 ICCs resected between 1997 and 2011 were included in the study. The cohort consisted of 26 men and 18 women with a mean age of 63±11. Tumors were subclassified as small duct or large duct types based on H&E morphology according to published criteria by at least two senior pathologists with consensus. One representative block of each case was selected for VHL immunostain (Sc-5575, rabbit polyclonal, 1:150; Santa Cruz Biotechnology). The staining results were graded as negative (<5%), 1+ (5-25%), 2+ (25-50%), 3+ (>50%). Electronic medical records were reviewed to determine patients' overall survival (OS) time and to extract pertinent demographic and tumor staging data. Statistical analysis was performed by two biostatisticians among the authors.

Results: Table 1 summarizes VHL immunostaining results in 44 tumors, including 32 small duct type and 12 large duct type. Positive VHL immunostain had a 93% sensitivity and 71% specificity for small duct type ($p<0.001$). Figure 1 shows Kaplan-Meier curves demonstrating better OS in patients with VHL positive tumors. This protective effect is observed in both early stage (AJCC

stage 1) and advanced stage (AJCC stage 2 and 3) patients. Additional multivariate analyses indicate that the protective effect of VHL is only for small duct ICCs with a hazard ratio (HR) of 0.127 (95% CL 0.036 to 0.45) and not significant in large duct ICCs (HR=0.991, 95% CL 0.207 to 4.748).

Histologic subtypes Total (n=44)	VHL Immunostaining Results		p-value
	Positive (n=30)	Negative (n=14))	
Small Duct Type (n=32)	28 (93.3%)	4 (28.6%)	<0.0001
Large Duct Type (n=12)	2 (6.7%)	10 (71.4%)	

Figure 1 - 1070

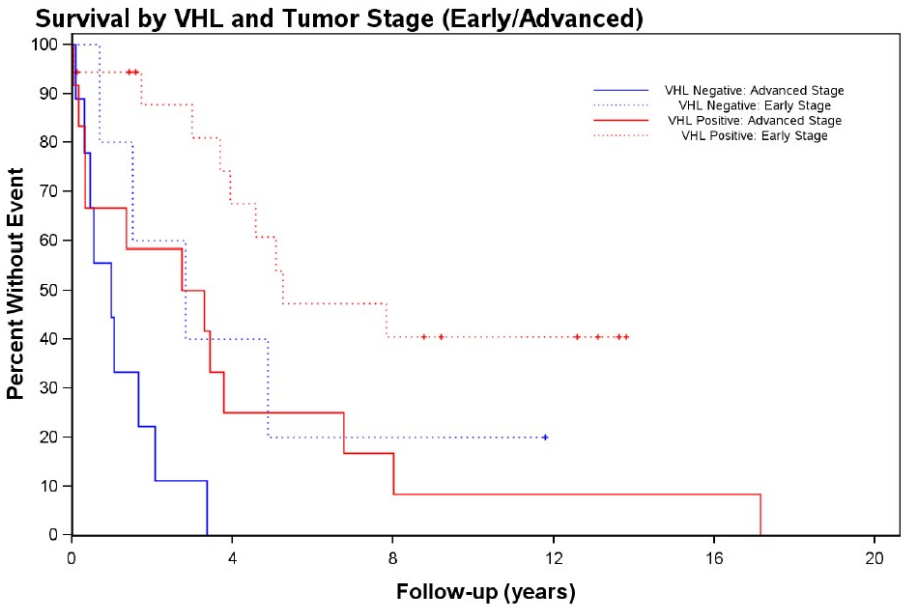

Conclusions: Our data indicate positive VHL immunostain can help subtype small duct ICC. VHL positive ICC have better OS, independent of tumor stages. Interestingly, multivariate analysis indicates this VHL protective effect is only observed in small duct subtype of ICCs.

1071 The Outcome of the Needle Biopsy Diagnosis of Acute Hepatitis: A Single Institution Experience

Rong Xia[1], Beena Ahsan[2], John Hart[2]
[1]University of Chicago Hospital, New York, NY, [2]University of Chicago, Chicago, IL

Disclosures: Rong Xia: None; Beena Ahsan: None; John Hart: None

Background: Acute hepatitis (AH) is defined histologically as lobular predominant inflammation & associated non-zonal hepatocyte injury (ballooning, necrosis & dropout) without fibrosis or dense portal inflammatory cell infiltrates (Fig. 1). It is associated with a hepatitic pattern of enzyme elevations. In this context the differential diagnosis is primarily drug induced liver injury & acute viral hepatitis (HAV, HBV, HCV & HEV). In some cases an etiology is never identified & an unknown toxic insult is assumed. An acute presentation of autoimmune hepatitis (AIH) can sometimes closely simulate AH of other etiologies, but usually the clinical, lab & histologic features are sufficiently distinct to allow these cases to be recognized separately, and steroid treatment is then instituted.

Design: We performed a retrospective review of native liver biopsies signed out as AH by a single senior liver pathologist from 1/1/01 to 12/30/06. The final reports included comments listing leading possible etiologies to aid in clinical management, including drug toxicity, AIH, drug triggered AIH, viral infection, and other. Each patient's clinical history, laboratory results, pathology results, & clinical follow-up (f/u) from the EMR were used to determine the final clinical diagnosis.

Results: A total of 68 needle biopsies were diagnosed as AH during the study period, of which 41 cases had sufficient clinical f/u to yield a final diagnosis. In 13 cases the report identified a single likely pathologic etiology (PE), & in 28 cases 2-3 possible etiologies were listed (Table 1). The final diagnosis was concordant with the suggested PE in 35 cases (85.4%). In 4 cases (4.9%) the final diagnosis was unclear (9.8%), and in 2 cases the final diagnosis differed from the suggested PE (Hemophagocytosis & AIH). There were significant differences in age & gender distribution depending on PEs (Fig 2). In 20 cases a final diagnosis of AIH was made, often despite limited justification from laboratory results. The 4 cases with unknown etiology all had limited clinical f/u at our center.

Table 1. Summary of the Demographic Information, Clinical History, Laboratory Tests, Pathologic Findings, and Clinical Follow-up

	Suggested Etiologies	Number*	Age (yr)	Gender (M:F)	Follow-up (m)	Progress (R:C)#	ALT (U/L)#	AST (U/L)#	ALP (U/L)#	TB (mg/dl)#	Viral workup(P:N)#^	Auto-antibodies(P:N)#@
Cases with Follow-up	Drug Toxicity	26	42.7 ±19.3	5:21	62.2 ±63.8	17:6	961.0 ±855.3	1017.3 ±1170.0	281.5 ±404.8	11.2 ±8.8	1:18	12:6
	AIH	25	41.0 ±16.0	5:20	70.3 ±62.4	15:9	966.7 ±860.3	1064.6 ±1192.2	278.1 ±425.3	9.0 ±9.1	0:16	16:6
	DAIH	N/A	N/A	N/A	N/A	N/A	N/A	N/A	N/A	N/A	N/A	N/A
	Viral Infection	12	30.3 ±16.3	5:7	60.2 ±55.7	8:3	1316.1 ±1198.1	1232.5 ±1467.2	436.9 ±560.4	16.6 ±6.9	6:6	3:5
	Others	1	29.0	1:0	1	N/A	16	30	541	3.6	0:1	N/A
	Resolving	8	43.3 ±16.3	0:8	19.5 ±21.3	8:0	205.9 ±271.6	176.25 ±177.6	91.5 ±54.6	4.6 ±4.3	1:7	5:2
	Total*	41	40.9 ±16.8	10:31	58.9± 62.0	26:12	702.1 ±793.5	721.4 ±1007.7	252.0 ±345.5	9.2 ±8.7	8:21	20:10
Cases without Follow-up	Drug Toxicity	17	42.4 ±23.5	9:9	N/A	N/A	1426.9 ±1404.4	1416.2 ±1611.0	143.8 ±76.6	12.65 ±9.0	0:9	6:5
	AIH	10	54.7 ±17.6	4:6	N/A	N/A	1052.8 ±797.2	1001.2 ±520.6	255.8 ±90.7	7.1 ±1.2	0:7	6:3
	DAIH	6	37.0 ±15.2	1:4	N/A	N/A	1239.6 ±1170.3	1036.5 ±1116.6	258.6 ±106.8	14.6 ±11.6	0:4	3:2
	Viral Infection	8	32.0 ±18.9	7:1	N/A	N/A	1316.1 ±1792.7	1336.3 ±2081.2	204.7 ±69.4	4.2 ±3.4	1:5	1:2
	Others	2	2, 23	0:2	N/A	N/A	N/A	N/A	N/A	N/A	N/A	N/A
	Resolving	N/A	N/A	N/A	N/A	N/A	N/A	N/A	N/A	N/A	N/A	N/A
	Total*	27	40.9 ±22.3	11:16	N/A	N/A	1250.8 ±1278.2	1203.9 ±1423.3	191.0 ±100.1	12.7 ±9.5	0:15	10:7

AIH, Autoimmune hepatitis; DAIH, Drug-triggered autoimmune hepatitis; AST, Aspartate aminotransferase; ALT, Alanine Aminotransferase; ALP, Alkaline phosphatase; TB: Total bilirubin; R:C, Resolved: chronic; P:N, Positive: negative; * Cases with multiple suggestive pathologic etiologies are present duplicatively in all relevant categories; # Only cases with available data are included; ^ Viral studies include available data for Hepatitis A, B, C, E, CMV, EBV , and HSV; @Auto-antibody studies include available data for anti-ANA, anti-dsDNA, anti-SMA, anti-mitochondrial antibodies.

Figure 1 - 1071

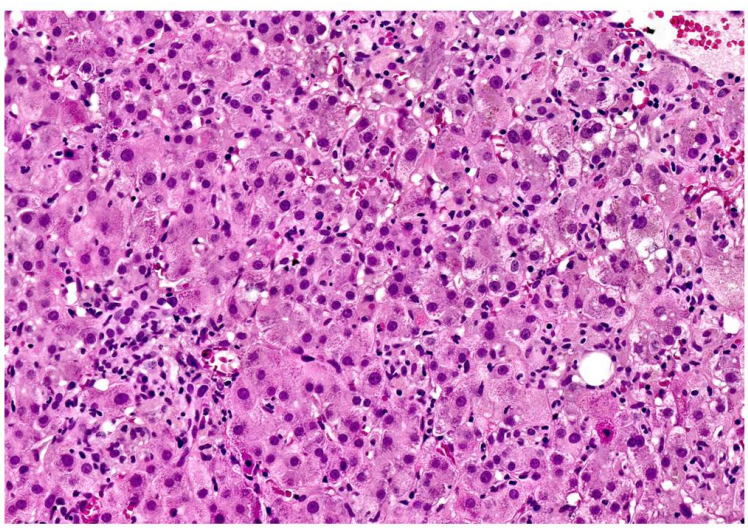

Figure 1. 47 y.o. F with a ANA = 1:320. The biopsy was signed out as acute hepatitis, with a comment favoring drug toxicity and specifically stating that AIH was unlikely. Nevertheless, the patient was treated with steroids for a clinical diagnosis of AIH. However, the steroids were quickly tapered off and the patient was done well since, suggesting that the clinical diagnosis was incorrect.

Figure 2 - 1071

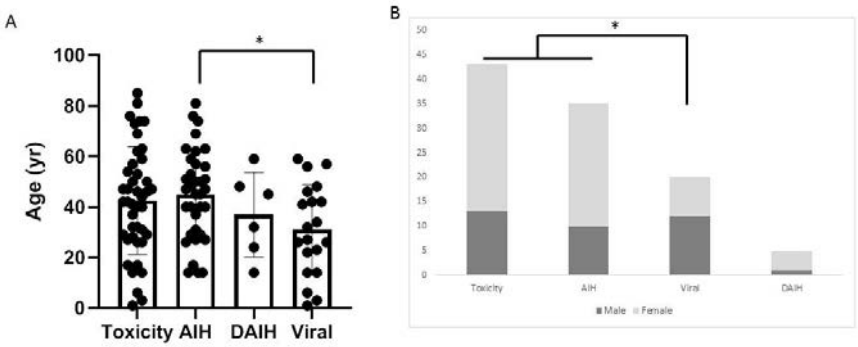

Figure 2 Age (A) and gender distribution (B) in patients with acute hepatitis of different pathologic etiologies. A. Significant age difference for patients with suggested pathologic etiology of AIH versus viral (one-way ANOVA with Tukey's post-hoc test). B. Significant difference in gender distribution in patients with suggested pathologic etiology of toxicity & AIH versus viral (Pearson's Chi-squared test). AIH, autoimmune hepatitis; DAIH, drug triggered autoimmune hepatitis.
* $p<0.05$

Conclusions: As there are several possible etiologies for the histologic pattern of AH, most of which do not have distinctive histologic features, final diagnosis usually require clinical f/u and integration of laboratory data. Often the clinical inflection point revolves around the recognition of AIH because steroid treatment needs to be begun promptly, and a presumptive diagnosis is made after other possibilities are excluded.

1072 USO1S Promotes Tumor Progression in Hepatocellular Carcinoma and Detection of Its mRNA Level Aid in Diagnostic Sensitivity

Ping Yang[1], Qun-sheng Huang[1], Jing-Ping Yun[1]
[1]Sun Yat-sen University Cancer Center, Guangzhou, China

Disclosures: Ping Yang: None; Qun-sheng Huang: None; Jing-Ping Yun: None

Background: Alternative splicing events contribute to the malignant progression of multiple solid tumors including hepatocellular carcinoma (HCC). The aim of this study was to identify the biological function of the truncated splicing variant of USO1 (USO1S) in HCC and to investigate the potential utility of combining USO1S mRNA RNAscope with traditional immunohistochemical (IHC) markers in the diagnosis of HCC.

Design: RNA sequence data were downloaded from The Cancer Genome Atlas (TCGA) and the association of alternative splicing events and overall survival were analyzed. The clinical relevance of USO1S in HCC was determined by RNAscope technology in fresh tissue and tissue microarray. CCK8 assays and colony formation were performed to determine the effect of USO1S on cell proliferation. Xenograft mouse models were used to evaluate the impact of USO1S on proliferation *in vivo*. Flow cytometry was applied to investigate the role of USO1S on cell apoptosis. A total of 892 patients with HCC and paired adjacent tissue, benign liver lesions, and non-hepatocytic tumors were examined. USO1S was detected using RNAscope. Glypican3 (GPC3) and α-fetoprotein (AFP) proteins were detected using IHC.

Results: USO1S was significantly overexpression in HCC tissues and correlated with unfavorable clinical outcome. Silencing of USO1S inhibited tumor growth and increased cell apoptosis in HCC. USO1S RNAscope improved the HCC detection sensitivity by 31.2% compared with AFP immunostaining. A panel of USO1S RNAscope and GPC3 immunostaining provided the best diagnostic value in diagnosing HCC (AUC = 0.867), comparing with USO1S, AFP and GPC3 alone. USO1S RNAscope shows high specificity when distinguishing HCC from benign lesions and non-hepatocytic malignancies.

Figure 1 - 1072

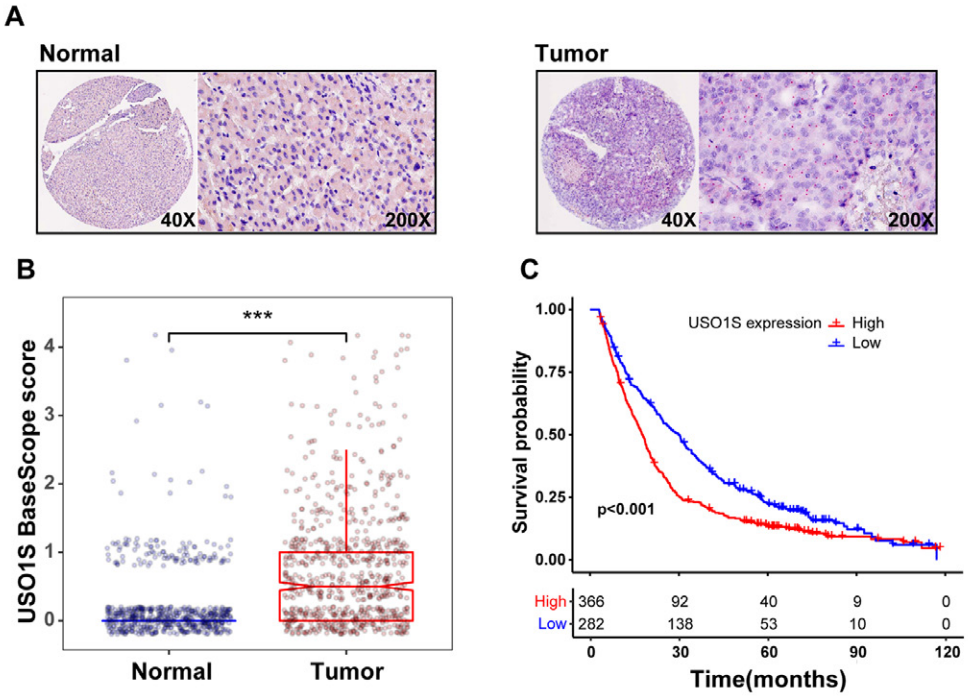

Figure 2 - 1072

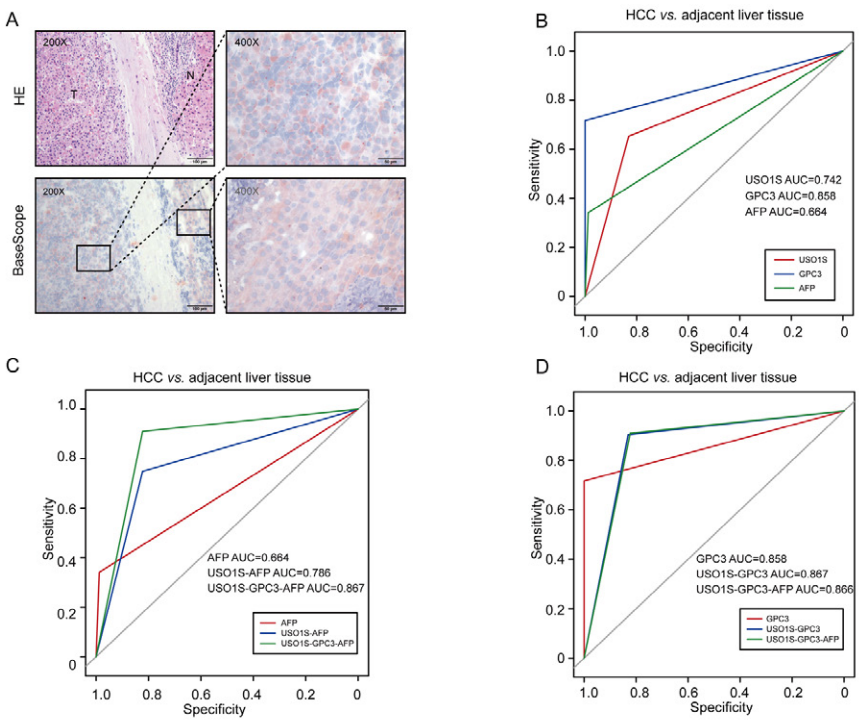

Conclusions: Our findings revealed an oncogenic role for USO1S in HCC. A panel including USO1S RNAscope and conventional biomarkers will improve the sensitivity in practical setting and together may aid new strategy in the diagnosis of HCC.

1073 Distinctive Histological Findings in Hereditary Hemorrhagic Telangiectasia Involving the Liver

Saba Yasir[1], Dora Lam-Himlin[2], Lindsey Westbrook[3], Tsung-Teh Wu[1], Hee Eun Lee[1], Aatur Singhi[4], Matthew Yeh[5], Sanjay Kakar[6], Vishal Chandan[7], Mojgan Hosseini-Varnamkhasti[8], Karen Matsukuma[9], Dhanpat Jain[10], Juan Silva Campos[11], Xuchen Zhang[10], Zongming (Eric) Chen[1], Michael Torbenson[1]

[1]Mayo Clinic, Rochester, MN, [2]Mayo Clinic, Scottsdale, AZ, [3]University of Colorado Anschutz Medical Campus, Aurora, CO, [4]University of Pittsburgh Medical Center, Pittsburgh, PA, [5]University of Washington Medical Center, Seattle, WA, [6]University of California, San Francisco, San Francisco, CA, [7]University of California, Irvine, Orange, CA, [8]University of California, San Diego, La Jolla, CA, [9]University of California, Davis, Sacramento, CA, [10]Yale School of Medicine, New Haven, CT, [11]Yale New Haven Hospital, New Haven, CT

Disclosures: Saba Yasir: None; Dora Lam-Himlin: None; Lindsey Westbrook: None; Tsung-Teh Wu: None; Hee Eun Lee: None; Aatur Singhi: *Consultant*, Foundation Medicine; Matthew Yeh: None; Sanjay Kakar: None; Vishal Chandan: None; Mojgan Hosseini-Varnamkhasti: None; Karen Matsukuma: *Advisory Board Member*, InCyte Corporation; *Consultant*, Diaceutics, Inc.; Dhanpat Jain: None; Juan Silva Campos: None; Xuchen Zhang: None; Zongming (Eric) Chen: None; Michael Torbenson: None

Background: Hereditary hemorrhagic telangiectasia (HHT) is an inherited disease leading to various vascular shunts. HHT commonly involves the liver, but the histological findings are poorly described.

Design: 33 cases were collected from 10 medical institutions and the clinical and histological findings reviewed.

Results: Twenty-two liver explants, 3 resections, 2 liver biopsy and 6 autopsy cases were reviewed from 30 women (average age 52 yrs, range 17-84 yrs) and 3 men (average age 55 yrs, range 52-60 yrs). The main histological findings were vascular malformations, which cluster into two general patterns. The most frequent pattern (N=26) was portal based shunts that were predominantly located in the small and medium sized portal tracts (Figure 1). In this group of cases, a distinctive shunt vessel (Figure 2) was seen in 8 cases, composed of small caliber vessels lined by hypercellular endothelium that appeared to directly connect the hepatic artery to the portal vein. As another finding, portal veins were often inconspicuous or absent in those portal tracts lacking telangiectasias (N=7). The second pattern (N=7) showed as a predominate finding dilated large-sized portal veins and portal vein branches in the hilum; some of the veins showed partial thrombosis and other showed eccentric thickening of the vessel walls. Other findings from the entire study group included biliary tract changes including periductal fibrosis (N=8), prominent bile ductular proliferation (N=5), and bile infarcts (N=8). One case with bile infarct also had an inflammatory pseudotumor. Other mass lesions included nodular elastosis (N=4), focal nodular hyperplasia (N=4), and a conventional cavernous hemangioma (N=1). One case also had a small duct cholangiocarcinoma, angiomyolipoma, and HNF1-alpha inactivated hepatic adenoma. Other microscopic findings included high grade biliary intraepithelial neoplasia (N=1), Von Meyenberg Complexes (N=4), web-like vascular telangiectasis (N=1), and nodular regenerative hyperplasia (N=5).

Figure 1 - 1073

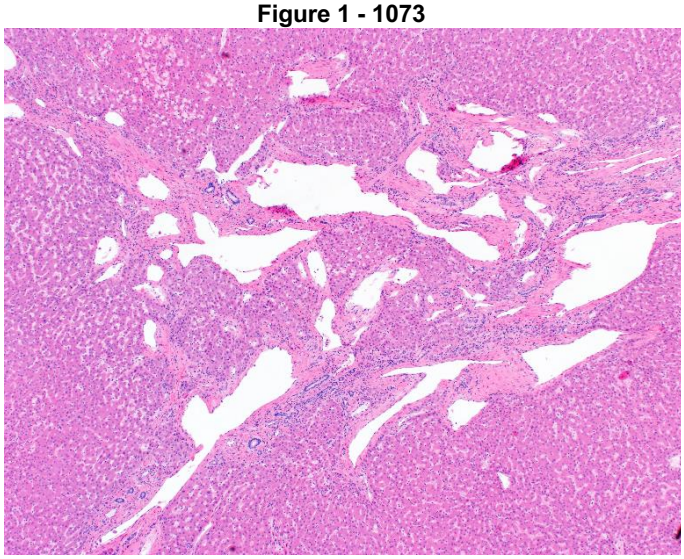

Figure 2 - 1073

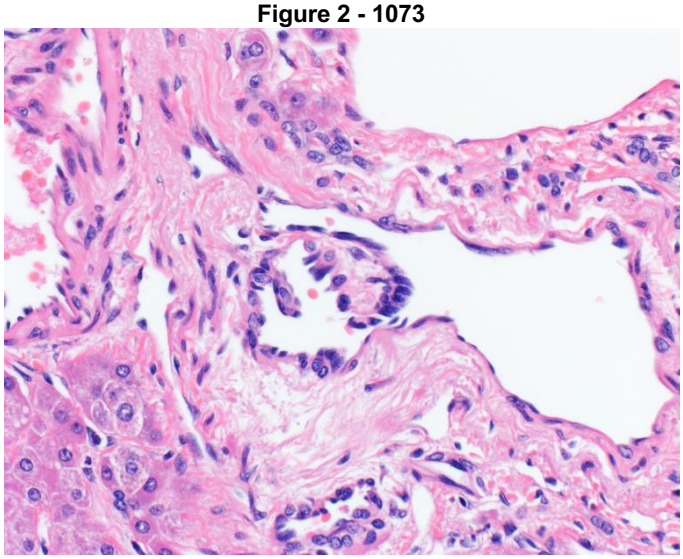

Conclusions: HHT involving the liver has a strong female predominance and is primarily a portal vein disease characterized by telangiectasias, as well as secondary biliary tract changes and vascular flow changes. The most common mass lesions are nodular elastosis and FNH.

1074 Genomic Profiling of LFABP-Negative Moderately to Poorly Differentiated Hepatocellular Carcinoma

Raymond Yip[1], Nancy Joseph[1], Sarah Umetsu[1], Michael Torbenson[2], Sanjay Kakar[1]
[1]University of California, San Francisco, San Francisco, CA, [2]Mayo Clinic, Rochester, MN

Disclosures: Raymond Yip: None; Nancy Joseph: None; Sarah Umetsu: None; Michael Torbenson: None; Sanjay Kakar: None

Background: Hepatocyte nuclear factor-alpha (*HNF1A)*-inactivated hepatocellular adenomas (H-HCA) are characterized by loss of liver fatty acid binding protein (LFABP) and somatic/germline *HNF1A* mutations. LFABP-negative well differentiated (WD) hepatocellular carcinoma (HCC) is rare but well described, shows *HNF1A* mutation and can closely resemble H-HCA (PMID: 31570768). LFABP loss has also been described in moderately (MD) and poorly differentiated (PD) HCCs (PMID: 26997447). Of the 8 *HNF1A*-mutated HCCs in the TCGA series, there were 4 MD and 1 PD case (PMID: 28622513). This study examines the correlation of LFABP loss and genomic features in MD and PD-HCC.

Design: The study cohort comprised 19 HCC (13MD, 6PD) with LFABP loss. The clinicopathologic features were compared to 7 previously characterized WD-HCC with LFABP loss. Capture-based sequencing using a 500 gene panel was performed in 7 LFABP-negative HCC (4MD, 3PD).

Results: LFABP-negative MD and PD-HCC frequently occurred in men (63%) and in the setting of viral hepatitis (53%) and advanced fibrosis/cirrhosis (63%). *HNF1A* mutation was seen in 1 MD-HCC and none of the PD-HCCs compared to all WD-HCC cases. Mutations in *TERT* promoter (57%), *TP53* (71%) and *RB1* (29%) were more common in LFABP-negative MD/PD-HCC. *CTNNB1* mutation was present in 2 LFABP-negative MD/PD-HCCs, but none of LFABP-negative WD-HCC.

	LFABP-negative WD-HCC (n=7)*	LFABP-negative MD/PD HCC (n=19)*	p value
Male gender	1/7 (14%)	12/19 (63%)	0.07
Age >50 years	4/7 (57%)	13/19 (68%)	0.66
Viral hepatitis	0	10/19 (53%)	0.02
Bridging fibrosis or cirrhosis	0	12/19 (63%)	<0.01
HNF1A mutation	5/5 (100%)	1/7 (14%)	0.02
TERT promoter mutation	2/5 (40%)	4/7 (57%)	1
TP53 mutation	0	5/7 (71%)	0.03
CTNNB1 mutation	0	2/7 (29%)	0.47
RB1 mutation	0	2/7 (29%)	0.47
NOTCH alterations	2/5 (40%)	0	0.15

* Genomic analysis in 7 MD/PD HCC and 5 WD-HCC.

Conclusions: LFABP-negative MD and PD-HCCs are more commonly associated with male gender, viral hepatitis and advanced fibrosis compared to LFABP-negative WD-HCC. These tumors are a heterogeneous group at the genomic level and show well known alterations of HCC such as mutations in *TERT* promoter, *TP53* and *CTNNB1*, while *HNF1A* mutation was observed in only 1/7 cases. In the absence of *HNF1A* mutations in a majority of these cases, the mechanism of LFABP loss is unclear.

1075 Fontan-Associated Liver Disease: Degree of Liver Damage is Not Always Reflected in Clinical and Radiological Parameters

Zhen Zhao[1], Thomas Schiano[2], Maria Isabel Fiel[1]
[1]Icahn School of Medicine at Mount Sinai, New York, NY, [2]Mount Sinai Medical Center, New York, NY

Disclosures: Zhen Zhao: None; Thomas Schiano: None; Maria Isabel Fiel: None

Background: The Fontan procedure directs systemic venous return into the pulmonary circulation with significant survival benefits but is associated with liver disease (FALD) mainly due to congestive hepatopathy. The congestive hepatopathy fibrosis score (CHFS) is a grading system that correlate well with chronic cardiac volume and/or pressure overload. Liver biopsy is the gold

standard in diagnosing and monitoring FALD associated fibrosis and cirrhosis, especially when imaging analysis is equivocal and degree of fibrosis is needed for decision making.

Design: Liver biopsy specimens (all obtained during cardiac catheterization) from 28 patients (median age 31 years [13-44] and 24 years [9-34] from the time of Fontan procedure), with average biopsy length 3.0 cm [1.5-4.7], were assessed by a single experienced liver pathologist for FALD with modified CHFS, fibrosis stage (Brunt classification) and sinusoidal fibrosis, steatosis grade (Brunt classification), portal activity (inflammation and bile duct status), and degree of congestion. Also collected were year-since-Fontan-procedure, mean Fontan pressure, degree of measured portal pressure, and radiological evidence of portal hypertension. Correlation of each and/or in combination with clinical data was analyzed.

Results: Mean Fontan pressure (MFP) was weakly correlated with year-since-Fontan-procedure (p=0.11) and portal pressure (p=0.12), but not with CHFS (range 1-4, median 2) (p=0.71). CHFS correlated significantly with Brunt fibrosis stage (p<1.00E-9), which correlated significantly with sinusoidal fibrosis (p=0.01). However, CHFS was not correlated with year-since-Fontan-procedure (p=0.70) or portal pressure (p=0.84). Grade 1 steatosis and portal alteration were each found in 5 patients (3 overlap) with no correlation with CHFS nor MFP level. MFP is likely the key clinical index and CHFS reflects pathology progression of FALD. Therefore, MFP was utilized to divide patients into 4 groups and with CHFS to count all other parameters for Naïve Bayes classification and data mining (Table 1).

Table 1. Probability of each score presenting in different MFL or CHFS levels by Naïve Bayes classification

Note: Potential valuable correlations or interest of study are marked in red.

		MFP				CHFS			
Score		1	2	3	4	1	2	3	4
Count		7	9	6	6	7	11	7	3
Probability		0.25	0.32	0.21	0.21	0.25	0.39	0.25	0.11
CHFS	1	0.29	0.33	0	0.33	1	0	0	0
	2	0.43	0.22	0.5	0.5	0	1	0	0
	3	0.29	0.44	0.17	0	0	0	1	0
	4	**0**	**0**	**0.33**	**0.17**	0	0	0	1
Fibrosis stage (Brunt)	1	0	0.22	0	0.33	0.57	0	0	0
	2	0.71	0.33	0.5	0.33	0.29	0.91	0.14	0
	3	0.14	0.44	0.17	0.17	0	0.09	0.86	0
	4	**0**	**0**	**0.33**	**0.17**	0	0	0	1
Sinusoidal fibrosis (1=patchy, 2=extensive)	1	0.43	0.22	0	0.17	**0.43**	**0.27**	**0**	**0**
	2	0.57	0.78	1	0.83	**0.57**	**0.73**	**1**	**1**
Sinusoidal dilation (1=mild patchy, 2=mild extensive or severe patchy, 4=severe extensive)	1	0	0.56	0.33	0.17	0.43	0.09	0.29	0.67
	2	0.29	0.11	0.33	0.17	0	0.18	0.43	0.33
	4	0.71	0.33	0.33	0.67	0.57	0.73	0.29	0
Sinusoidal congestion (1=mild patchy, 2=mild extensive or severe patchy, 4=severe extensive)	1	0.43	0.67	0.67	0.33	0.57	0.36	0.71	0.67
	2	0.43	0.22	0	0.17	0.43	0.18	0.14	0
	4	**0.14**	**0.11**	**0.33**	**0.5**	0	0.45	0.14	0.33
RBC trapped in space of Disse (0= non, 1=mild patchy, 2=mild extensive or severe patchy, 4=severe extensive)	0	0	0.11	0	0.17	0.29	0	0	0
	1	0.57	0.67	0.67	0.17	0.57	0.45	0.71	0.33
	2	0.29	0.11	0.17	0.17	0.14	0.18	0.14	0.33
	4	0.14	0.11	0.17	0.5	0	0.36	0.14	0.33
Hepatocyte necrosis	N	0.86	0.89	0.67	0.5	1	0.55	0.71	1
	Y	0.14	0.11	0.33	0.5	0	0.45	0.29	0

Hepatocyte plate atrophy	N	0	0.56	0	0.17	0.43	0.09	0.29	0
	Y	1	0.44	1	0.83	0.57	0.91	0.71	1
Nodular regenerative hyperplasia	N	0.57	0.78	1	0.67	**0.57**	**0.73**	**0.86**	**1**
	Y	0.43	0.22	0	0.33	**0.43**	**0.27**	**0.14**	**0**
Steatosis	N	1	0.67	0.83	0.83	0.86	0.82	0.71	1
	Y	0	0.33	0.17	0.17	0.14	0.18	0.29	0
Portal activity	N	0.86	0.44	0.83	0.5	0.43	0.64	0.71	1
	Y	0.14	0.56	0.17	0.5	0.57	0.36	0.29	0
Portal pressure (HTN only when >5-6)	1	0.86	0.56	0.5	0.5	0.57	0.73	0.57	0.33
	2	0.14	0.44	0.5	0.33	0.29	0.27	0.43	0.67
	3	**0**	**0**	**0**	**0.17**	0.14	0	0	0
Radiological evidence of portal HTN	Y	0.71	0.78	0.83	1	0.71	0.82	0.86	1
	N	0.14	0.11	0.17	0	0.29	0.09	0	0

Conclusions: CHFS is applicable in evaluating FALD, however stage of fibrosis is not associated with the period since the Fontan procedure nor with the circulating pressure. Also noted is that radiological evidence of portal HTN does not correlate with degree of portal hypertension nor by fibrosis, indicating the necessity of biopsy for effective FALD monitoring. Liver biopsies taken at the time of cardiac catheterization can obtain adequate length specimens.